Biomechanical effectiveness assessment of motorcyclist airbags in realistic impact scenarios using human body models

Raúl Aranda Marco

München 2022

Aus dem Institut für Rechtsmedizin
Institut der Universität München
Vorstand: Prof. Dr. med. Matthias Graw

Biomechanical effectiveness assessment of motorcyclist airbags in realistic impact scenarios using human body models

Dissertation
zum Erwerb des Doktorgrades der Humanbiologie
an der Medizinischen Fakultät der
Ludwig-Maximilians-Universität zu München

vorgelegt von
Raúl Aranda Marco
aus Zaragoza

2022

Mit Genehmigung der Medizinischen Fakultät
der Universität München

Berichterstatter:	Prof. Dr. rer. biol. hum. Steffen Peldschus
Mitberichterstatter:	PD Dr. Tobias Helfen Prof. Dr. Rudolf Hatz
Mitbetreuung durch die promovierte Mitarbeiterin:	Dr. med Sylvia Schick
Dekan:	Prof. Dr. Thomas Gudermann
Tag der mündlichen Prüfung:	25.11.2022

Acknowledges

This thesis presents the results of some years working as PhD Student in the Biomechanics and Accident Analysis area at the Institute of Legal Medicine in Munich.

My sincere gratitude goes to Prof. Dr. Steffen Peldschus for supervising my doctoral thesis. Your advice and orientation helped me to finish this thesis and your expertise and dedication inspired me during this way. I am also very thankful to my co-supervisor Dr. Sylvia Schick and her guidance about the medical aspects of this work.

I would like also to express my gratitude to Prof. Dr. Matthias Graw for giving me the possibility of developing my work at the Institute of Legal Medicine.

I was very lucky to be part of a great team of people during my time as PhD Candidate. For that reason, I would like to mention all my colleagues for their support: Dr. Julia Mühlbauer, Felicitas Lanzl, Dr. Therese Fuchs, Eva Nuspl, Laura Rahm, Dr. Katrin Brodbeck, Anja Wagner and Dr. Klaus Bauer. I am very thankful for their helpfulness, the interesting multidisciplinary discussions and specially for our coffee breaks. I will not forget your moral support and the good atmosphere inside and outside our office.

Finally, I would like to express my deepest gratitude to my family, specially my to parents Carmen and Salvador, who always believed in me and encouraged me to keep fighting.

A mis dos soles.

A mi luna.

Zusammenfassung

Das primäre passive Schutzsystem für die Sicherheit von Motorradfahrern, das die Verletzungen bei einem Unfallgeschehen mindern oder verhindern kann, stellt die persönliche Schutzausrüstung dar. Allerdings ist die Benutzung von tragbarer Schutzausrüstung auffallend gering [94], auch wenn das Sterberisiko der Motorradfahrer 20 mal höher als das Risiko der Autofahrer ist[37]. Nur das Tragen eines Schutzhelms ist weiter verbreitet, naheliegenderweise aufgrund der gesetzlichen Helmpflicht. Um den Brustkorb zu schützen, wurde die Verwendung von aufblasbaren Schutzsystemen vorgeschlagen[93]. Diese Protektoren bestehen aus einem Airbag, der in der Bekleidung der Motorradfahrer integriert ist und sich bei einem Unfall aufblasen würde. Die Vorteile beim Tragen eines Helms sowie seine Fähigkeit, schwere Kopfverletzungen zu reduzieren, wurden bereits aufgezeigt. [26, 56]. Trotz der Verfügbarkeit mehrerer Airbagjacken auf dem Markt, sind sowohl ihr Schutzpotenzial als auch ihre Wirksamkeit in konkreten Unfallszenarien noch unklar. Im ersten Teil dieser Dissertation wird diese Fragekomplex untersucht.

Nach einem kurzen Überblick über den Stand der Technik (Kapitel 2), wird die Modellierung und Charakterisierung eines Finite Elemente Modells eines frontalen Airbags für den Thorax vorgestellt, welches einen existierenden und üblichen Airbag abbildet. Die Charakterisierung des FE Airbag-Modells wird durchgeführt, indem die Simulationsergebnisse mit dem Verhalten eines realen Airbags in zwei verschiedenen Fallversuchen verglichen werden. Zuerst wird der Betriebsdruck des Airbags in Tests mit geringer Impaktenergie ermittelt. Danach wird in einem zweiten Schritt die Aufprallreaktion des Airbags in einer Reihe von stärker belastenden Tests bestimmt untersucht. Dieses Airbag-Modell wird im folgenden Kapitel verwendet, um das Schutzpotential und die Effektivität eines repräsentativen frontalen Airbags für den Brustkorb unter realistischen Aufprallbedingungen zu bestimmen und zu analysieren. Verschiedene Impaktsituationen werden in einer numerischen Umgebung mit dem FE Menschmodell GHBM simuliert. Die simulierten Impaktszenarien wurden in einer bisherigen Unfallanalyse [17] als Häufungen mit einer hohen Konzentration von Unfällen mit schweren Brustverletzungen identifiziert. Um das derzeitige Schutzpotenzial eines repräsentativen frontalen Airbags für den Thorax abschätzen zu können, wird jede Aufprallsituation zwei Mal simuliert: mit und ohne Airbag Protektor. Die Effektivität des Airbags wird anhand einer Analyse von biomechanischen Parametern und der Anwendung von biomechanischen Kriterien bestimmt. In diesem Fall werden die Anzahl von Rippenfrakturen basierend auf einer Bruchdehnungsanalyse des Brustkorbs

in der gemessenen Thoraxverformung und die Anwendung des Kompressionskriteriums genutzt, um die mögliche Verletzungsminderung des Airbags einzuschätzen. Die erhaltenen Ergebnisse aus den Simulationen zeigen, dass die Leistungsfähigkeit eines frontalen Airbags für den Thorax im Hinblick auf die Reduktion der Verletzungsschwere stark von der Aufprallgeschwindigkeit beeinflusst wird und in geringerem Umfang auch von der Konfiguration des Aufprallobjekts. Ein Airbag könnte einen eingeschränkten Schutz bis zu einer Aufprallgeschwindigkeit von 30 km/h bieten. Der Airbag Protektor konnte bei einer niedrigen Aufprallgeschwindigkeit (17 km/h analysiert in Cluster 4 und 20 km/h von Cluster 1) eine Schutzwirkung erzeugen, da er die Anzahl von Rippenfrakturen sowie die Verformung des Thorax deutlich reduzieren konnte, und würde allgemein auch einen wesentlichen Einfluss auf die Verletzungsentschärfung bei 30 km/h ausüben. Außer für einen Impakt bei 40 km/h mit einer horizontalen Orientierung des Objekts, wurde jedoch kein offenbarer Einfluss des Airbags für Aufprallgeschwindigkeiten über 30 km/h erzielt.

Die Zertifizierung der auf dem europäischen Markt verfügbaren Airbags für den Thorax wird gemäß den in der Norm EN 1621-4 aufgeführten Anforderungen duchgeführt. Allerdings haben sich Zweifel entwickelt, ob das EN 1621-4 Normtestverfahren für die Bewertung der Schutzwirkung von Thorax Airbags geeignet ist [11]. Insbesondere sind die geringe Übereinstimmung der Aufprallbedingungen im Testverfahren mit einem realen Unfall und die geringe Biofidelität angemerkt worden. Motiviert durch den Bedarf an einem neuen Testverfahren, das näher an der Realität liegen sollte, wurde im Rahmen des PIONEERS Projekt eine Testmethode vorgeschlagen, bei der ein bewegliches (Aufprall-)objekt gegen den fixierten Thorax des Hybrid III Dummy stößt [71]. Dieses potenzielle Testverfahren wird im zweiten Teil dieser Dissertation analysiert.

Das beim PIONEERS Projekt vorgeschlagene Testverfahren stellt die umgekehrte Aufprallkonfiguration eines Motorradunfalls dar, die als „Objekt-gegen-Fahrer“ bezeichnet werden könnte. Allerdings wird bei einem Motorradunfall die Belastung des Thorax durch den Stoß des Motorradfahrers gegen einen Hindernis ausgelöst. Diese Aufprallkonfiguration könnte als „Fahrer-gegen-Objekt“ bezeichnet werden, weil eine bewegte Masse (der Körper des Motorradfahrers) gegen ein festes Objekt stößt. Aufgrund ihrer technischen Komplexität und ihrer möglicherweise geringen Reproduzierbarkeit stellt jedoch die Umsetzbarkeit dieser „Fahrer-gegen-Objekt“ Aufprallkonfiguration in ein wiederholbares, einfaches, biomechanisch valides und realistisches Testverfahren viele Schwierigkeiten dar, weshalb die umgekehrte Konfiguration bevorzugt wird. Es ist noch unbekannt, ob eine Äquivalenz zwischen beiden Aufprallkonfigurationen gefunden werden könnte. Das fünfte Kapitel befasst sich mit dieser noch offenen Frage, indem eine Logik für eine biomechanisch belastbare Umsetzung der „Fahrer-gegen-Objekt“ Konfiguration in die umgekehrte Konfiguration vorgeschlagen und die nachfolgenden Zwischenschritte mittels einer numerischen Studie analysiert werden. Auf Basis des Thoraxverhaltens hinsichtlich der Brustkorbverformung und des viskosen Verletzungskriteriums wurde zuerst die Überführbarkeit der „Fahrer-gegen-Objekt“ Konfiguration in eine „Objekt-gegen-Fahrer“ Konfiguration über die Berechnung der Masse des Aufprallobjekts oder der äquivalenten Masse eingeschätzt.

Das bedeutet, es wird an der Aufprallsituation beteiligte Massenanteil des Motorradfahrers identifizert, der das gleiche Thoraxverhalten hervorrufen würde. In einem zweiten Schritt werden in Kapitel 5 die zu erwartenden Unterschiede zwischen dem Verhalten eines menschliches Brustkorbs (abgebildet durch das Menschmodell GHBM) und dem Verhalten eines Hybrid III Dummy Brustkorbs analysiert. Da sich dieses neue Testverfahren möglicherweise zu einer Ergänzung oder zu einem Ersatz des aktuellen Normtestverfahrens entwickeln könnte, wurde in diesem Kapitel auch eine Bewertung und Einstufung der Airbag-Schutzwirkung auf Basis des Verletzungsrisikos vorgeschlagen.

In Summe befasst sich diese Dissertation mit der Verbesserung der Sicherheit von Motorradfahrern, wobei Untersuchungen zum Schutz des frontalen Thorax im Fokus stehen. Die Analysen zu effektiver Schutzwirkung durh Airbagsysteme basieren dabei auf der Verwendung von FE Menschmodellen und biomechanischen Parametern.

Abstract

The principal passive safety protection system for motorcycle riders which could mitigate and prevent injuries in case of accident is Personal Protective Equipment (PPE). However, even if the risk of death for motorcyclists is 20 times higher than for car occupants [37], the use of wearable protectors is significantly low [94]. Only wearing a helmet is widely extended probably because of its mandatory statement. To protect the thorax, the use of inflatable protection systems has been proposed [93]. Those protectors consist of an airbag integrated in the garments worn by the motorcyclists which would inflate in case of accident. The benefits of wearing a helmet and its effectiveness in the reduction of head injury severity has been demonstrated [26, 56]. However, despite several airbag jackets are available on the market, the protection potential and effectiveness of such a device on an accident situation is still unclear. The first part of this thesis investigates this question.

After a brief review of the state of the art (chapter 2), the modelling and characterization of a finite element model of a frontal thorax airbag representative of a real world standard airbag is exposed in chapter 3. The characterization of the model was conducted comparing simulation results of the FE airbag model with the performance of a real airbag in two different kind of drop tests. Firstly, the working pressure of the airbag was determined through low-severity tests and secondly, the impact response of the airbag was obtained on a set of more severe tests. This model is used in the following chapter 4 to analyse and determine the protection potential and effectiveness of a representative frontal thorax airbag under realistic impact conditions. Using the human body model GHBMC, different impact situations are simulated on a numerical environment. The impact scenarios simulated were identified in previous accident analyses [17] as clusters with a high concentration of accident with severe thorax injuries. In order to assess the current protection potential of a representative frontal thorax airbag, every impact situation is simulated twice: with and without airbag protector. The effectiveness of the airbag is determined by the analysis of biomechanical paramenters and the application criterion. In this case, the number of rib fractures on the basis of an ultimate strain analysis of the rib cage together with the measurement of the thorax deflection and the application of the Compression Criterion are used to calculate the possible injury mitigation. The results obtained from the simulation study showed that the effectiveness of a frontal thorax aibag in the reduction of the injury severity is highly conditioned by the impact speed and also by the object configuration on a lesser degree. An airbag could provide a limited protection up to 30

km/h of impact velocity. The airbag was able to provide a protective effect, reducing considerably the number of rib fractures and the thorax deflection, at a lower impact velocity (the 17 km/h analysed in Cluster 4 or the 20 km/h of Cluster 1) and would also globally present a significant influence on the injury mitigation at 30 km/h. However, except for the case of an impact at 40 km/h in horizontal object configuration, no obvious influence of the airbag in the injury mitigation was obtained for impact velocities over 30 km/h.

The certification of thorax airbags available in the European market is conducted by the fulfilment of the requirements established by the standard EN1621-4. However, some doubts have emerged about the suitability of the standard EN1621-4 test procedure used for the evaluation of the impact protection abilities of thorax airbags [11]. Specially its low biofidelity and the low correspondence of its impact conditions with a real accident have been remarked. Motivated by the need of a new test procedure as close as possible to the reality, the PIONEERS project proposed a test where a moving object would impact a fixed thorax of Hybrid III dummy [71]. This potential test procedure is analysed in the second part of this thesis.

The test proposed by the PIONEERS project represents the inverse impact configuration of a motorcycle accident, what could be called as "object-to-rider" configuration. However, in a motorcycle accident, the rider usually impacts another object causing the loading of the thorax. This impact configuration could be denominated "rider-to-object" configuration because a moving mass (the body of the rider) impacts a fixed object. However, due to its technical complexity and its possible low reproducibility, the translation of those impact condition into a repeatable, simple, more biofidelic and realistic test procedure implies some difficulties and the inverse configuration (object-to-rider) is preferred. If an equivalence between both impact configurations could be found is still unknown. Chapter 5 addresses this remaining open question suggesting a logic for a biofidelic translation of the rider-to-object configuration into the reverse one and analysing the subsequent intermediate steps in a numerical study. Based on the thorax response in terms of thorax deflection and Viscous Criterion, the translation of the rider-to-object configuration into an object-to-rider configuration was firstly assessed by the calculation of the object impact mass or equivalent mass. That means, the portion of the mass of the rider involved in the impact situation which would provide the same thorax response. On a second step, chapter 5 analyses the expected differences between the thorax responses of a human thorax (represented by the human body model GHBMC) and the thorax of the Hybrid III dummy. Considering the option of this new test to become a complement or a substitute of the current standard procedure, an airbag performance classification rating in terms of injury risk was proposed in this chapter.

In general terms, this thesis addresses the necessary improvement of motorcyclist safety focussing its investigations in the protection of the frontal thorax through the research of effective airbag protectors based on the use of human body models and biomechanical parameters.

Contents

1 Introduction **1**

1.1 Contributions and research projects 3

2 State of the Art **5**

2.1 Human Body Models (HBMs) 5

2.2 Wearable Airbag Protector 6

2.3 Standard EN 1621-4 7

2.3.1 Impact attenuation test and requirements 7

2.4 Compression Criterion 9

2.5 Viscous Criterion 12

2.6 LMU accident database 13

3 Modelling and characterization of a frontal thorax airbag finite element model **15**

3.1 Methodology 15

3.1.1 First experimental stage: Working pressure 17

3.1.2 Second experimental stage: Severe impact conditions 17

3.2 Results 18

3.2.1 Results: Working pressure 18

3.2.2 Results: Severe impact conditions 20

3.3 Discussion 21

4 Protection potential of current thorax airbag devices **23**

4.1 Introduction 23

4.2 Methodology 26

4.2.1 Definition of impact boundary conditions 26
4.2.2 Numerical simulations 27
4.3 Results 32
4.3.1 Cluster 1 33
4.3.2 Cluster 2 43
4.3.3 Cluster 3 53
4.3.4 Cluster 4 57
4.3.5 Analogy between vehicle's roof edge and idealized object - Results . 59
4.4 Discussion 61

5 Analysis of a potential test procedure for frontal thorax airbags 67
5.1 Introduction 67
5.2 Methodology 69
5.2.1 Bridging the gap between the accident scenario and the test impact conditions 69
5.2.2 Feasibility of the new test procedure 71
5.3 Results 74
5.3.1 Sensitivity analysis 74
5.3.2 HBM vs Dummy thorax response: Results 78
5.4 Discussion 81

6 Conclusions and Outlook 85

List of Figures

2.1 THUMS family models of the pedestrian version [1] 5

2.2 HUman MOdel For Safety (HUMOS) [51] and Strassbourg University Finite Element Head Model (SUFEHM) [80]. 6

2.3 Examples of airbag protectors available in the market from Helite [2] and Motoairbag [3] 7

2.4 Label indicating a protector is certified according to EN 1621-4 [33] 8

2.5 a.Kerbstone impactor b.Anvil [32] 8

2.6 Levels of protection according to EN 1621-4 [33]. 9

2.7 Cadaver test to apply an anteroposterior load to the thorax[52] 9

2.8 Force-deflection results from the experiments done by Kroell *et al.*[52] . . . 10

2.9 Non-age dependent risk curves for AIS $\geq$ 3 injury [60] and age dependent risk curves for AIS $\geq$ 3 injury [74] produced by distributed, anterior impacts to the thoraces of mid-size males. 11

2.10 Sternal compression injury risk. (A) Injury risk functions developed by Mertz et al. (1997) [60], (B) NHTSA FVMSS 208 injury risk functions (NHTSA, 1998), and (C) NHTSA NCAP chest injury risk by age (NHTSA, 2008) [89]. 11

2.11 Risk of severe thorax injury as a function of the maximu viscous response for frontal impacts [97]. 12

3.1 Original airbag jacket and its correspond back airbag 16

3.2 Airbag FE model and its position by GHBMC model 16

3.3 Small drop-tower used for obtaining the airbag working pressure 17

3.4 Drop-tower used for obtaining the airbag response under severe impact conditions 18

3.5 Airbag response for different pressure values compared to the simulation result 19

3.6 Numerical airbag response inflated with air or carbon dioxide 19
3.7 Numerical airbag response inflated with air or carbon dioxide 20
3.8 Numerical airbag response inflated with air or carbon dioxide 20
3.9 Response of the airbag FE model to the standardization test 21

4.1 Impact boundary conditions, velocity (top) and object radius (bottom), selected at each cluster. 27
4.2 Simulation example with the GHBMC equipped with a FE airbag model. . 28
4.3 Initial position of GHBMC M50 Detailed Pedestrian Version 1.5 28
4.4 Impact configurations against a small radius obstacle. 29
4.5 Impact configuration against a large radius obstacle. 30
4.6 Impact configuration against a flat object. 30
4.7 Selected nodes for the chest deflection measurement. 31
4.8 Impact against a vehicle's roof edge. 32
4.9 Cluster 1 impact conditions 33
4.10 Maximum principal maximal strain contour plot at cortical and trabecular bone for an impact at 30 km/h in diagonal configuration. 34
4.11 Thorax deformation by an impact of 30 km/h in diagonal configuration . . 35
4.12 Rib strain at cortical and trabecular bone for an impact at 30 km/h in horizontal configuration 36
4.13 Thorax deformation by an impact of 30 km/h in horizontal configuration . 37
4.14 Thorax deformation by an impact of 30 km/h in vertical configuration . . . 38
4.15 Rib strain at cortical and trabecular bone for an impact at 30 km/h in vertical configuration 39
4.16 Cluster 2 impact conditions 43
4.17 Rib principal strain at cortical and trabecular bone for an impact at 60 km/h in diagonal configuration 44
4.18 Thorax deformation by an impact of 60 km/h in diagonal configuration . . 45
4.19 Rib principal strain at cortical and trabecular bone for an impact at 60 km/h in horizontal configuration 46
4.20 Thorax deformation by an impact of 60 km/h in horizontal configuration . 47
4.21 Thorax deformation by an impact of 60 km/h in vertical configuration . . . 48
4.22 Rib principal strain at cortical and trabecular bone for an impact at 60 km/h in horizontal configuration 49

4.23 Cluster 3 impact conditions 53
4.24 Rib principal strain at cortical and trabecular bone for an impact at 50 km/h in horizontal configuration 54
4.25 Thorax deformation by an impact of 50 km/h in horizontal configuration . 55
4.26 Cluster 3 impact conditions 57
4.27 Rib principal strain at cortical and trabecular bone for an impact at 17 km/h against a flat object 58
4.28 Thorax deformation by an impact at 17km/h to a flat surface. 59
4.29 Rib principal strain at cortical and trabecular bone for an impact against a vehicle's roof edge and a cylinder with a radius of 0.075 m. 60

5.1 Summary of initial procedure states: accident and test impact conditions. . 69
5.2 Intermediate step: Determination of the equivalent mass. 70
5.3 Possible equivalence between the real accident scenario and the new test procedure. 71
5.4 Simulation of the object-to-rider impact configuration with the Hybrid III dummy model. 72
5.5 Impact conditions of the sensitivity study. 73
5.6 Simulation of the object-to-rider impact configuration with the Hybrid III dummy model. 74
5.7 Comparison of thorax deflection and maximal Viscous Criterion response of both impact configurations under three different protective conditions for a variable equivalent mass and the applied velocities. 77
5.8 Thorax deflection and Viscous Criterion response as a function of the combination of equivalent-mass velocity for three different protection levels. . . 78
5.9 Comparison of thorax deflection and maximal Viscous Criterion response in rider-to-object configuration between the GHBMC and the Hybrid III dummy FE model. 80

List of Tables

2.1 Linear relationship between chest compression and AIS severity [65]. 10

2.2 Clusters obtained from the accident analysis of the representative impact conditions for the airbag performance analysis 13

4.1 Intervals of impact boundary conditions of each cluster. 26

4.2 Cluster 1 - Simulation Results 41

4.3 Cluster 2 - Simulation Results 51

4.4 Cluster 3 - Simulation Results 56

4.5 Cluster 4 - Simulation Results 57

5.1 Main characteristics of the airbag models used in the sensitivity study. . . 73

5.2 Thorax deflection values obtained from the rider-to-object configuration and possible equivalent masses in object-to-rider configuration. 75

5.3 Maximal Viscous Criterion response values obtained from the rider-to-object configuration and possible equivalent masses in object-to-rider configuration. 76

5.4 Thorax response in terms of thorax deflection and Viscous Criterion response obtained from the simulation of the rider-to-object configuration with GHBMC pedestrian. 79

Chapter 1

Introduction

Powered-Two-Wheelers are one of the most dangerous mode of transportation and their users are considered as vulnerable road users because of their higher risk of being involved in a fatal accident [16]. Traffic accidents involving motorcyclists users represent the 17% of the traffic deaths in the European Union [36]. Considering all world traffic fatalities, a 28% of fatalities were accounted for Powered-Two-Wheelers users [98]. Low extremities are the most frequent body region injured, however the head and the thorax are usually the most severely body region injured in an accident. According to the Motorcycle Accident In-Depth Study (MAIDS) report published in 2008 [58], the thorax was remarked as the body region with the highest rate of MAIS3+ (more than 50%) while it was only the fourth most common body region injured.

The principal passive safety protection system for motorcycle riders which could mitigate and prevent injuries in case of accident is Personal Protective Equipment (PPE). However, even if the risk of death for motorcyclists is 20 times higher than for car occupants [37], the use of wearable protectors is significantly low [94]. Only wearing a helmet is widely extended probably because of its mandatory statement. To protect the thorax, the use of inflatable protection systems has been proposed [93]. Those protectors consist of an airbag integrated in the garments worn by the motorcyclists which would inflate in case of accident. The benefits of wearing a helmet and its effectiveness in the reduction of head injury severity has been demonstrated [26, 56]. However, despite the diversity of weareable airbags available in the market, how effective a frontal thorax airbag could be under realistic impact conditions is still unknown. The existence of the standard EN1621-4 [33], which certifies most of the airbags in the European market, appears to be insufficient to answer this question. Not only because of its simple and low-severity impact conditions but also because its low biofidelity and the unknown background for its established impact thresholds to classify the airbags protection performance. Some researchers, like Serre *et al.* (2019) [84], conducted some single crash tests to evaluate the real airbag effectiveness but focusing more on the activation parameters. Other, like Cherta *et al.* (2019b), tried to give an overview about the airbag effectiveness simulating some impact conditions derived

from the accident analysis but not in a realistic impact configuration, where the body of the rider hits an obstacle, rather in the inverse one. However, a systematic study based on biomechanical parameters about an airbag impact protection effectiveness which provides a global overview about its potential and limitations is still missing. Questions like which is the maximal impact velocity whereby a thorax airbag is still able to provide significant injury mitigation or how much protection an airbag could provide in impacts against statistically recorded obstacles in accident data (like trees or car roof edges) considering different radius and orientations are still open issues.

The current standard EN1621-4 for the certification of thorax motorcyclists airbags established three different levels of protection (fail, level 1 and level 2) depending on the values of transmitted force measured during the impact attenuation testing procedure. However, from a biomechanical perspective, the background and fundamentals of these thresholds are totally unknown. The low biofidelity of the test procedure together with the limitations of this test to distinguish the optimal inflated thickness/pressure combination [11] have turned the current standard into a questionable procedure for the evaluation of thorax airbags. Those factors motivate the research of a new test procedure which could substitute or at least complement the current standard. This possible new method should be as close as possible to a real accident being able to reproduce more realistic impact conditions. How to translate the impact conditions of an identified most common accident situation into a repeatable, simple, cost-effective and more biofidelic and realistic laboratory test entails the main challenge in the development of a new test procedure for the evaluation of thorax airbags. In addition, a new test method should be implemented including a rating of the airbags impact perfomance based on biomechanical criteria which not only assures a determined minimum level of protection but also motivates the improvement of the injury mitigation effectiveness of the frontal thorax airbags.

The assessment of the protection effectiveness of a representative frontal thorax airbag as well as the analysis of the fundamentals of a new test procedure to evaluate the airbag protection performance based on biomechanical criteria are both addressed in this thesis. This work contributes generally to the improvement of motorcyclists safety and more specifically to the protection of riders frontal thorax using an airbag protector. In addition, the method and tools presented in the following chapters contributes to the widening of human body models and virtual assessment in the development of future airbag protectors.

1.1 Contributions and research projects

During my time as PhD Candidate in the Biomechanics and Accident Analysis department at the Institute of Legal Medicine of the Ludwig-Maximilian University (LMU), I was directly involved in three research projects about motorcyclist safety:

- EU Marie Curie Action FP7 Project MOTORIST - MOTOrcycle Rider Integrated SafeTy (Grant Agreement 608092) [5].
- EU Horizon 2020 PIONEERS - Protective Innovations of New Equipment for Enhanced Rider Safety (Grant Agreement No. 769054) [4].
- Intelligente Schutzbekleidung für Motorradfahrer in Auftrag der Unfallforschung der Versicherer (UDV) [6, 17].

I want to thank the European Commission and the Unfallforschung der Versicherer for financing part of my investigation.

Chapter 2

State of the Art

2.1 Human Body Models (HBMs)

A Human Body Model is a Finite Element Model of the human body which is usually used to the calculation of the human body kinematics and the prediction of injuries on the human body. The most widespread models are the Total Human Model for Safety (THUMS) and the Global Human Body Model Consortium (GHBMC). The first was developed by Toyota Motor Corporation and Toyota Central R&D Labs. Currently, the participants included in the GHBM Consortium are General Motors Corp., FCA US LLC, Honda R&D Co., Hyundai Motor Co., Nissan Motor Corp. Ltd., PSA Peugeot-Citroën, Renault s.a.s., and Joyson Safety Systems. Ford Motor Co., NHTSA (National Highway Transportation Safety Administration) and Autoliv Inc. Both developers offer a family of models providing occupant and pedestrian versions in different percentiles (see Figure 2.1).

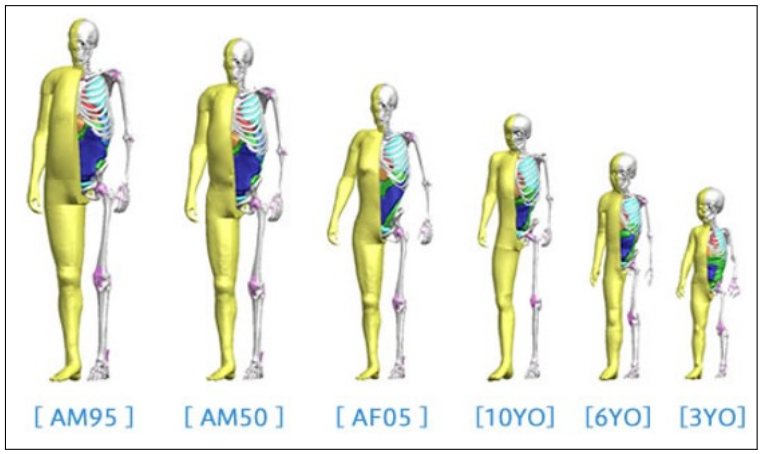

Figure 2.1: THUMS family models of the pedestrian version [1]

The THUMS and the GHBMC models are the most used models but there are more models representing the whole human body like the HUman MOdel For Safety (HUMOS) [78] or others which only reproduce a part of the human body, specially the head, like the Strassbourg University Finite Element Head Model (SUFEHM) [24]. Figure 2.2 shows both models. The HBMs are used in several fields specially in the automotive for the calculation of the occupant safety [39] or the safety of vulnerable road users [99]. But they are also used in fields like sports [22] and military [88].

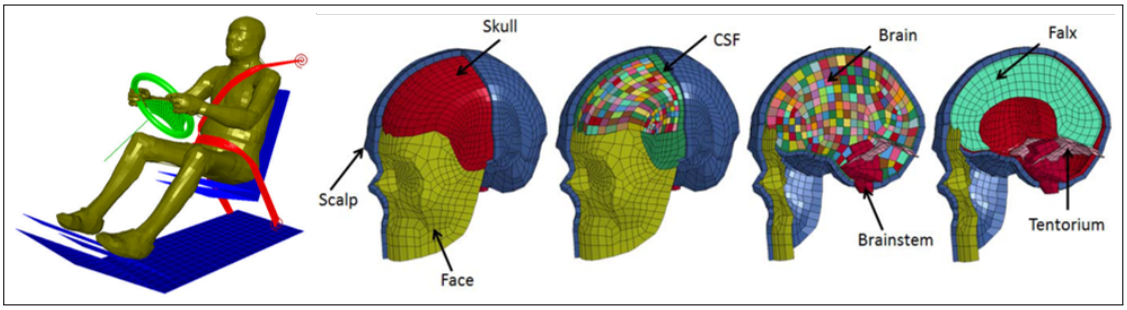

Figure 2.2: HUman MOdel For Safety (HUMOS) [51] and Strassbourg University Finite Element Head Model (SUFEHM) [80].

2.2 Wearable Airbag Protector

A wearable airbag protector is an inflatable system integrated in the garments worn by motorcyclists, usually a jacket or a vest. This passive safety system inflates in case of accident trying to protect the rider from possible injuries.

There are many airbag protectors for the thorax available on the market and they differ on many parameters airbag pressure (usually not communicated by the manufacturer), activation time after the first impact (in general between 20 and 200 ms), volume of the bag (mainly between 5 and 20 litres), inflation time, location of the gas cartridges or gas composition. They are also available on several shapse and with different covering areas. Therefore, wearable airbag protectors are usually classified attending to its activation method: mechanical or electronic activation.

- Mechanical activation: The airbag system worn by the rider is physically linked to the motorcycle by a cable. In case of impact, the cable is unhooked initiating the inflation of the airbag.
- Electronic activation: The airbag system is not physically linked to the motorcycle and an impact will be detected by some sensors which will activate the inflation. Two types are found depending on the sensors location:

– The sensors are located on the front wheel and in case of impact, a radio signal is sent to activate the airbag.
– The sensors are integrated in the jacket and the jacket is indepedent from the motorcycle.

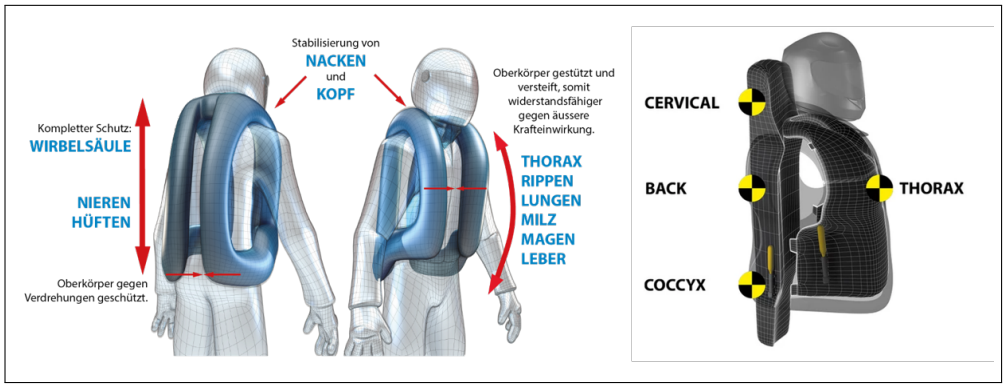

Figure 2.3: Examples of airbag protectors available in the market from Helite [2] and Motoairbag [3]

2.3 Standard EN 1621-4

An wearable airbag protector is considered an standard airbag if its performance fulfil all the requirements contemplated in the European Standard EN 1621-4 Motorcyclists' protective clothing against mechanical impact Part 4: Motorcyclists' inflatable protectors - Requirements and test methods [33]. This Standard specifies the minimum intervention time of inflated, the minimum duration time, the minimum level of and the minimum covering protection provided by the motorcyclists' protectors. It determines also requirements for the performance of the system like the activation force and activation energy and also requirements for sizing, ergonomics and innocuousness. An airbag protector certified according to the Standard requirements is marked with the label shown in figure 2.4. For this work, the attenuation impact performance and test are the most relevant part. Other requirements are out of scope of this study.

2.3.1 Impact attenuation test and requirements

The test machine used for the impact attenuation evaluation of an airbag chest protector is the same as for the testing of non-inflatable protectors described by the Standard EN 1621-3 [32]. The testing procedure is conducted in a drop-tower machine where an impactor falls freely along a vertical guide onto the testing sample placed on an anvil. The impactor is a bar with kerbstone shape with a length, h_1, of (160 $\pm$ 2) mm, a width, h_2, of (50 $\pm$

Figure 2.4: Label indicating a protector is certified according to EN 1621-4 [33]

1) mm and with a radius hemispherical face, R, of (12,5 ± 0,1) mm (see figure 2.5). The total mass of the impactor should be (5000 ± 50) g and the kinetic energy on impact is (50 ± 1,5) J. The anvil, shown in figure 2.5b, should be made of polished steel with the dimensions l_1 equal to (190 ± 20) mm, l_2 equal to (100 ± 2) mm and a radius, r_1, of (150 ± 5) mm. The anvil should be attached to a load cell in order to measure the force transmitted during the impact.

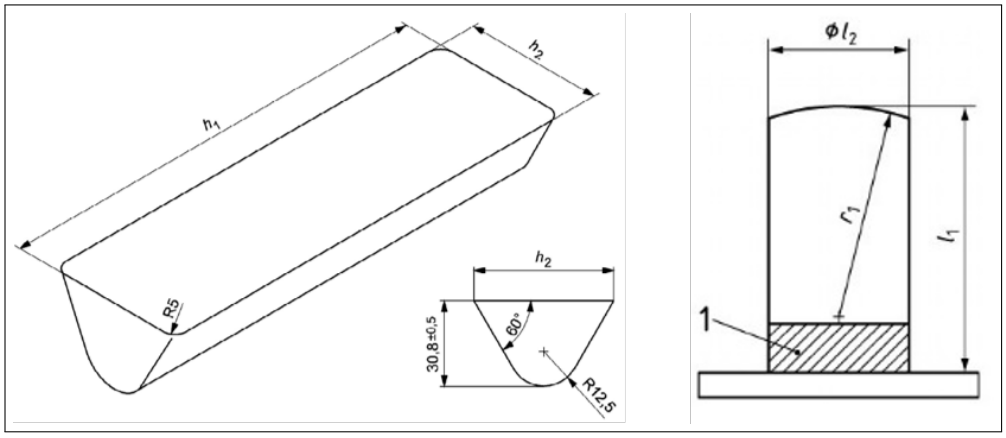

Figure 2.5: a.Kerbstone impactor b.Anvil [32]

Impact drop-tests should be performed at the inflated time declared by the manufacturer and each protective zone should be tested three times. A test result (pass) is considered positive if the results of each single impact is possitive. According to the force transmission values obtained during the test, the Standard EN 1621-4 established two possible levels of protection for a pass airbag protector: level 1 or level 2. The thresholds values of force transmitted of each level to classified a pass protector are exposed in figure 2.6.

	Level 1	Level 2
Overall Mean value	≤ 4,5 kN	≤ 2,5 kN
Single strike	≤ 6 kN	≤ 3 kN

Figure 2.6: Levels of protection according to EN 1621-4 [33].

2.4 Compression Criterion

The Compression Criterion tries to predict the injury severity derived from frontal chest impacts based on the measurement of the thorax deflection. The development of this criterion is based on the experimental work carried out by Kroell *et al.* [52]. In their experiments, Kroell *et al.* subjected a set of unembalmed specimens to dynamic, anteroposterior blunt loading of the thorax. The force was applied at the midsternum in the horizontal direction by a rigid impacting mass with a diameter of 15.24 cm moving at constant velocity (see figure 2.7).

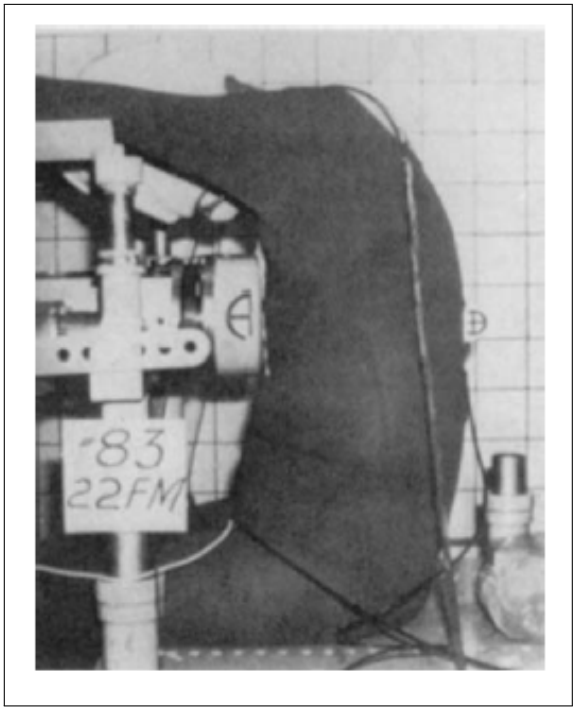

Figure 2.7: Cadaver test to apply an anteroposterior load to the thorax[52]

Responses to the impacts in terms of force-time and deflection-time were measured in order to find the injury tolerances and mechanical response of the thorax. Figure 2.8 shows the forces versus deflection crossplots obtained from some tests.

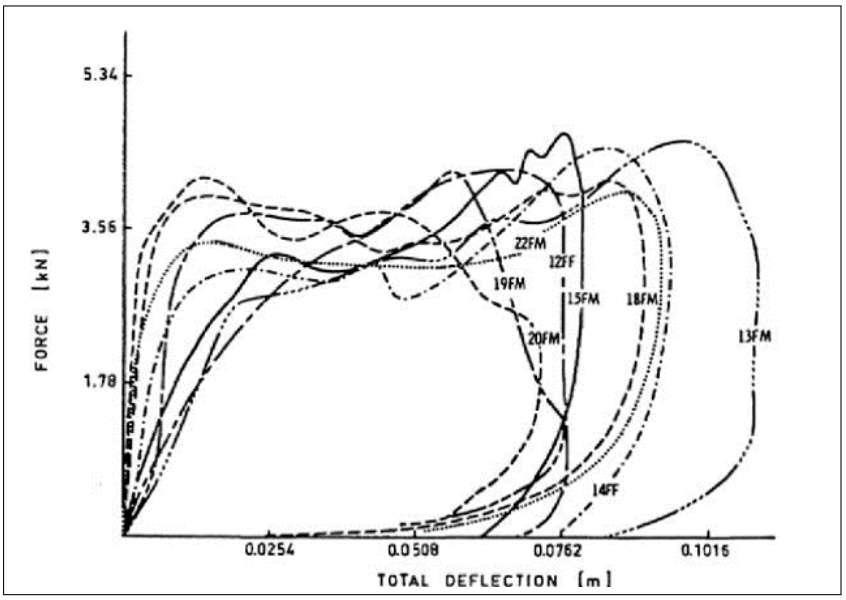

Figure 2.8: Force-deflection results from the experiments done by Kroell *et al.*[52]

In their study, Kroell *et al.* found a linear relationship between AIS and chest compression. This AIS correlation is based on skeletal injuries because the tests were done on unembalmed cadavers. The correlation is expressed in the next ecuation 2.1.

$$AIS = -3.78 + 19.56C \tag{2.1}$$

Where C is the chest compression divided by chest depth. As an example, for a 50th percentile male with a chest depth of 230 mm, a deflection of 69 mm (30% compression, C=0.3) will result in 2-3 ribs fractures. Similarly, for a compression of 40%, the AIS would be 4. The next table (Table 2.1) summarizes the linear relationship between chest compression and AIS.

No. of rib fractures	AIS	% Compression	Deflection (mm)
1	1	24	55.2
2 - 3	2	30	69
4 or more	3	35	80.5
Flail chest	4	40	92
Bilateral flail chest	5	45	103.5

Table 2.1: Linear relationship between chest compression and AIS severity [65].

Several authors proposed injury risk curves for different population [60, 74] and surrogate [89] based on the thorax deflection criterion. Figures 2.9 and 2.10 show some of those curves.

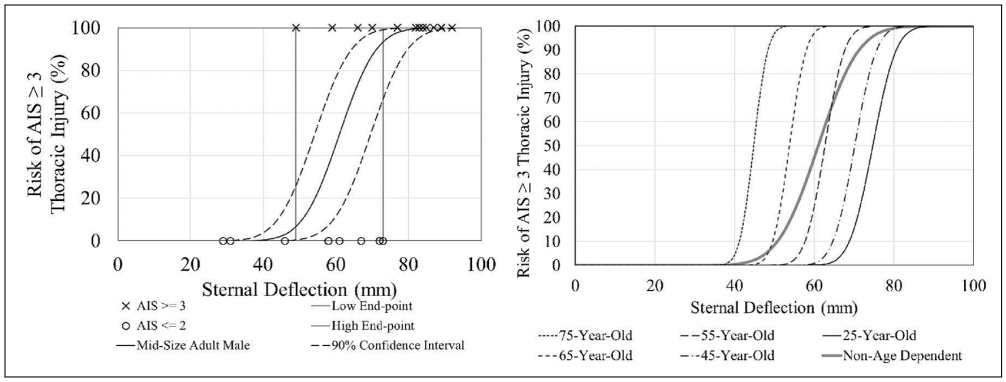

Figure 2.9: Non-age dependent risk curves for AIS $\geq$ 3 injury [60] and age dependent risk curves for AIS $\geq$ 3 injury [74] produced by distributed, anterior impacts to the thoraces of mid-size males.

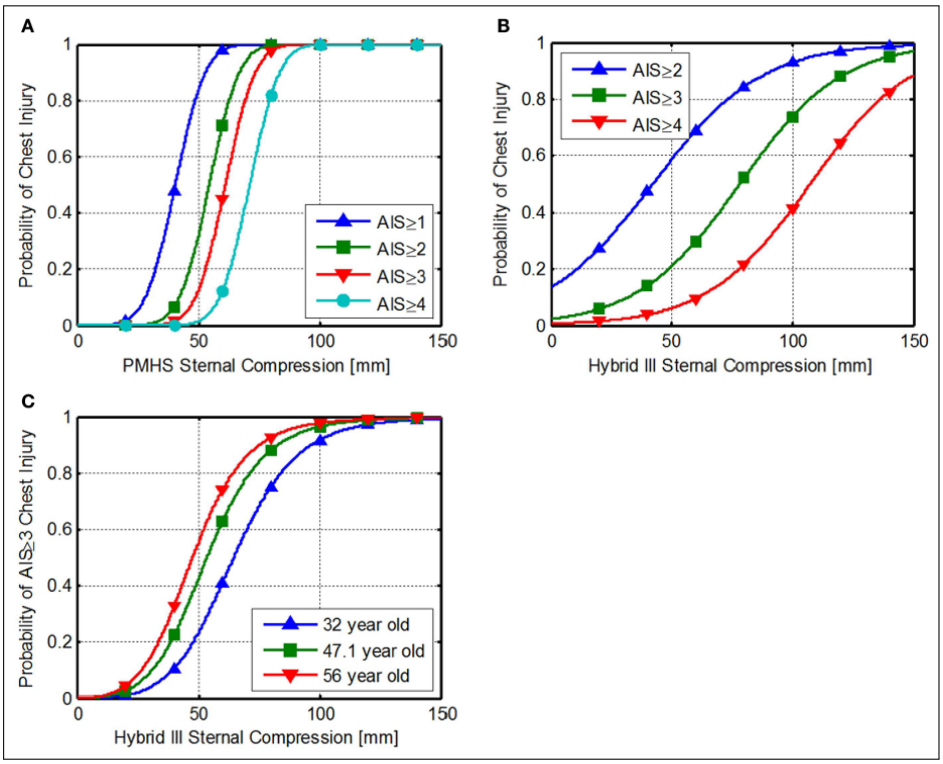

Figure 2.10: Sternal compression injury risk. (A) Injury risk functions developed by Mertz et al. (1997) [60], (B) NHTSA FVMSS 208 injury risk functions (NHTSA, 1998), and (C) NHTSA NCAP chest injury risk by age (NHTSA, 2008) [89].

2.5 Viscous Criterion

The viscous criterion (VC) is an injury criterion that considers the rate-dependency and compression-dependency of the soft tissue injuries (see equation 2.2). The VC value (m/s) is the maximum product of the momentary product of the thorax deformation speed and thorax compresion. Both of them are determined by measuring the rib deflection (side impact) or the thorax deflection (frontal impact):

$$VC = V(t) \times C(t) = \frac{d[D(t)]}{dt} \times \frac{D(t)}{b} \tag{2.2}$$

where *V(t)* is the velocity of the deformation calculated by differentiation of the deformation *D(t)*, and *C(t)* denotes the instantaneous compression function, which is defined as the radio of the deformation *D(t)* and the initial torso depth b [83]. VCmax of 1.3m/s was found to correspond to a 50% probability of thoracic AIS+3 while VCmax of 1.3m/s to a 25% probability of AIS+3. Viano *et al.* [97, 54] also proposed a VCmax based injury risk curve for AIS 4+ severity (see Figure 2.11).

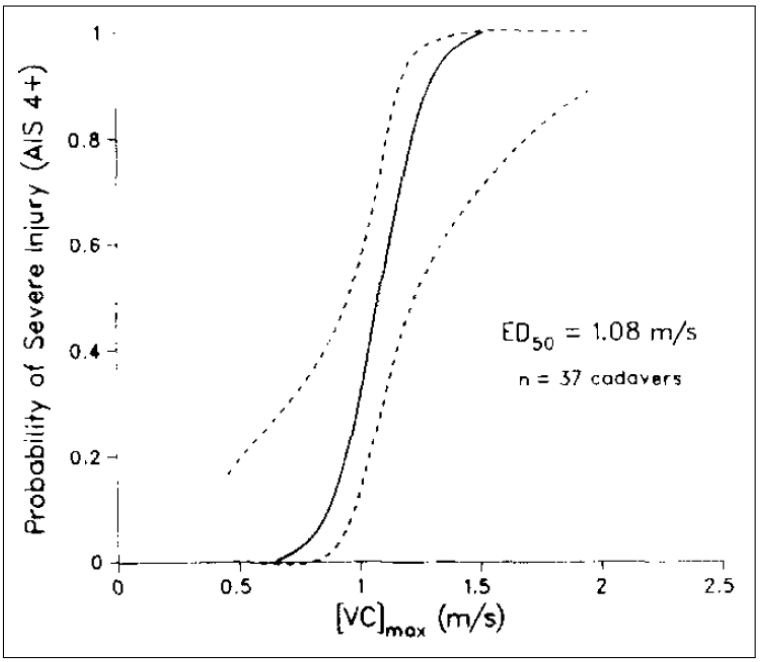

Figure 2.11: Risk of severe thorax injury as a function of the maximu viscous response for frontal impacts [97].

To correlate the internally measured Viscous response to an externally measured one, which correspond with the measurement on a Hybrid III dummy, Viano *et al.* defined the following expression (equation 2.3):

$$VCext = 1.3 \times VCint \tag{2.3}$$

2.6 LMU accident database

The LMU-accident database is a collection of accidents and injuries data from autopsied traffic fatalities. The database is financed by the Institute of Legal Medicine in Munich and managed by the department of Biomechanics and Accident Analysis. The data collection started in 2004 and is still going on and its geographical coverage is localized in the region of Southern Bavaria. In the period of time between 2004 and 2014, approximately the total number of accidents recorded were 1000, among them around 160 were motorcycle accidents. The specific data selection is focused on road traffic accident or accident with transport vehicle finished in fatality. Every accident recorded is exhaustively documented with police report, analytical accident report, autopsy report and other possible additional documents like pictures and alcohol/drugs reports increasing the number of variables collected per accident up to 950. This database was deeply analyzed attending specially to the thorax injuries by Andreas Thalhammer in his PhD Thesis [92] with the purpose of determining adequate impact conditions for the following evaluation of the effectiveness of airbag thorax protectors. Therefore, those impact conditions should be representative of the most frequent accidents recorded into the database and as close as possible to real situations accident situations. Firstly, all cases where classified attending to two criteria simultaneously: the normal component to the impacted obstacle of the impact speed and the radius of the impacted object. Then, this classification was filtered in order to consider only those accidents in which an AIS2+ thorax injury was reported. In the analysis of the filtered accident data, three interval areas or clusters were identified as basis for the study of airbags protectors due to the concentration of several accidents under these impact conditions (See table 2.2).

	Velocity	Object radius
Cluster 1	20 - 40 km/h	0.05 - 0.1 m
Cluster 2	50 - 70 km/h	0.05 - 0.1 m
Cluster 3	40 - 60 km/h	0.2 - 0.3 m

Table 2.2: Clusters obtained from the accident analysis of the representative impact conditions for the airbag performance analysis

The first cluster identified were the accidents occurred within an impact against an object with radius between 0.05 m and 0.1 m at a range of velocity from 20 km/h to 40 km/h. The second area with several accidents recorded comprehends those fatalities also occurred because of an impact against the same object radius as in the first cluster but with a higher impact velocity (50 km/h to 70 km/h). The last cluster includes all those accidents happened with an impact velocity between 40 km/h and 60 km/h against an obstacle with a radius of 0.2m to 0.3m. Those clusters were selected as the representative impact conditions for the analysis of the effectiveness of airbag protectors.

Chapter 3

Modelling and characterization of a frontal thorax airbag finite element model

This chapter explains the creation of a finite element model of a frontal thorax standard airbag according to the main parameters of a real standard airbag protector available in the market. The characterization of the model was conducted comparing simulation results of the FE airbag model with the performance of a real airbag in different drop tests.
The model here presented is used in the next chapter as a representative model of a current standard airbag for the protection the frontal thorax and the evaluation of its performance in a realistic impact scenario.

3.1 Methodology

The objective of the work presented in this chapter is to develop a FE model of a thoracic frontal airbag representative of a current state of the art standard airbag protector. In order to obtain the main parameters of a real airbag, a protector available on the market was acquired and tested. The product chosen is an airbag jacket composed by two parts: one airbag for the thorax and another bag for the back. Both airbags are inflated independently because each one is equipped with its own gas bottle and both of them are certified according to the standard EN1621-4. This airbag system was selected in comparison with other products on the market because of its activation simplicity. In this case the airbag is mechanically activated by pulling a cable, making possible to activate the inflation without triggering the airbag or without manipulating any electronical algorithm. Once inflated, the airbag reached a thickness of 8.5 cm. The test samples were acquired in a comparable manner to that a consumer rating organisations acquiring their samples.

Figure 3.1: Original airbag jacket and its correspond back airbag

The created FE airbag model is composed by two identical inflatable elements. Each inflatable element is 370 mm length and 160 mm width and it is constructed by two components. The first one delimits the external geometry and defines the content volume and the second consist in two straps limiting the thickness of the inflatable element (see first illustration on figure 3.2). Those dimensions cover the whole frontal thorax of the GHBMC (see figure 3.2). Both parts are implemented with the textile material MAT-FABRIC (034) and a Young's modulus of 0.1 GPa. Once inflated, the final thickness of the airbag is 8.5 cm.

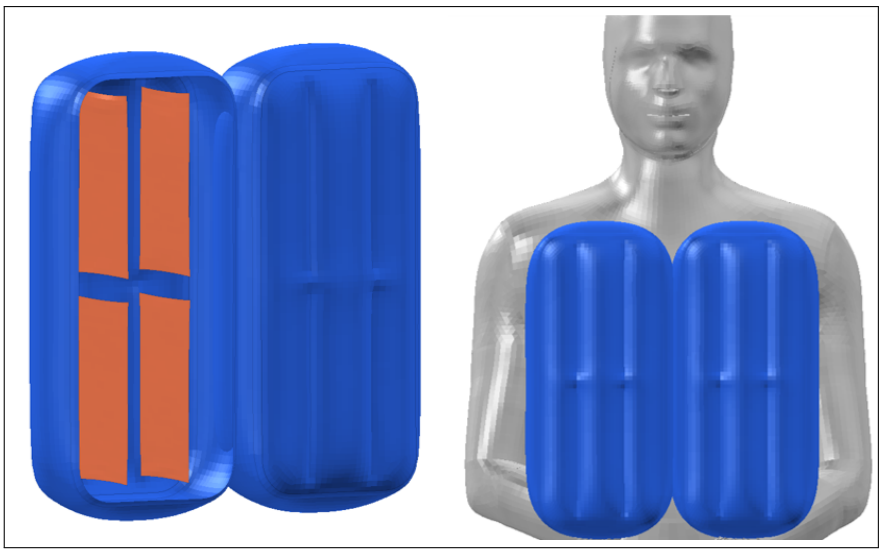

Figure 3.2: Airbag FE model and its position by GHBMC model

In order to understand the performance of the real airbag, several tests were conducted in two different stages. Firstly, a group of drop-tests were conducted to determine the pressure of the airbag after its activation and inflation. Secondly, another group of drop-tests were made to determine the response of the airbag under severe impact conditions.

In all experiments, the back airbag of the jacket was tested because it offered a more extensive and stable impact surface (see figure 3.1). All the test conducted were numerically replicated in simulation reproducing the same boundary conditions. The two experimental stages are described in the following.

3.1.1 First experimental stage: Working pressure

The working pressure of the airbag is usually not specified by the manufacturer. Thereby, the main objective of this stage was to find this value to characterize the FE model. For that purpose, using a small drop-tower (1.2 m height) and a 0.5 kg half sphere aluminum striker equipped with an accelerometer, a group of tests were conducted to obtain the airbag impact response at different pressure levels (see figure 3.3).

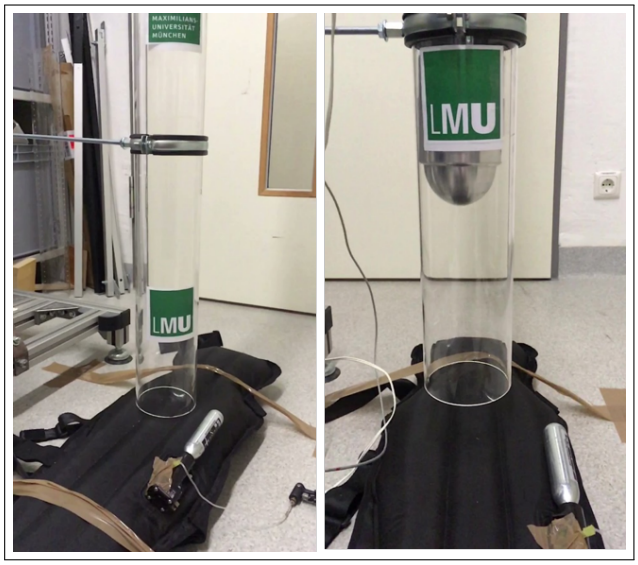

Figure 3.3: Small drop-tower used for obtaining the airbag working pressure

Firstly, the airbag was tested after its activation and its quick inflation with the gas from its own bottle (CO2) at different moments. Afterward, the airbag was inflated with air up to different levels of pressure from 0.2 to 0.8 bar. Therefore, the FE model of the airbag was initially calibrated with air gas properties to match the experimental response. Afterwards, following ideal gas law $PV = nRT$, the airbag FE model was characterized with carbon dioxide gas properties to obtain a similar impact response. Finally, both impact response curves were compared to determine the working pressure.

3.1.2 Second experimental stage: Severe impact conditions

In order to obtain the airbag response under severe impact conditions, two series of tests were conducted using two heavier half spherical strikers: 8 kg and 10 kg. In both cases,

the airbag was inflated at its working pressure and the drop impacts tests were conducted at an impact speed of 3.5 m/s, 4.5 m/s and 5.5 m/s (see figure 3.4). The results of these rows of experiments were used to evaluate the appropriate response under severe impact conditions of the FE model as a simplified representation of an standard airbag available on the market.

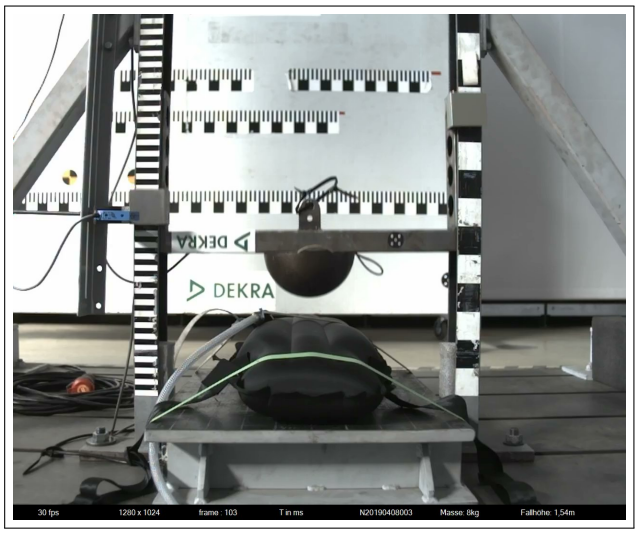

Figure 3.4: Drop-tower used for obtaining the airbag response under severe impact conditions

In addition to the simulations of the stage 1 and 2 experiments, the impact attenuation test established by the European Standard EN 1621-4 [33] was also numerically reproduced to check if the developed airbag FE model would pass an hypothetical standardization test.

3.2 Results

The airbag response at the different experimental stages as well as its comparison with the numerical response of the airbag FE model is exposed in the following sections.

3.2.1 Results: Working pressure

From the analysis and comparison of the test conducted with its own bottle gas at unknown pressure and the subsequent test conducted with well-known pressure values using air, it was concluded that the real airbag is initially inflated at a pressure between 0.6 and 0.8 bars (see figure 3.5). Lower pressure values were measured in other test impacts conducted several seconds (later than 5s) after the inflation. Therefore, the FE model was then characterized with a pressure of 0.65 bar. Figure 3.5 shows the acceleration response

experimentally obtained for different pressure values together with the numerical response obtained for an inflated pressure of 0.65 bar. The simulations were performed at one inflatable element.

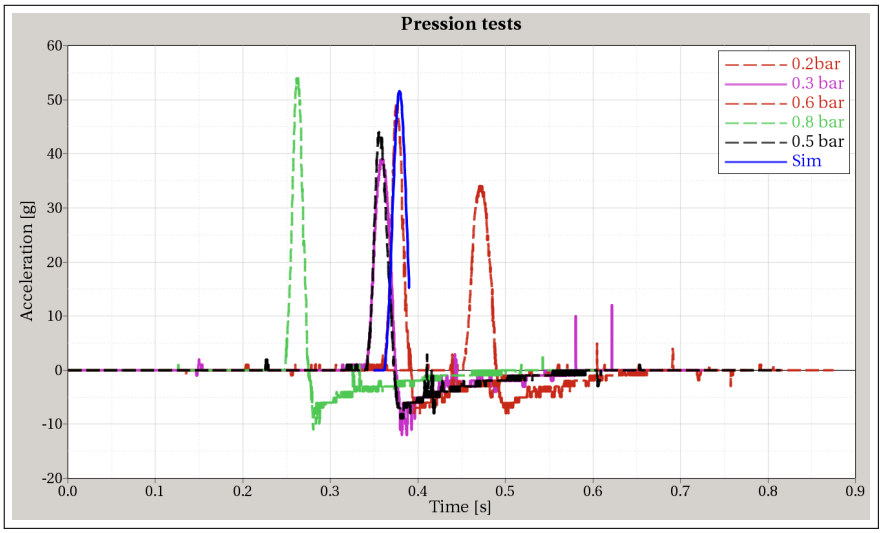

Figure 3.5: Airbag response for different pressure values compared to the simulation result

As it was mentioned before, air was used to determine the working pressure of the airbag instead of carbon dioxide, gas which is usually used to inflate the airbag. Similar response were obtained characterizing the airbag FE model with air or carbon dioxide gas properties (see figure 3.6).

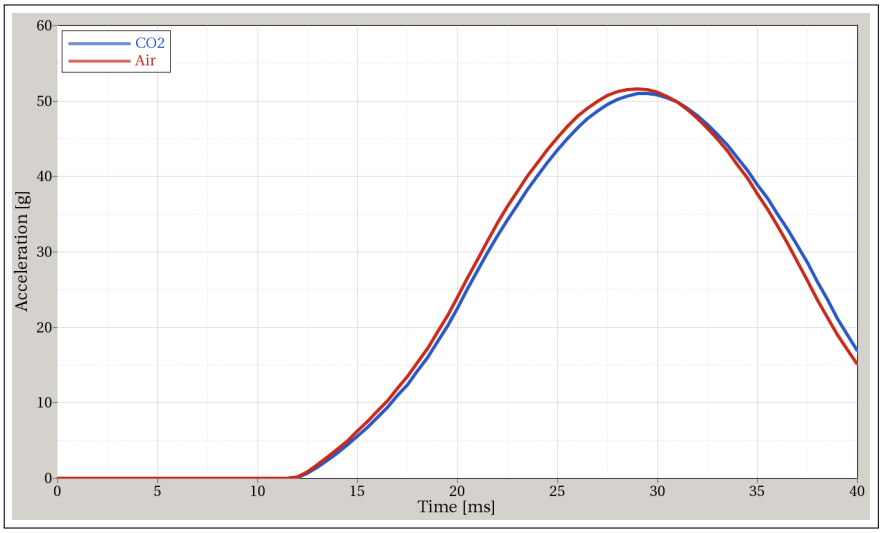

Figure 3.6: Numerical airbag response inflated with air or carbon dioxide

3.2.2 Results: Severe impact conditions

The experimental setup and the series of experiments described in the stage 2 were numerically replicated for one inflatable element in order to evaluate the airbag FE model under severe impact conditions. Figures 3.7 and 3.8 show respectively, for the cases of 8kg or 10 kg striker, the FE model response for the three considered impact speeds in comparison with the corresponding test results.

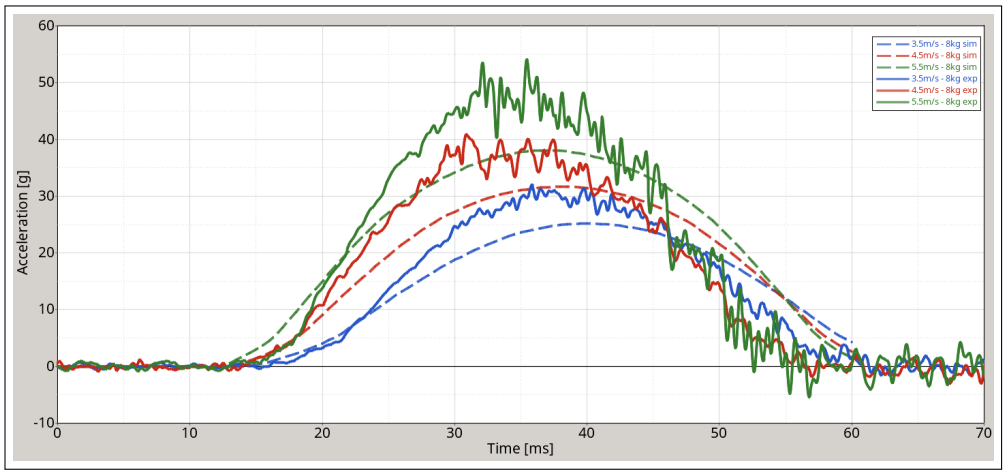

Figure 3.7: Numerical airbag response inflated with air or carbon dioxide

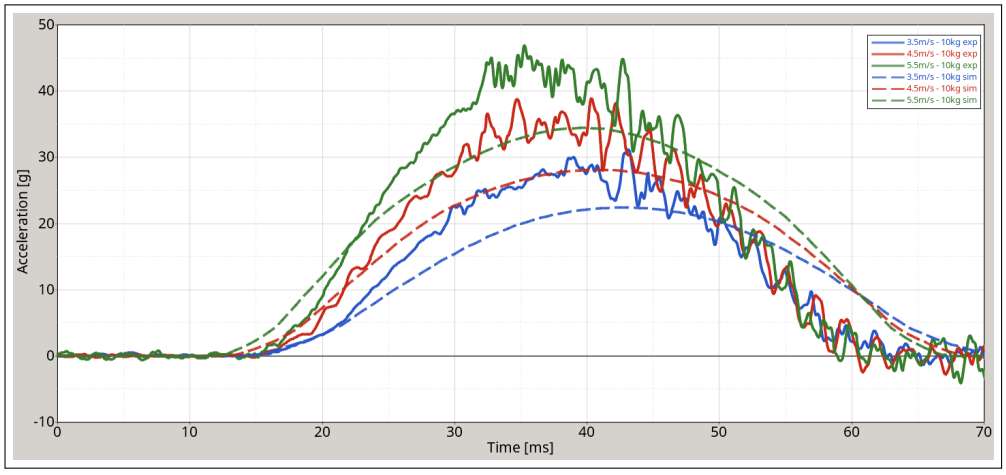

Figure 3.8: Numerical airbag response inflated with air or carbon dioxide

Airbag FE model response to the impact conditions established by the standard EN1621-4 is presented in figure 3.9 and the maximal force transmitted corresponds with the force value reported by the manufacturer.

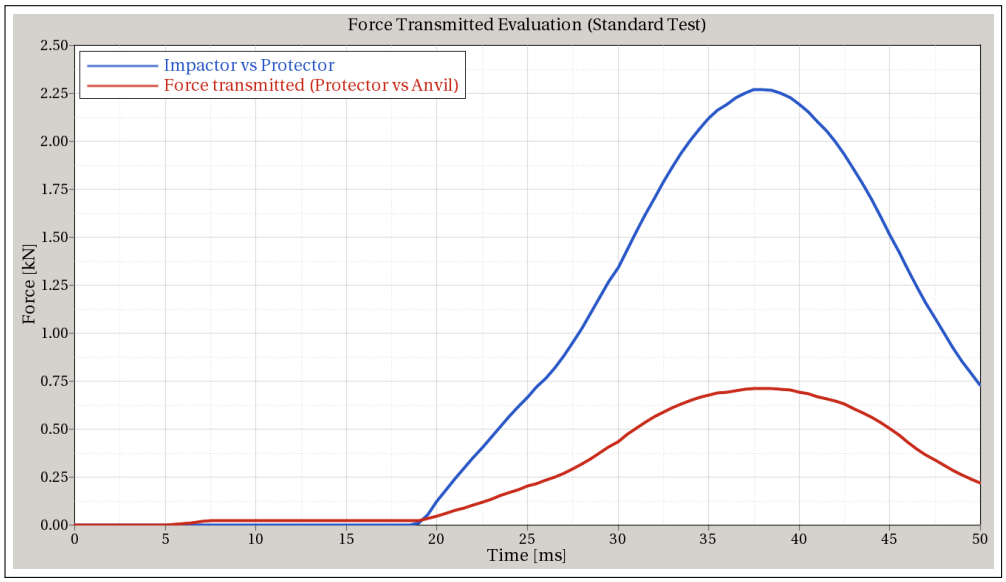

Figure 3.9: Response of the airbag FE model to the standardization test

3.3 Discussion

This chapter explained how a FE model of an airbag for motorcyclists' was modelled and characterized for the simulation of frontal impacts at the thorax. The airbag FE model created is based on the inflated thickness and pressure obtained experimentally from a real airbag device available in the market. According to Serre *et al.* (2012) [85], an intervention time of 4 s after the activation is recommended to prevent trunk injuries. Thereby, a pressure between 0.6 and 0.8 bar was assumed as working pressure of the airbag in case of accident and the lower pressure values obtained experimentally later than this intervention time were discarded. A series of drop-test were conducted using impact masses of 8kg and 10 kg in order to obtain the performance of the real airbag under severe impact conditions. The numerical response of the airbag FE model was compared with those experimental measurements showing satisfactory results. The simulation of those test conditions showed a similar response of the airbag FE model and in consequence it was considered a representative model of a current state of the art airbag's performance.

Despite the realistic response and behaviour of the airbag FE model, some limitations during this process should be considered. Firstly, the standard test procedure indicated in the standard EN1621-4 [33] was only numerically calculated. Peak values of force transmitted were compared with those values reported by the manufacturer within his EN1621 certificate. Secondly, the shape of the FE model differs from the original one observed at the real airbag. It was not possible to obtain a numerical geometry of the airbag and consequently the airbag could not be exactly replicated. Based on the results obtained by Marconi *et al.* (2018) [59], the relation between inflation pressure and inflated thick-

ness determine the chest deflection during an impact. Therefore, this study was primarily focused on reproducing this pressure/thickness combination of a real airbag jacket. However, a possible influence of the airbag form should not be discarded and further studied. Thirdly, the slightly higher peak value measured together with the shorter duration of the acceleration response indicate a stiffer behaviour of the real airbag than the FE model. A possible explanation could be that the Young's modulus used for characterizing the airbag material might not correspond with the elasticity properties of the real airbag material. Those considerations indicate also an influence of the airbag textile material in the energy absorption and a sensitivity study could be conducted to quantify this effect with more detail. Another limitation is that the severe impact conditions tested do not correspond with those observed in accident statistics in terms of impact velocity and mass resulting in different kinematic energy involved in the impact. An impact test accounting a maximum kinetic energy of 151.25 J (5.5 m/s, 10 kg) was conducted while in some accident analysis works is reported that a moving rider (at least 23.4 kg corresponding with the thorax) impacts a fixed object at a velocity of 25 km/h (6.94 m/s) [6], [14] which implies a minimum kinetic energy of 564.24 J. However, the impact energy generated during the test conditions presented in this work were higher than the energy provided (50 J) in the test procedure of the standard EN1621-4 [33].Despite the discussed limitations, the developed numerical airbag model is seen to be appropriate for being applied in subsequent steps, as the focus of its application is the simplified representation of an airbag realistically representing today's products on the market.

Chapter 4

Protection potential of current thorax airbag devices

4.1 Introduction

The risk of being involved in a fatal accident is higher for Powered Two Wheeler (PTW) users than for car occupants [16] and motorcyclists are considered as vulnerable road users because of their limited structural protection. Traffic accidents involving motorcyclist and moped users account for 28% [98] of all world traffic fatalities and the 17% of the traffic deaths in the European Union [36]. Only in Germany, 619 riders dead and 10220 PTW users were severe injured in 2018 [28]. Low extremities are the most frequent body regions injured, but the thorax, together with the head, is the most severely body region injured in motorcycle accidents [63, 64]. In the Motorcycle Accident In-Depth Study (MAIDS) report published in 2008 [58], thorax was pointed out to be the fourth most common region injured but with the highest rate of MAIS3+ injuries (more than 50%). The importance of thorax injuries in motorcyclists' fatality was also signed by Serre *et al.* (2012) [85] in his epidemiological and accidentological analysis about motorcyclists' impact against light vehicles. In this study, it was concluded that the necessity of protecting the trunk should be considered as important as the protection of the head, signing the protection of the thorax as a significant issue in PTW users passive safety.

Personal Protective Equipment (PPE) is the main passive safety system for motorcycle riders which can help in the mitigation and prevention of injuries in case of accident. The benefits of wearing a helmet and its effectiveness in the reduction of head injury severity has been demonstrated [26, 56]. Other studies concluded that protective clothing can prevent or reduce light injuries, specially soft tissue injuries such as cuts and abrasions [27] but they might not be necessary effective against more severe injuries like fractures [7, 10]. Concerning thorax region, Thollon *et al.* (2008) [93] presented the first study indicating the possible benefits of an airbag protector for the mitigation of thoracic injuries. After

the numerical simulation of impact tests with cylindrical impactors, Thollon *et al.* (2008) [93] pointed out the capacity of the airbag of reducing the loading sustained by the ribcage providing the partially dissipation of the impact energy. In alignment with these findings, Capitani *et al.* (2010) [23] remarked not only the energy dissipation capacity but also the energy distribution effect as a benefit provided by inflatable protectors. After the modelling in Finite Element and validation of an airbag protector according to the EN1621-4 [33] test conditions, Marconi *et al.* (2018) [59] simulated a frontal test used for the certification and calibration of dummies and determined that chest deflection after impact depends on the relationship between inflated airbag thickness and airbag pressure. However, the behaviour and effectiveness of an airbag protector for the frontal thorax under the impact conditions of a real impact scenario are still in study.

Several works analysed the possible accident scenarios involving PTW users reporting collisions with occupant cars as the most frequent impact situation [55, 58]. Thorax was identified as the most injured body region by Piantini *et al.* (2016) [69] in his analysis about 40 collisions between PTW and passenger cars. Similarly, Fredriksson and Sui in their in-depth accident analysis published in 2015 about fatal PTW crashes in Germany [42] and about accidents also in Germany with severe injured outcome published in 2016 [43] signed thorax as the second most frequent body region for fatal injuries and the first for severe injuries. In both studies, passenger cars were remarked as the main injury source followed by surrounding objects, specially trees, for the case of fatal injuries. Since the necessity of reducing the severity of motorcyclist thoracic injuries became an evidence [15], the definition of motorcyclists thorax impact conditions such as impact velocity and impact obstacle dominating in crash scenarios became also more relevant in order to evaluate the effectiveness of airbag jackets and the development of new safety devices.

Based on the data collected in a dedicated survey of PTW accidents performed in the trauma centres of Lyon and Marseille and after the simulation of several PTW crashes in a multibody platform, Cherta Ballester *et al.* (2019a) [14] proposed two impact levels of protection for the thorax representative of the most impact scenarios analysed. The first proposed level should protect the frontal thorax from an impact of 7 m/s and the lateral from an impact of 5 m/s. The second level recommended protection from am impact of 13 m/s for both areas. In parallel, the research project "Optimierte Schutzkleidung für Motorradfahrer" [17] funded by the Traffic Insurance Association in Germany (UDV) tried to define realistic impact conditions for the evaluation of frontal thorax airbag protectors in terms of impact velocity and obstacle radius. Based on a in-depth analysis of its own accident database (UDB) and the Institute of Legal Medicine from the University of Munich (LMU) database, authors identified an impact against a structural part of a passenger car (mean object radius of 0.075 m) at two different mean impact velocities (25 km/h and 60 km/h) and an impact at a velocity of 50 km/h against a surrounding obstacle like a tree with a mean radius of 0.25 m as the most frequently recorded crash scenarios.

The diversity of wearable airbag protectors available in the market [35] together with some limitations recently published of the current standard method for motorcyclists' airbags for assessing protection in crash scenarios [11] led to the necessity of understanding the performance of such airbag devices under realistic accident impact conditions and the evaluation of their effectiveness in thoracic injury mitigation. Some authors tried to analyse this airbag behavior experimentally like for example Serre *et al.* (2019) [84] who conducted crash tests with PMHS to evaluate real airbag effectiveness. Other studies, tried to evaluate airbag jacket performance by a method extensively used in automotive for passive safety assessment [104]: numerical simulations with Finite Elements Human Body Models (HBM).

Numerical models of human body has been previously used for the assessment of PPE, specially motorcycle [38] and bicycle helmets [62] and more recently neck braces [61]. Concerning thorax region, Cherta Ballester *et al.* (2019b) [25] presented an evaluation methodology of airbag protectors using the HUman Model for Safety (HUMOS II). In his study, Cherta Ballester *et al.* simulated frontal thoracic impacts using an equipped and unequipped with airbag HUMOS II, for three different velocities (5 m/s, 7 m/s and 9 m/s) combining with three different impactor shapes (plate, pillar and kerbstone). Following the findings of Bauer *et al.* [17] in motorcyclists statistics, an analysis of the frontal airbag effectiveness was also conducted in the research project "Optimierte Schutzkleidung für Motorradfahrer". In this case, the realistic impact conditions previously mentioned were simulated using the Global Human Body Model Consortium (GHBMC) and a finite element model representative of a certified airbag protector available in the market at the moment. The study presented in this chapter is in alignment with the works referred to above regarding the use of Finite Element HBMs for the evaluation of motorcyclist PPE.

The objective of this chapter is to analyse the ability of injury mitigation of a representative current standard frontal thorax airbag under realistic accident impact conditions. For that purpose, a set of frontal impacts at different impact velocities were simulated using the GHBMC 50th percentile male pedestrian v1.5 and the FE model representative of a frontal standard airbag available in the market explained in chapter 3. In every simulation, the HBM at a determined velocity would impact frontally a fixed cylindrical object representing a possible real obstacle depending on its radius. The number of rib fractures at the rib cage obtained on the basis of an ultimate strain analysis at the cortical and trabecular rib bone together with the measurement of the chest deflection and the application of the Compression Criterion would determine the injury mitigation effectiveness of the airbag under those specific impact conditions. The evaluation of the airbag protection potential is conducted by the comparison of the results of the same impact situation simulated with and without protector. The impact conditions presented in the research project "Optimierte Schutzkleidung für Motorradfahrer" [17] are the basis for the numerical simulations here computed and the results here presented are formulated as a deeper analysis and a complementary extension of those existing in this project final report.

4.2 Methodology

4.2.1 Definition of impact boundary conditions

The conclusions obtained from the accident statistical analysis presented in section 2.6 are the basis to determine the impact conditions for the numerical study. From this analysis, three interval areas or clusters were identified as those with a higher concentration of severe accidents with thorax injuries. These clusters signed three different situations to study in numerical simulations: a low velocity impact against a structural part of a passenger car, the same impact but at a high velocity and a high velocity impact against a big obstacle which could be, for example, a tree [6]. In addition to these three situations, a fourth situation was added to the study: a very low velocity impact against a rigid flat surface. This load case would be representative of an impact against the ground due to a fall of the rider from his own motorcycle. In terms of impact conditions it would occur at 17 km/h, equivalent to a 1.15 m fall, similar to the impact velocity tested in the standard EN 1621-4 for motorcyclists' airbag protectors [33]. Table 4.1 summarizes the corresponding impact conditions of each cluster and defines the boundary conditions frame for the numerical study of the protection potential of thoracic frontal airbags.

	Velocity	Object radius
Cluster 1	20 - 40 km/h	0.05 - 0.1 m
Cluster 2	50 - 70 km/h	0.05 - 0.1 m
Cluster 3	40 - 60 km/h	0.2 - 0.3 m
Cluster 4	17 km/h	∞ (flat object)

Table 4.1: Intervals of impact boundary conditions of each cluster.

In order to obtain a global vision of the behavior of an airbag protector attending to its protection effectiveness, some combinations of impact conditions were selected within the intervals of velocity and object radius considered by each cluster. Each cluster is defined by their limit values in terms of object radius and impact velocity. These limit values were numerically simulated and were subsequently analysed and the analysis is completed with the simulation of the mean combination of impact conditions. For example, regarding Cluster 2 (object radius from 0.05m to 0.1m and velocity from 50km/h to 70 km/h), a simulation combining every extreme boundary condition was conducted: impact velocity of 50 km/h and 0.05 m object radius, 50 km/h and 0.01 m, 70 km/h and 0.05 m and 70 km/h and 0.1 m, together with the simulation of an impact at 60 km/h against an object of 0.075 m radius. Applying this method of selection to all clusters, except for the case of Cluster 4 which is considered as a single case, a table of simulations was defined. Figure 4.1 shows all impact conditions analysed.

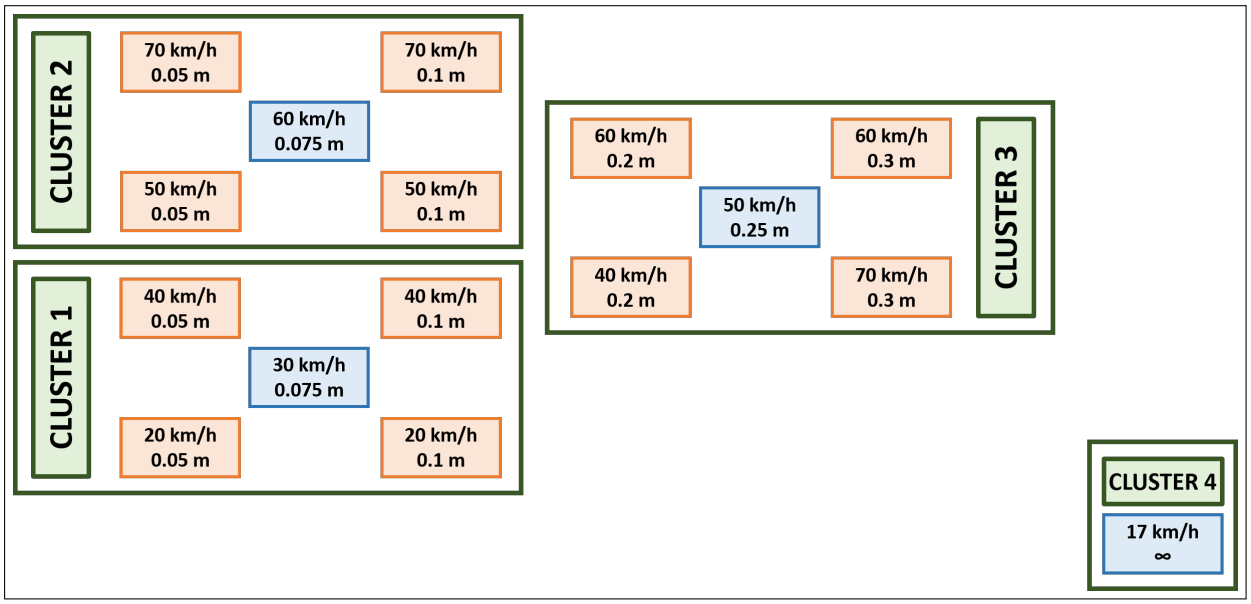

Figure 4.1: Impact boundary conditions, velocity (top) and object radius (bottom), selected at each cluster.

4.2.2 Numerical simulations

The evaluation of the effectiveness of an airbag thorax protector for motorcyclist was conducted using numerical simulations. A total of 72 FE simulations were launched to understand and determine the current protection potential and limits of a frontal thorax airbag. All simulations were conducted in LS-Dyna solver code using the human body model GHBMC M50 Detailed Pedestrian Version 1.5 [95]. The GHBMC M50 Detailed Pedestrian Version 1.5 is a current state of the art FE human body model formed by 1.25 million of nodes and 2.35 million of elements which compound its 1005 parts. The model represents the anthropometric data of a 50th percentile male with a height of 1.75 m and a weight of 77.5 kg. The geometry of the model was developed based on several MRI and CT scans obtained from a 50th percentile male volunteer.

Every accident situation was simulated twice. Firstly, it was simulated without any protector to assess the possible injuries derived from such an impact. Secondly, the same situation was simulated under the same boundary conditions using a FE model of a current standardized airbag protector to assess the capacity of the airbag device of avoiding or reducing the severity of the expected injuries. The standard airbag model was the same for all simulated cases and it was characterized to be representative of a current airbag protector available in the market. The FE airbag model used in this study consists in two inflatable elements with a total volume of 12 liters (6 liter each of them), a thickness of 8.5 cm and a pressure of 0.65 bar. How this standard airbag was modelled and validated is explained in chapter 3. The airbag was positioned to cover the whole frontal thorax of

the GHBMC pedestrian model (See figure 4.2).

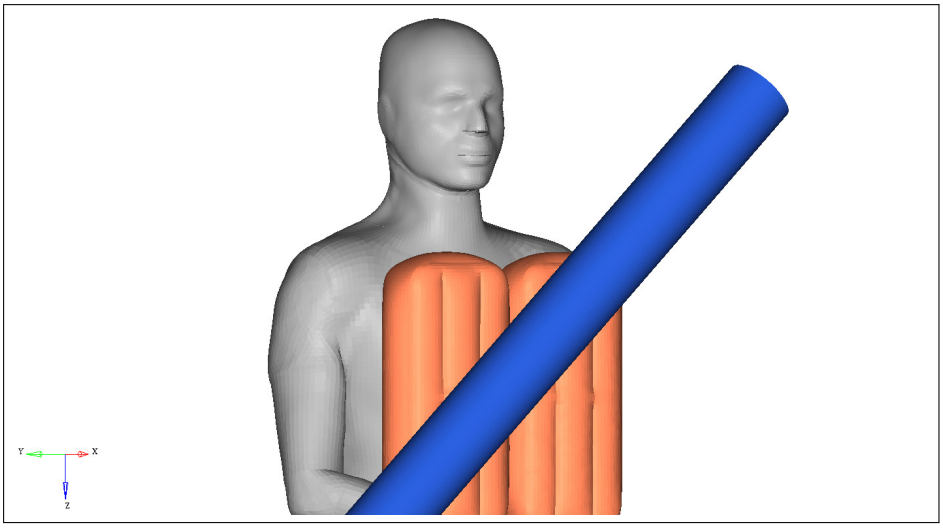

Figure 4.2: Simulation example with the GHBMC equipped with a FE airbag model.

Several FE cylinders were modelled as idealized obstacle for the impact simulations. Cylinders with a radius of 0.05, 0.075 and 0.1 meters were implemented to be representative of the obstacle considered in Clusters 1 and 2. Regarding Cluster 3, cylinders with a radius of 0.2, 0.25 and 0.3 meters were modelled to represent those kind of large impact objects. A rigid wall was chosen to represent the flat surface object in Cluster 4 simulations.

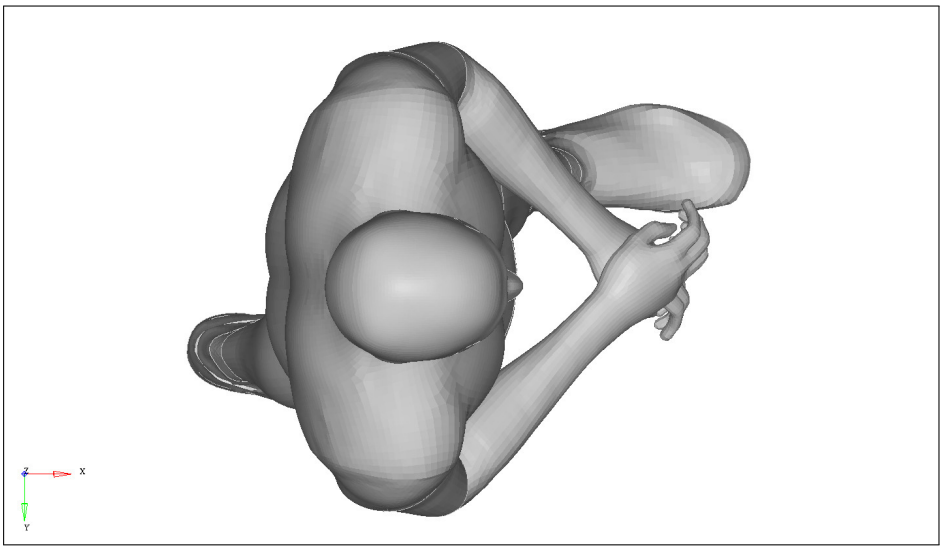

Figure 4.3: Initial position of GHBMC M50 Detailed Pedestrian Version 1.5

In all simulations conducted, some nodes at the ends of the impact objects were con-

strained and an initial velocity corresponding to impact speed was given to GHBMC in order to simulate a moving mass (75 kg, corresponding to 50th percentile human body [47]) impacting against a fixed obstacle. GHBMC pedestrian model is initially positioned in such a way that its arms are folded in front of the abdomen (See figure 4.3). As the main objective of this study is to evaluate the effectiveness of an frontal thoracic airbag protector, the contact between the parts corresponding to HBM upper extremities and the impact object as well as the contact between those parts and the airbag model were not implemented. The avoidance of potentially numerical errors at model parts which are not the focus of this analysis was considered in the decision. Other specifications of the simulations conducted are briefly explained hereunder attending to the size of the object:

Small radius object

Clusters 1 and 2 encompass an impact against a small radius object at two different severities: low speed and high speed impact. Cylinders with radius from 0.05 to 0.1 m were used in all simulations enclosed in these clusters. Due to the small radius of the impact object in comparison with the GHBMC thorax dimension, three different impact configurations were considered attending to the orientation of the obstacle: horizontal, vertical and diagonal. Vertical configuration is not considered as realistic as the other ones because in an crash against a completely vertical object, the first impact would happen at the head level and thorax would not be so severely loaded. As it was shown in Figure 4.4, the vertical object is positioned under the head to avoid this first impact and to evaluate directly hypothetical thorax injuries derived from such an impact. For Cluster 1 as well as for Cluster 2, 30 simulations were required to consider all boundary conditions in each case. Impact objects were positioned at mid-sternum height.

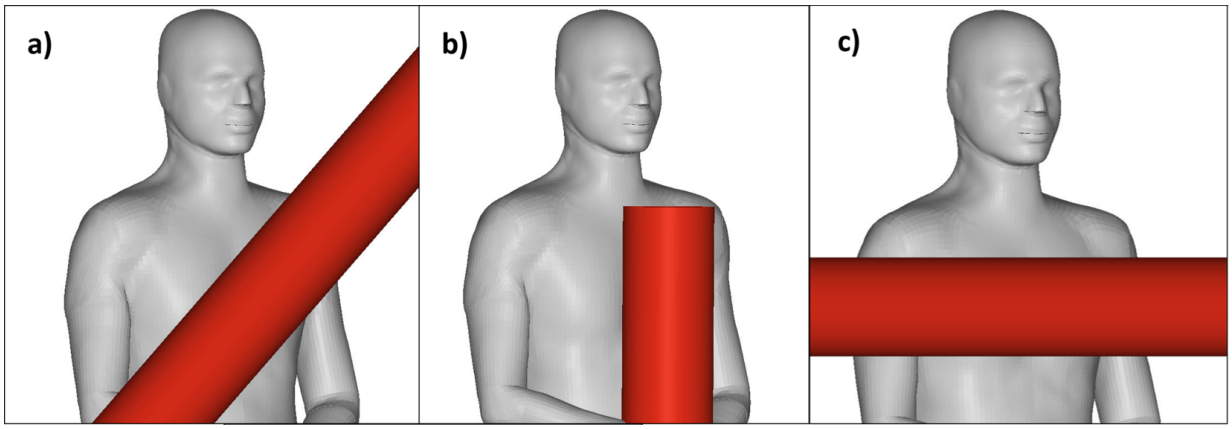

Figure 4.4: Impact configurations against a small radius obstacle.

Large radius object

Impact accident situations included in Cluster 2 occurred against a large radius object. Cylinders with radius from 0.2 to 0.3 m were used as obstacle in their corresponding simulations. The large impact surface of these obstacles cover the whole thorax of the human body. Thereby, only an impact against an obstacle horizontally oriented was considered (see Figure 4.5). Cylinders were positioned at mid-sternum height. Due to its large dimension and to avoid potential numerical errors on the parts corresponding to the HBM head, those parts were not included in the contact formulation.

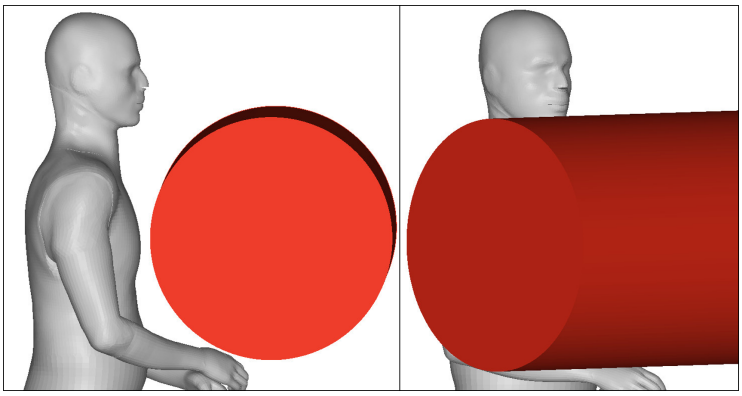

Figure 4.5: Impact configuration against a large radius obstacle.

Flat object

A flat object was used in Cluster 4 simulations. The object surface covers the whole thorax of the human body model and its movement its totally constrained (Figure 4.6).

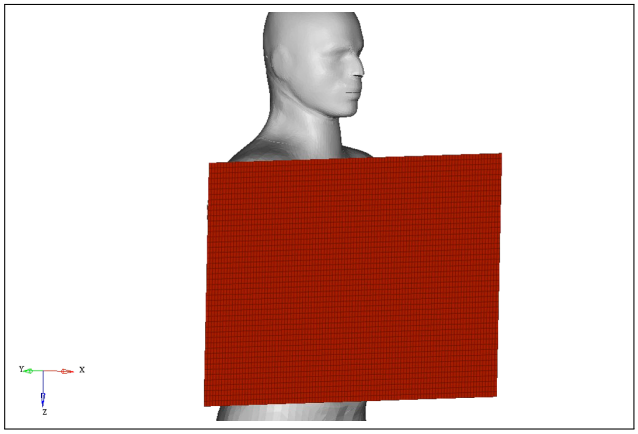

Figure 4.6: Impact configuration against a flat object.

All simulations were evaluated attending to the effects of the impact at the thorax region and the possible derived thoracic injuries. Two parameters were obtained: the number of rib fractures and the chest deflection. Chest deflection was defined as the variation of the distance between the midpoint of two nodes taken on the pectoral muscles and a node taken on the skin at the level of the center of the 8th thoracic vertebra (T8) [96, 73]. This method, originally implanted for the occupant version of GHBMC, was transferred to the pedestrian GHBMC by the selection of equivalent nodes. Figure 4.7 shows the selected nodes. The kinematic of node A was automatically calculated by the interpolation of nodes 4027556 and 4002148 kinematic using the LS-Dyna keyword *CONSTRAINED_INTERPOLATION*. Based on those chest deflection values, the Compression Criterion developed by Kroell *et al.* [57, 52], was applied to determine the predicted injury severity as AIS value. Additionally, a strain-based prediction of possible rib fractures was done. Ultimate strain values of 1.8% and 13% were set for the cortical and trabecular bone rib materials respectively [73].

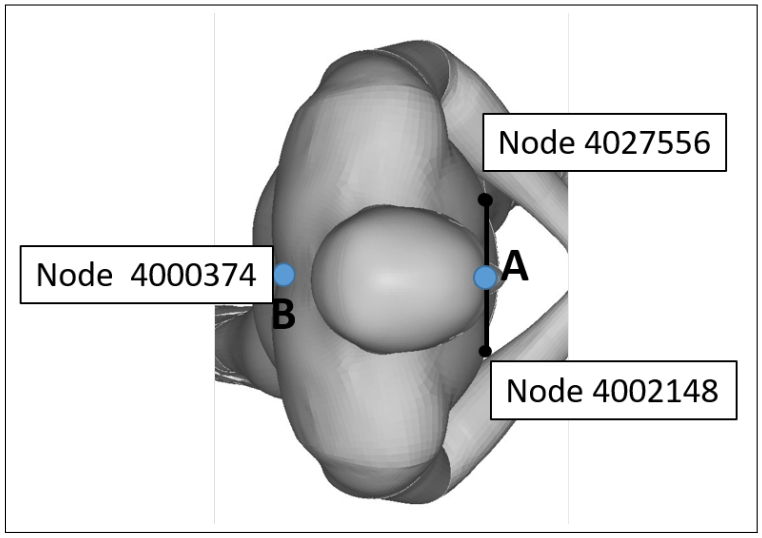

Figure 4.7: Selected nodes for the chest deflection measurement.

4.2.2.1 Analogy between a vehicle's structural part and the idealized impact object

The representation in a finite element simulation of the kinetics and dynamics of all elements involved in a complex motorcycle accident scenario could be very expensive in terms of computational time. Consequently, due to the high number of simulations needed (72 simulations in total), simplified impact objects were used to represent the real impact object reported in the accident database. A structural part of a vehicle or a tree was idealized in an impact cylinder dimensioning with its related representative radius.

To investigate the analogy between the idealized impact cylinder and a real impact object in terms of thorax injuries derived from a frontal impact, this study was completed with an additional simulation of an impact against the roof edge of a car. In this simulation, a moving GHBMC pedestrian model impacted with its thorax directly to the roof edge of a FE car model at a velocity of 30 km/h, see Figure 4.8. The model of the vehicle is a finite element model of a Ford Taurus developed by George Washington University National Crash Analysis Center (NCAC) and available at the National Highway Traffic Safety Administration (NHSTA) online FE models repository [66].

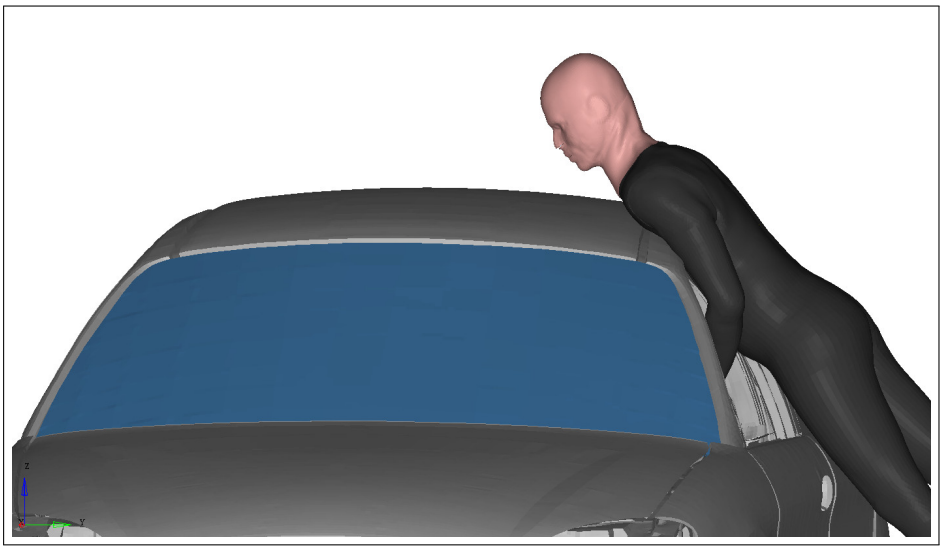

Figure 4.8: Impact against a vehicle's roof edge.

4.3 Results

In this part of the study, the results obtained from the numerical simulations are exposed. In total, 72 simulations were conducted to fulfil the analysis of the four clusters in order to obtain a global vision of the behavior of an airbag protector attending to its protection effectiveness in frontal thoracic impacts. The next sections expose in detail the results obtained from the numerical simulations of the mean combination of impact conditions in every considered impact configurations (blue boxes in 4.1) together with a summary of the main results obtained from those boundary conditions (orange boxes in 4.1) delimiting each cluster.

To simplify the explanation of the results, every single simulation is designated using a code reflecting its correspond cluster (CX), velocity in km/h (VXX), object radius in mm (RXXX), object configuration (D=Diagonal, H=Horizontal or V=Vertical) and the integration of the airbag in the calculation (Air or NoAir). Following this code, as example, the simulation of the situation enclosed in cluster 2 that corresponds to an impact at 70

km/h against an obstacle with a radiuos of 0.075 m and positioned diagonally without an airbag protector would be referred to as the simulation *C2_V70_R075_D_NoAir*.

Additionally to the results derived from the study of the four clusters, numerical results showing the analogy between the roof edge of a passenger car and the idealized impact cylinder used in this work are also presented.

4.3.1 Cluster 1

In cluster 1, the effects of an airbag protector in a low impact speed against a small radius object were analysed. To fulfil the study of all impact conditions and configurations included in this cluster (see figure 4.9), a total of 30 simulations were conducted. Then, the results of an impact at 30 km/h against a 0.075 m radius object are in detail exposed in the next sections 4.3.1.1, 4.3.1.2 and 4.3.1.3 for diagonal, horizontal and vertical impact configurations respectively. Section 4.3.1.4 summarizes the main results corresponding to all impact conditions studied in Cluster 1.

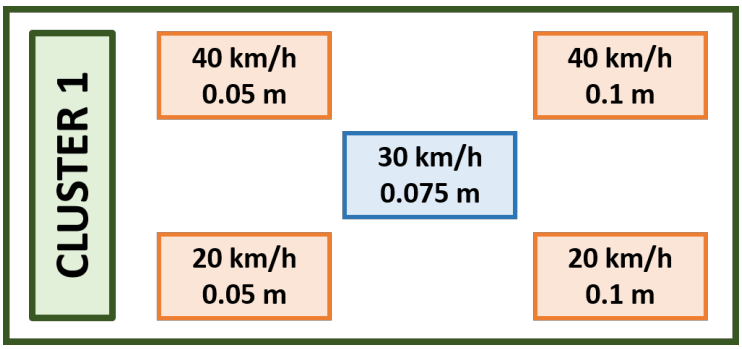

Figure 4.9: Cluster 1 impact conditions

4.3.1.1 Diagonal impact configuration at 30km/h

The strain-based analysis of the rib cage after the impact corresponding to the simulation *C1_V30_R075_D_NoAir* showed that the fracture of the 3rd, 4th and 5th ribs at both sides together with a fracture of the 2nd rib at the left side and the 6th, 7th and 8th ribs at the right side are expected. On the other hand, the use of the airbag protector shows a positive effect for the same impact situation reducing the number of expected fractures to four: 2nd and 5th rib on the left side and 5th and 8th rib on the right side. Figure 4.10 shows the contour plots for both situations.

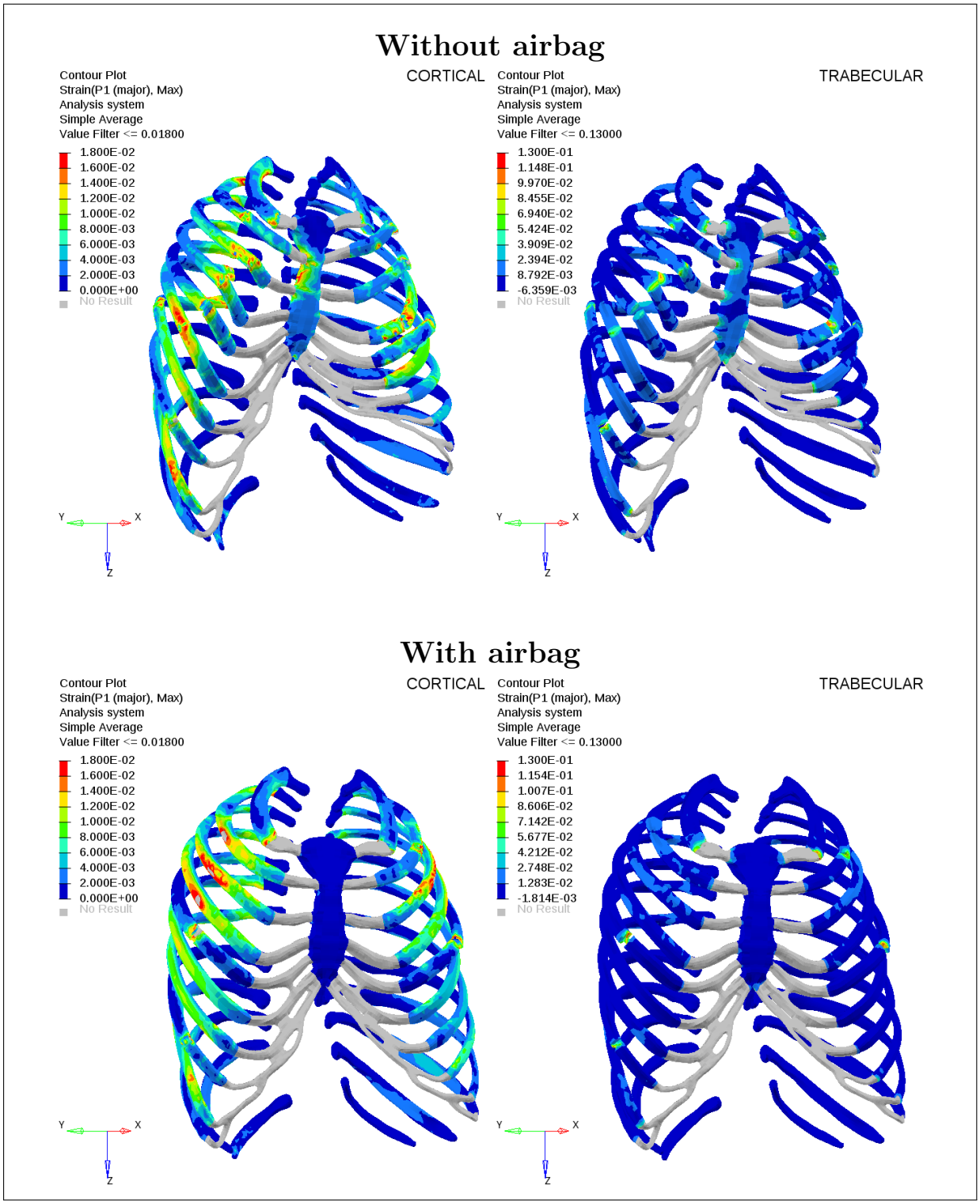

Figure 4.10: Maximum principal maximal strain contour plot at cortical and trabecular bone for an impact at 30 km/h in diagonal configuration.

The protective potential of the airbag protector is also observed in the analysis of the thorax deflection. In this impact situation, the airbag is able to reduce the thorax deflection from 80.5 mm to 71.5 mm. This positive effect is also observed assessing the predicted injury severity applying the Compression Criterion [52], which relates the values to injuries of AIS 3 and AIS 2, respectively. Figure 4.11 shows the thorax deformation for both cases.

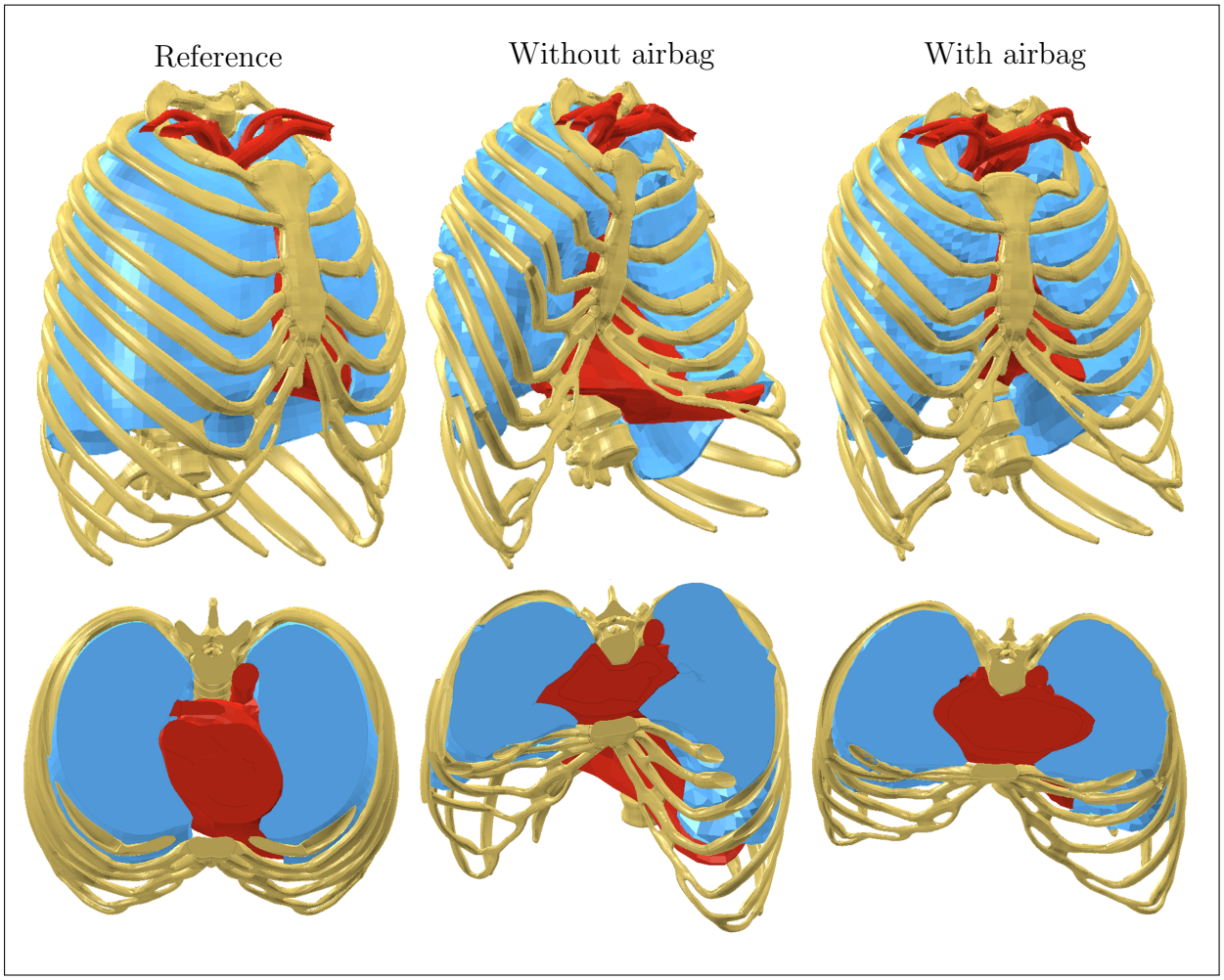

Figure 4.11: Thorax deformation by an impact of 30 km/h in diagonal configuration

4.3.1.2 Horizontal impact configuration at 30km/h

In an impact against a horizontal object at 30 km/h, fractures of the 3rd, 4th and 5th ribs on both sides are observed for the impact without airbag. Only the first rib fractures on both sides in the simulation with airbag, thereby a positive effect of the airbag is observed for these boundary conditions. Figure 4.12 shows contour plots for both situations.

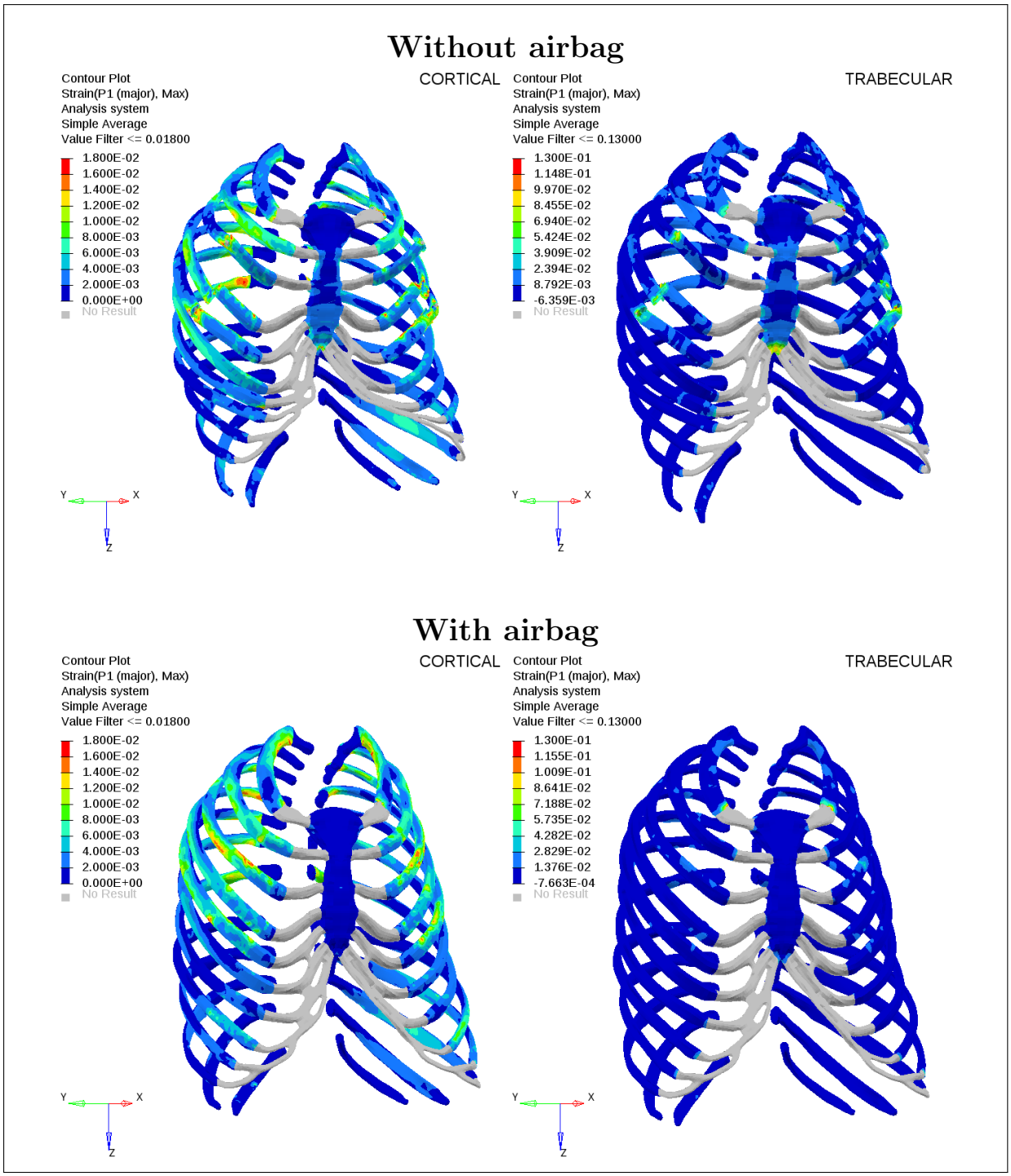

Figure 4.12: Rib strain at cortical and trabecular bone for an impact at 30 km/h in horizontal configuration

The positive contribution of the airbag is also significant in terms of thorax deflection, which is reduced by the airbag of 20 mm, from the 98 mm measured in *C1_V30_R075_H_NoAir* to the 78 mm in *C1_V30_R075_D_Air*. According with the Compression Criterion [52], at these impact conditions an airbag would reduce the injury severity from AIS 4 to AIS 3. Figure 4.13 shows thorax deformation for both cases.

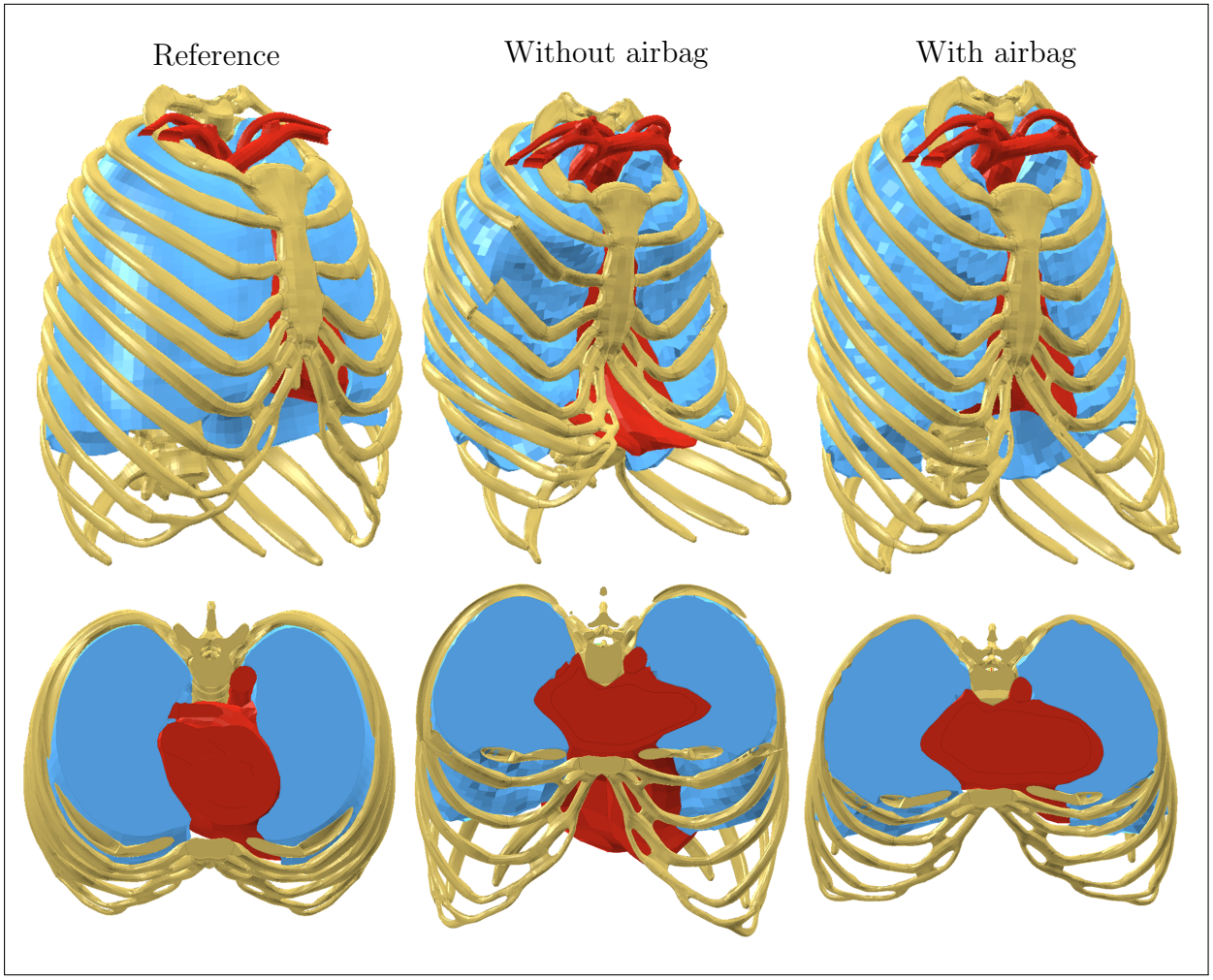

Figure 4.13: Thorax deformation by an impact of 30 km/h in horizontal configuration

4.3.1.3 Vertical impact configuration at 30 km/h

During the running process of the simulation of the impacts correspondent with vertical configuration numerical errors occurred. For this reason, it was not possible to run both simulations (*C1_V30_R075_V_NoAir* and *C1_V30_R075_V_Air*) until the same time horizon used for the other configurations. Simulations were interrupted before the whole impact was calculated. The reason of these interruptions is the high pressure concentrated in a

few number of elements, which generates negative volume errors in soft tissue parts.

The deflection values obtained (56 mm without airbag and 66 mm with airbag) should not be considered as definitive values because the simulations were both interrupted before the whole impact was completely simulated. It was not possible to calculate the maximal deflection because at the moment at the simulation was stopped, the HBM was still in motion. According to the Compression Criterion [52], for those deflection values an injury AIS 1 would be expected. Figure 4.14 shows the deformation of the thorax for both simulations.

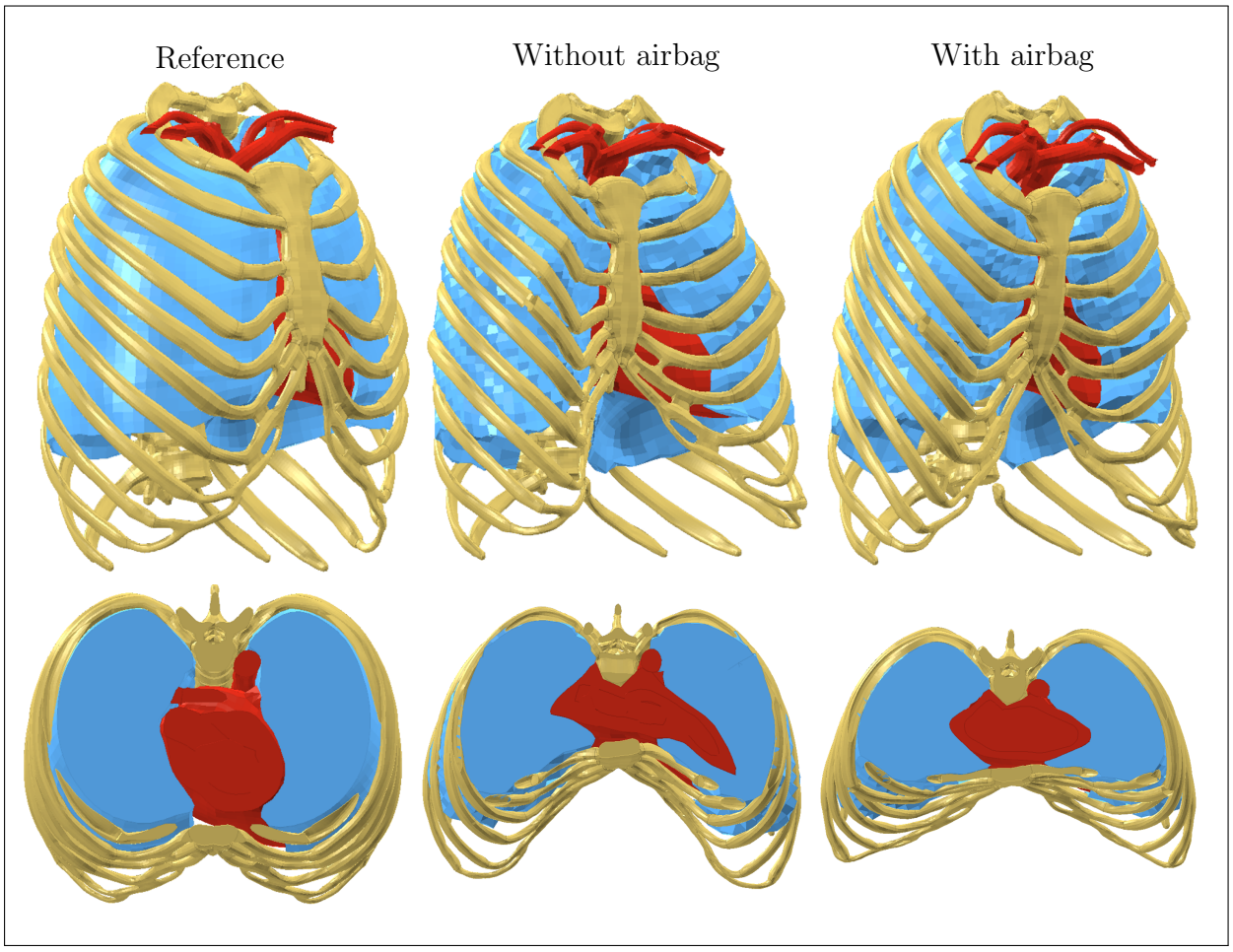

Figure 4.14: Thorax deformation by an impact of 30 km/h in vertical configuration

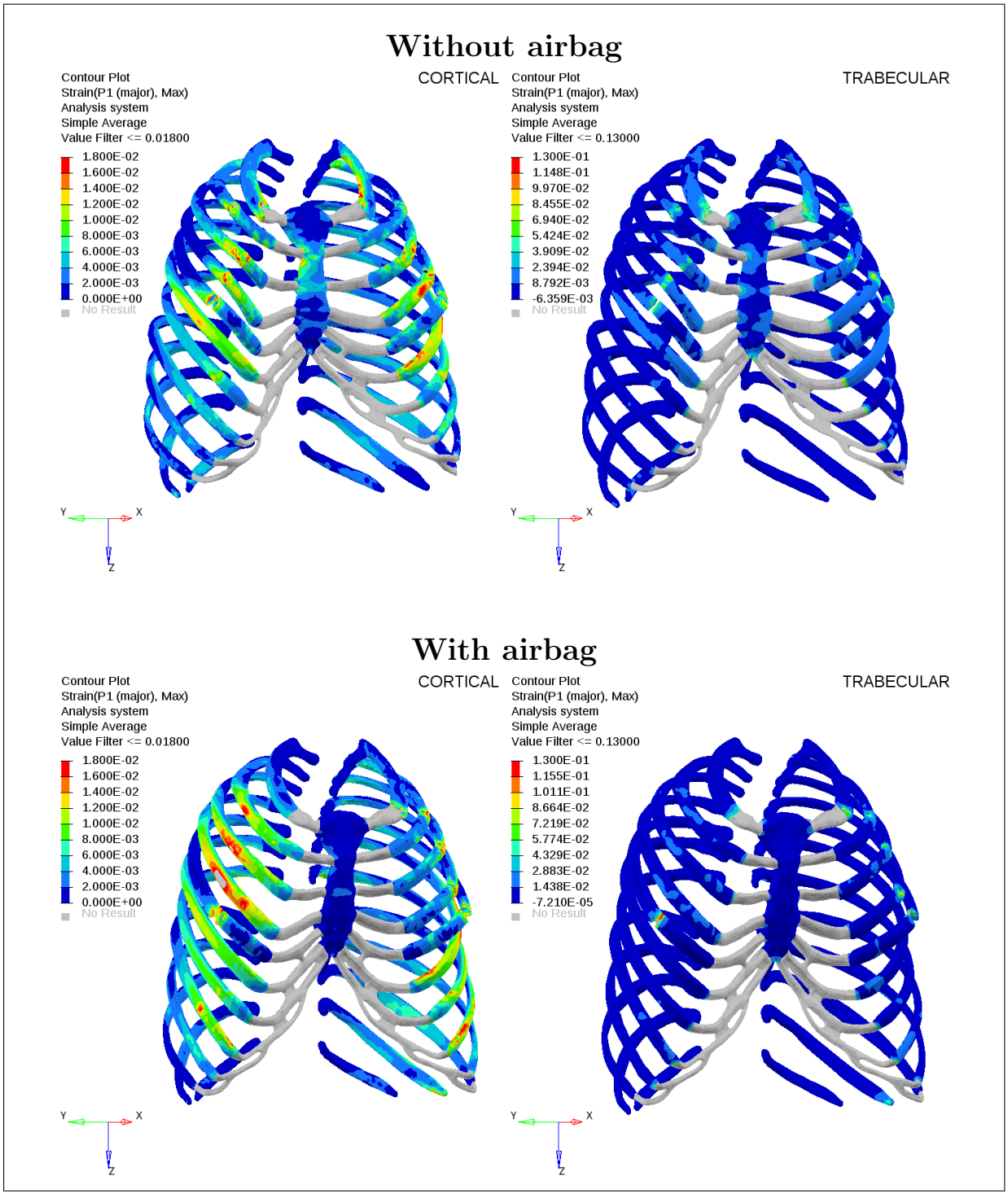

Figure 4.15: Rib strain at cortical and trabecular bone for an impact at 30 km/h in vertical configuration

Despite of the shorter simulation time calculated, as figure 4.15 shows, a fracture of the 2nd, 3rd, 4th and 5th ribs on both sides occurs for the impact without airbag resulting in a prediction of a coded AIS 3 injury. In case of using an airbag, no significant effect of the protector is observed. Fractures of the 2nd, 3rd, 4th and 5th ribs on the left are obtained together with fractures of the 5th rib on the right side. Also strain values exceed 1.8% at the cortical bone of the 3rd and 4th ribs on the right side, which indicates an upcoming fracture of the trabecular bone. The number of fractures expected signs discrepancy with the low chest deflection values measured and the low injury severity established by the Compression Criterion [52].

4.3.1.4 Results synthesis: Cluster 1

This section summarizes the main results obtained from the impact simulation of all boundary conditions enclosed in Cluster 1. Table 4.2 presents the number of rib fractures on the left and right side, the thorax deflection measured, the injury severity according to the Compression Criterion and the total time simulated for every impact in diagonal, horizontal and vertical configurations.

The results obtained from an impact against an obstacle with a radius of 0.075 m at an impact velocity of 30 km/h show that an airbag protector at the frontal thorax might be able to reduce the injury severity at this body region. The clear positive contribution of the airbag is observed at the horizontal configuration where the protector would reduce the number of rib fractures from six to zero and decreases the injury severity from AIS 4 to AIS 2 due to a relative thorax deflection reduction of 19 mm. At diagonal configuration, from the eight rib fractures observed in *C1_V30_R075_H_NoAir*, six of them would be prevented by the airbag protector also allowing to mitigate the possible injury severity from AIS 3 to AIS 2 derived from the chest compression. However, this protection benefit of the airbag may be limited at the vertical configuration where only one rib fracture would be prevented in comparison with a non-protected impact situation. The deflection values measured in simulation *C1_V30_R075_V_NoAir* as well as simulation *C1_V30_R075_V_NoAir* would imply an injury severity of AIS 1 and the airbag protector would not reduce this severity. However, as it was mentioned in the section 4.3.1.3, some discrepancies are observed between the deflection measured and the number of rib fractures determined for the vertical configuration compared to the results obtained at other configurations.

Simulation	Rib fractures		Deflection (mm)	Compression Criterion	Time (ms)
	Left side	Right side			
Diagonal object configuration					
C1_V20_R050_D_NoAir	2nd 3rd 4th 5th	3rd 4th 5th 6th	64	AIS 1	63,2
C1_V20_R050_D_Air	None	None	55	AIS 0	70
C1_V20_R100_D_NoAir	3rd 4th 5th	3rd 4th 5th	65	AIS 1	55
C1_V20_R100_D_Air	None	None	56	AIS 1	70
C1_V30_R075_D_NoAir	2nd 3rd 4th 5th	3rd 4th 5th 6th 7th 8th	80,5	AIS 3	40
C1_V30_R075_D_Air	2nd 5th	5th 8th	71,5	AIS 2	70
C1_V40_R050_D_NoAir	2nd 3rd 4th 5th	3rd 4th 5th 6th 7th 8th 9th	88	AIS 3	27
C1_V40_R050_D_Air	2nd 3rd 4th 5th	2nd 3rd 4th 5th	80	AIS 3	43
C1_V40_R100_D_NoAir	3rd flail 4th 5th	2nd 3rd 4th 5th 8th	90	AIS 3	27,3
C1_V40_R100_D_Air	2nd 3rd 4th 5th	2nd 3rd 4th 5th 8th	82	AIS 3	43
Horizontal object configuration					
C1_V20_R050_H_NoAir	3rd	3rd	86	AIS 3	53,2
C1_V20_R050_H_Air	None	None	62	AIS 1	70
C1_V20_R100_H_NoAir	3rd	3rd	81	AIS 3	38,2
C1_V20_R100_H_Air	None	None	61	AIS 1	70
C1_V30_R075_H_NoAir	3rd 4th 5th	3rd 4th 5th	97,2	AIS 4	33,5
C1_V30_R075_H_Air	None	None	78,3	AIS 2	70
C1_V40_R050_H_NoAir	3rd 4th 5th	3rd 4th 5th	110	AIS 5	27
C1_V40_R050_H_Air	2nd 3rd 4th 5th	2nd 3rdn5th	98	AIS 3	47
C1_V40_R100_H_NoAir	2nd 3rd 4th 5th	2nd 3rd 4th 5th	105	AIS 5	17
C1_V40_R100_H_Air	2nd 3rd 4th 5th	1st 2nd 3rd	91	AIS 3	41
Vertical object configuration					
C1_V20_R050_V_NoAir	5th	5th	37	AIS 0	48
C1_V20_R050_V_Air	5th	5th	50	AIS 0	70
C1_V20_R100_V_NoAir	4th 5th	5th	37	AIS 0	47
C1_V20_R100_V_Air	5th	5th	37	AIS 0	50
C1_V30_R075_V_NoAir	2nd 3rd 4th 5th	2nd 3rd 4th 5th	55,8	AIS 1	25
C1_V30_R075_V_Air	2nd 3rd 4th 5th	2nd 4th 5th	62,7	AIS 1	49
C1_V40_R050_V_NoAir	2nd 3rd 4th 5th 7th	2nd 3rd 4th 5th	56	AIS 1	31
C1_V40_R050_V_Air	2nd 3rd 4th 5th	2nd 3rd 4th 5th	62	AIS 1	37
C1_V40_R100_V_NoAir	2nd 3rd 4th 5th 6th 7th	2nd 3rd 4th 5th 6th 7th	72	AIS 2	22
C1_V40_R100_V_Air	2nd 3rd 4th 5th	2nd 3rd 4th 5th	64	AIS 1	30

Table 4.2: Cluster 1 - Simulation Results

The maximal deflection for an impact at 20 km/h was measured in the horizontal configuration (86 mm in *C1_V20_R050_H_NoAir*) and the highest number of rib fractures for the diagonal configuration were obtained in the *C1_V20_R050_D_NoAir* simulation where the fracture of the 2nd, 3rd, 4th 5th ribs on the left side and the 3rd, 4th, 5th and 6th ribs on the right side of the rib cage are expected. However, in both scenarios the airbag protector is able to provide effective protection avoiding every rib fracture and reducing the chest deflection up to 14 mm. The reduction of the thorax deflection would mean also a descent of the injury severity level from AIS 3 to AIS 1 according to the Compression Criterion. This airbag's ability of reducing the thorax compression is observed in all impact situations at 20 km/h. The same positive effect is observed by preventing rib fractures, except for the vertical configuration where, despite the airbag protector, the fracture of the 5th rib on both sides is still expected. No significance of the obstacle radius was observed for this velocity.

The maximum number of rib fractures in the whole cluster 1 were obtained in the simulation *C1_V40_R100_V_NoAir* where twelve ribs would be fractured. In this impact with the obstacle in vertical configuration, the airbag would be able to avoid four of them (6th and 7th ribs on both sides). Despite the airbag, the fracture of the 2nd, 3rd, 4th and 5th ribs on both sides would still occur in an impact against smaller object's radius. As it was mentioned before, also in these two impact situations, relatively low thorax deflection values were measured for the high number of rib fractures calculated. A total of eleven rib fractures were counted in an impact at 40 km/h against an obstacle with a radius of 0.05m without airbag at diagonal configuration (*C1_V40_R050_D_NoAir*). Close results are observed at this diagonal configuration when the radius of the impact object is 0.1 m where a total of seven single rib fractures plus a double fracture at the third rib on the left side would be expected. The contribution of the airbag is very limited in both situations. In both cases, the airbag is able to reduce the thorax deflection by 8 mm but maintaining the same AIS 3 level of severity. Regarding the protection of the rib cage, the fracture of the 6th, 7th, 8th and 9th ribs would be prevented on the left side but the fracture of the 2nd rib on the right side would be counted additionally for the case of the smaller radius. In the results from *C1_V40_R100_D_Air*, instead of the double fracture of the 3rd rib on the left side, a single one would be predicted but again with the addition of the fracture of the 2nd rib which is not observed in an impact without airbag. These results point out a possible shielding behaviour of the airbag. In other words, the thorax of the GHBMC equipped with airbag might be not support such a high concentrated load because of the load distribution effect provided by the airbag protector. Due to the shielding effect, the load could be transmitted to other ribs which were not hit directly. Following the trends observed at other impact velocities, the maximum deflection was obtained at the horizontal configuration. The values obtained for both simulations without airbag would mean an AIS 5 injury severity according to the Compression Criterion.

4.3.2 Cluster 2

The performance of an airbag protector at a high impact speed against a small radius object were studied in cluster 2. A total of 30 simulations were calculated to analyse all impact configurations included in this cluster(see Figure 4.16). Results of the mean impact situation (an impact at 60 km/h against an obstacle with a 0.075 m radius) are exposed extensively for diagonal, horizontal and vertical impact configurations in the next three sections. Finally, in section 4.3.2.4 the principal results obtained from every simulation are summarized.

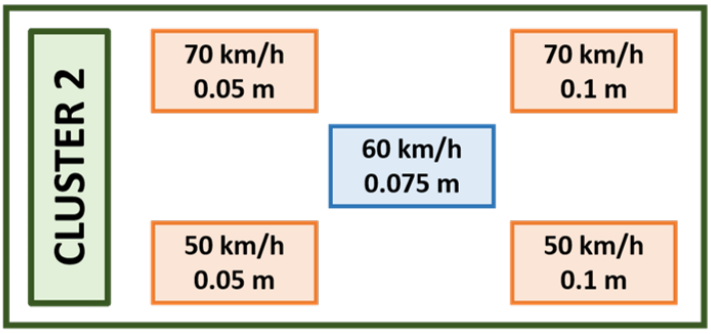

Figure 4.16: Cluster 2 impact conditions

4.3.2.1 Diagonal impact configuration at 60 km/h

The analysis of the principal strain values obtained from the simulation *C2_V60_R075_D_No Air* at the cortical and trabecular of the rib cage shows after the impact a simple fracture at the 1st, 2nd, 6th, 7th and 8th and and a double point fracture at the 3rd, 4th and 5th ribs on the right side, which would indicate an unilateral flail chest. On the left side, a single fracture at the 2nd, 3rd, 4th, 6th and 7th rib is expected together with the double point fracture of the 5th rib. The calculation of the same impact conditions with an airbag protector *C2_V60_R075_D_Air* shows a reduction of the number of rib fractures avoiding any double point fracture. However, still ten rib fractures are obtained: single fracture of the 2nd, 3rd, 4th and 5th ribs on both sides, single fracture of the 6th rib on the right side and the fracture of the 7th on the left side. Figure 4.17 shows contour plots for both situations.

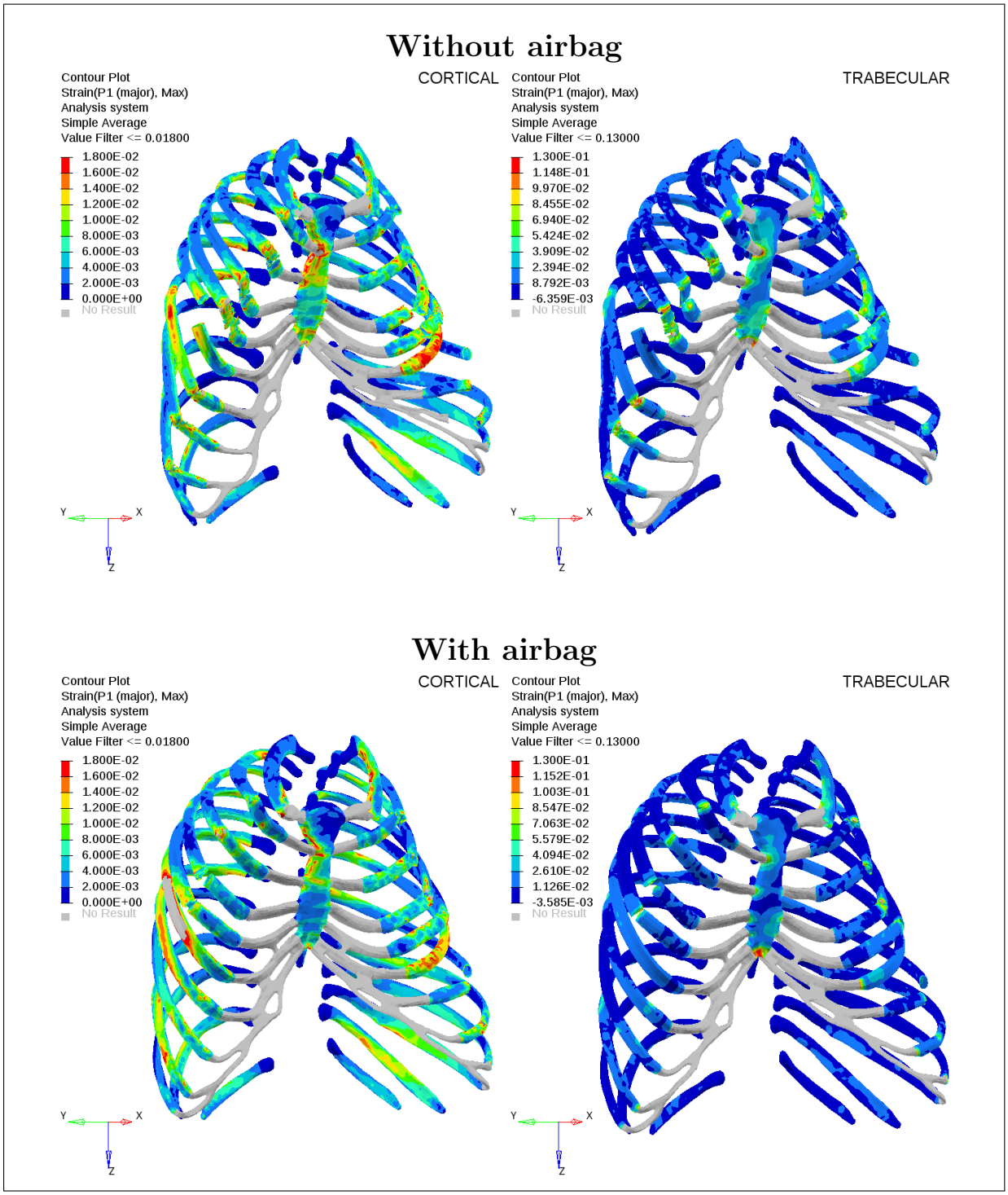

Figure 4.17: Rib principal strain at cortical and trabecular bone for an impact at 60 km/h in diagonal configuration

The chest deflection measured are 103 mm and 94 mm for the impacts without and with airbag respectively. Despite the airbag protector is able to reduce the thorax compression for these impact conditions, according to the Compression Criterion both cases would be classified with an AIS 4 injury severity. Figure 4.18 shows thorax deformation for both cases.

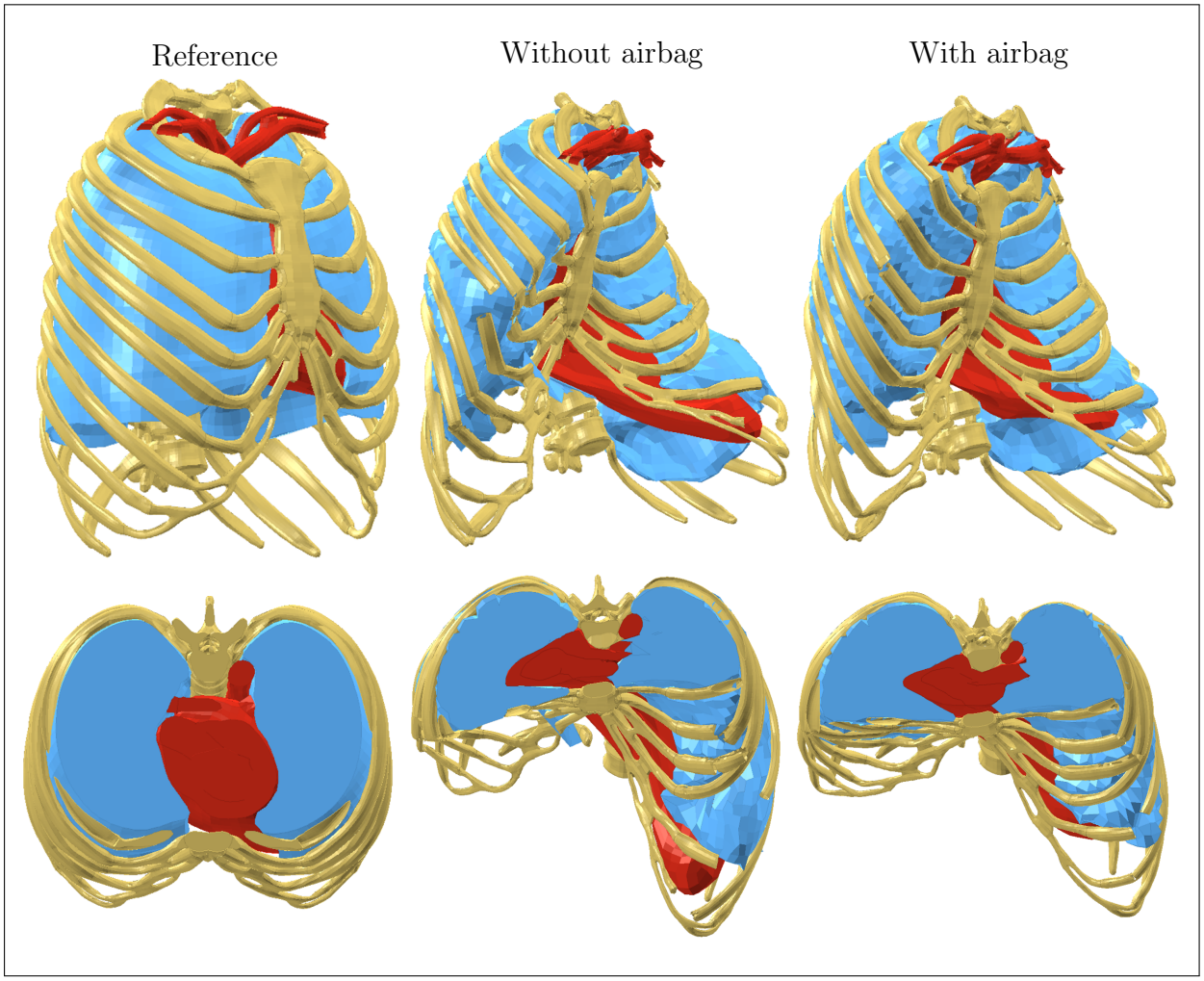

Figure 4.18: Thorax deformation by an impact of 60 km/h in diagonal configuration

4.3.2.2 Horizontal impact configuration at 60 km/h

Multiple fractures are observed in this impact scenario. For the *C2_V60_R075_H_NoAir* case, the 2nd and 3rd ribs presented a simple fracture and a double point fracture of the 4th and 5th ribs on both sides. An airbag protector did not bring any significant reduction on the injury severity. Simple fractures are observed from the 2nd to the 5th ribs on both side except the 3rd rib on the left that presents a double point fracture (See Figure 4.19).

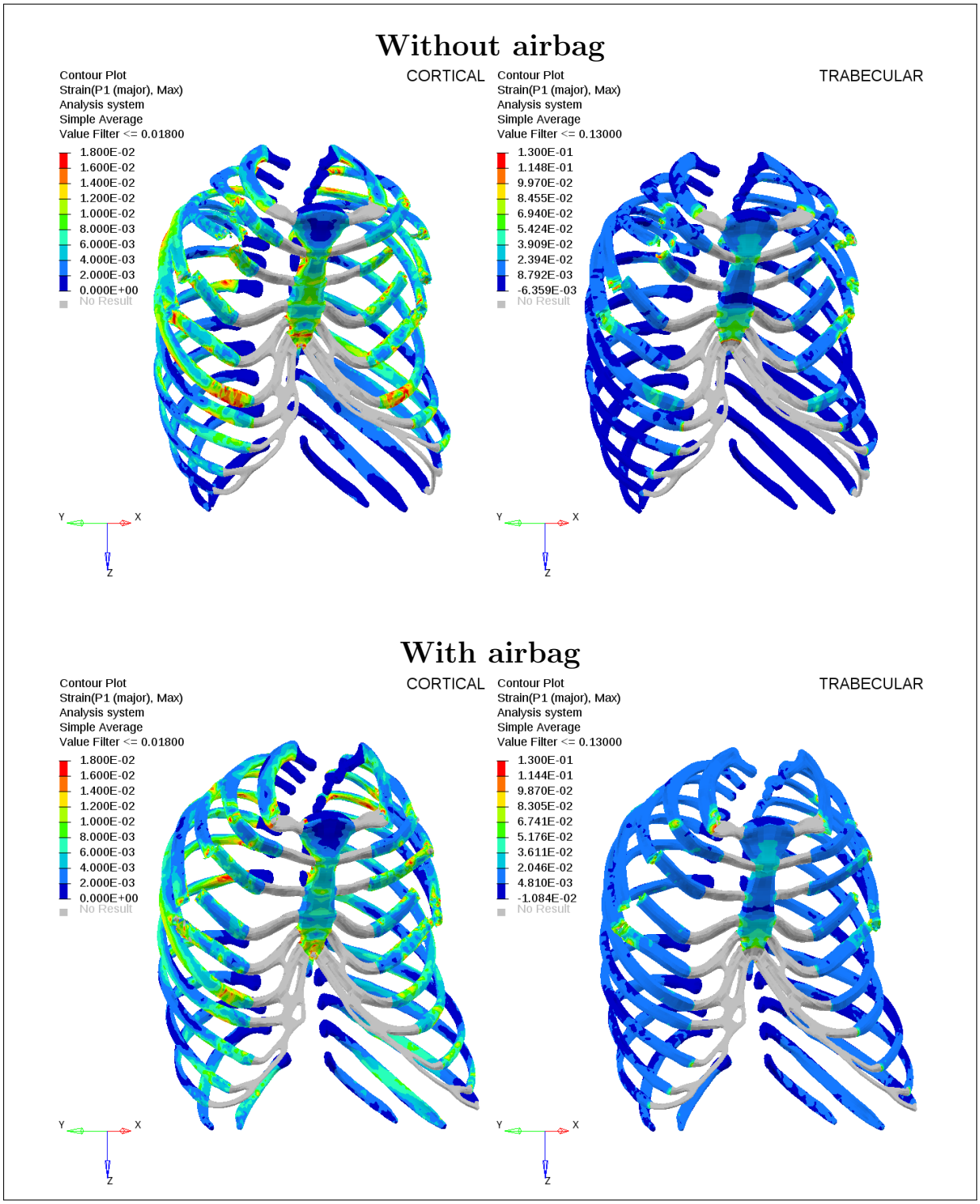

Figure 4.19: Rib principal strain at cortical and trabecular bone for an impact at 60 km/h in horizontal configuration

A deflection of 108 mm was obtained for the simulation without airbag and a value of 111 mm for the case with airbag. These values could suggest a negative performance of the airbag protector because of the slightly higher deflection obtained. Nevertheless, these results are a consequence of the simulation time achieved. The simulation without protector were interrupted before the impact was completely simulated because of numerical errors generated by the high compression rates (7 ms of impact simulated). These effect was attenuated by the initial energy absorption provided by the airbag protector allowing a longer simulation of the impact (14 ms). Although higher deflection values are definitely expected for an impact without airbag than for the case with airbag, with the values obtained both impacts derived in a a very high thorax compression and they would be classified as critical (AIS 5) according to the Compression Criterion. Figure 4.20 shows thorax deformation for both cases.

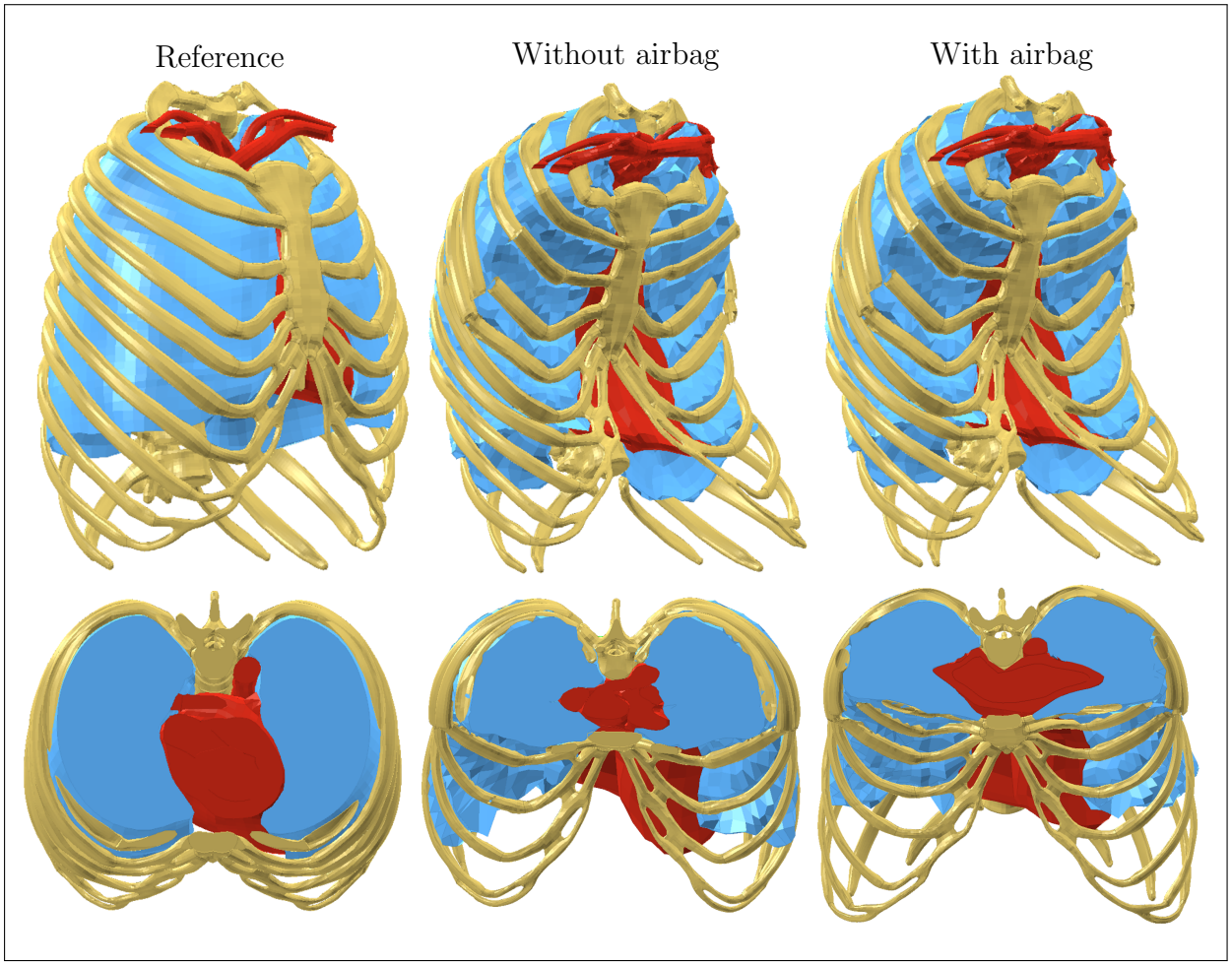

Figure 4.20: Thorax deformation by an impact of 60 km/h in horizontal configuration

4.3.2.3 Vertical impact configuration at 60 km/h

The analysis of the here exposed impact scenario could not be totally completed because of numerical errors during the simulation *C2_V60_R075_V_Air*. The calculation of this situation was broken due to some nodes having out-of-range forces resulting in an insufficient simulated time which allowed an evaluation of the possible injuries. Therefore, the results related to this case showed in this section correspond with the last state of the simulation.

The chest deflection measured for an impact without airbag was 69 mm which, according to the Compression Criterion, would be classified as an AIS 2 injury. However, this value should be taken carefully because a visual evaluation of the deformed thorax (see figure 4.21) suggest a higher thorax compression.

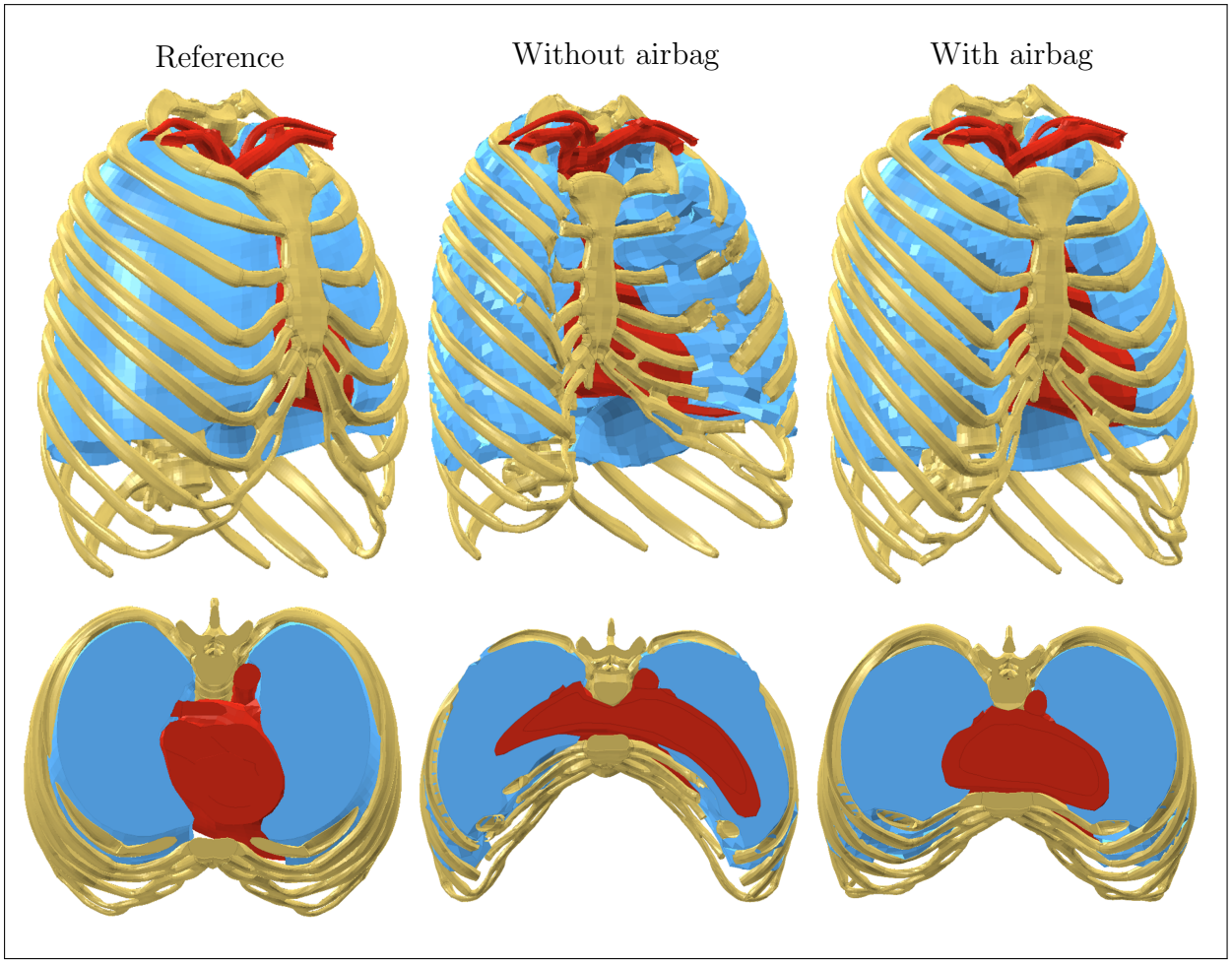

Figure 4.21: Thorax deformation by an impact of 60 km/h in vertical configuration

Attending to the number of rib fractures, the single fracture of the 2nd, 5th and 6th ribs on both sides were counted together with the double point fracture of the 3rd and 4th ribs also on both sides (see figure 4.22).

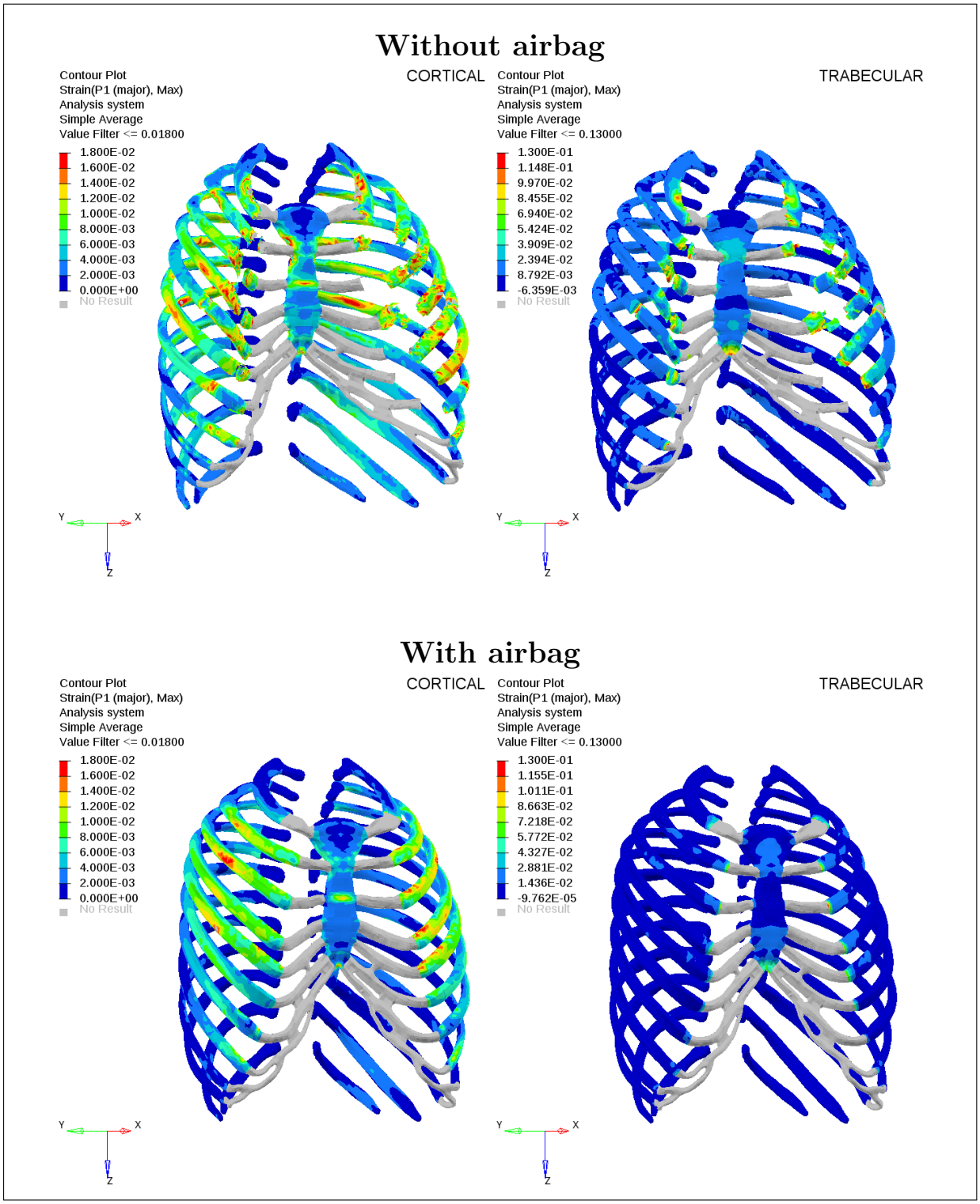

Figure 4.22: Rib principal strain at cortical and trabecular bone for an impact at 60 km/h in horizontal configuration

4.3.2.4 Results synthesis: Cluster 2

This section groups together all the main results obtained from the simulation of Cluster 2 impact conditions. These results are summarized for every impact configurations in table 4.3 exposing the number of rib fractures and chest deflection measured of each case. Some of the simulations in this table are labelled with an asterisk. This mark indicates that for those cases it was not possible to simulate totally the impact phase because of a numerical error during the calculation due to some nodes having out-of-range forces in some thorax soft tissue parts. Therefore, the results presented for the labelled simulations correspond to those ones obtained at the last state calculated and they should not be considered as definitive values. The inability of calculate the total impact phase occurred especially frequently Cluster 2 impact scenarios with the obstacle in vertical configuration. The injury severity level as well as the number of rib fractures obtained from these simulations seem to be very low and a much higher severity would be expected considering the results observed at the other impact configurations for the same impact conditions. As the results of the vertical configuration were obtained at a very earlier stage of the impact simulation than for the diagonal and horizontal configuration, it was not possible to stablish a direct comparison and they are not further commented in this section.

Simulation	Rib fractures		Deflection (mm)	Compression Criterion	Time (ms)
	Left side	Right side			
Diagonal object configuration					
C2_V50_R050_D_NoAir	2nd 3rd 4th 5th 6th 7th 8th flail 9th	2nd 3rd 4th 5th 7th	97	AIS 4	22
C2_V50_R050_D_Air	2nd 3rd 4th 5th	2nd 3rd 4th 5th	92	AIS 4	33
C2_V50_R100_D_NoAir*	2nd 3rd 4th 5th	3rd 4th 5th 6th	76	AIS 2	10
C2_V50_R100_D_Air	2nd 3rd 4th 5th 6th 7th 8th	2nd 3rd 4th 5th 6th 7th 8th	105	AIS 5	44
C2_V60_R075_D_NoAir	2nd 3rd 4th 5th flail 6th 7th	2nd 3rd flail 4th flail 5th flail 6th 7th 8th 9th	103	AIS 4	14
C2_V60_R075_D_Air	2nd 3rd 4th 5th 7th	2nd 3rd 4th 5th 6th	94	AIS 4	30
C2_V70_R050_D_NoAir*	1st 2nd 3rd flail 4th 5th	3rd 4th 5th flail 6th flail 7th 8th	73	AIS 2	8
C2_V70_R050_D_Air*	2nd 3rd 4th 5th 6th	2nd 3rd 4th 5th 6th 7th	86	AIS 3	23
C2_V70_R100_D_NoAir*	1st 2nd 3rd 4th 5th flail 6th	2nd 3rdflail 4th 5th flail 6th 7th 8th	89	AIS 3	8
C2_V70_R100_D_Air*	2nd 3rd flail 4th 5th	2nd 3rd 4th 5th 6th 7th	104	AIS 5	24

Simulation	Rib fractures		Deflection (mm)	Compression Criterion	Time (ms)
	Left side	Right side			
Horizontal object configuration					
C2_V50_R050_H_NoAir	2nd 3rd 4th 5th	2nd 3rd 4th 5th	120	AIS 5	16
C2_V50_R050_H_Air	2nd 3rd 4th 5th	2nd 3rd 4th 5th	111	AIS 5	37
C2_V50_R100_H_NoAir	2nd 3rd 4th 5th	2nd 3rd 4th 5th	109	AIS 5	13
C2_V50_R100_H_Air	2nd 3rd 4th 5th	2nd 3rd 4th 5th	105	AIS 5	36
C2_V60_R075_H_NoAir	2nd 3rd 4th 5th 6th	2nd 3rd 4th 5th 6th	108	AIS 5	8,5
C2_V60_R075_H_Air	2nd 3rd 4th 5th	2nd 3rd 4th 5th	110	AIS 5	26
C2_V70_R050_H_NoAir	2nd 3rd 4th 5th flail 6th	2nd 3rd 4th 5th flail 6th 7th	129,5	AIS 5	11
C2_V70_R050_H_Air	2nd 3rd flail 4th flail 5th 6th	2nd 3rd 4th 5th flail 6th 7th	127	AIS 5	30
C2_V70_R100_H_NoAir*	2nd 3rd flail 4th 5th	2nd 3rd 4th 5th	90	AIS 3	7
C2_V70_R100_H_Air	2nd 3rd flail 4th 5th	2nd 3rd 4th 5th	109	AIS 5	22
Vertical object configuration					
C2_V50_R050_V_NoAir	2nd 3rd 4th flail 5th 6th 7th 8th	2nd 3rd 4th 5th 6th 7th	60	AIS 1	18
C2_V50_R050_V_Air*	2nd 3rd 4th 5th 6th 7th	2nd 3rd 4th 5th 6th 7th	70	AIS 3	32
C2_V50_R100_V_NoAir*	2nd 3rd flail 4th 5th 6th 7th	2nd 3rd 4th 5th 6th 7th	68	AIS 1	11
C2_V50_R100_V_Air*	None	None	48	AIS 0	24
C2_V60_R075_V_NoAir	2nd 3rd 4th flail 5th 6th	2nd 3rd 4th 5th 6th	69	AIS 1	8,6
C2_V60_R075_V_Air*	None	None	40	AIS 0	22
C2_V70_R050_V_NoAir*	4th	4th	28	AIS 0	6
C2_V70_R050_V_Air*	None	None	36	AIS 0	22
C2_V70_R100_V_NoAir*	2nd 3rd flail 4th flail 5th 6th	2nd 3rd 4th 5th 6th	72	AIS 2	8
C2_V70_R100_V_Air*	None	None	42	AIS 0	19

*Results for the last state calculated.

Table 4.3: Cluster 2 - Simulation Results

As it was exposed in the previous sections, a low significat effect of the airbag was observed in am impact at 60 km/h against an obstacle with a 0.075m radius. A high number of rib fractures, eighteen in total, were counted for the impact without airbag with the object in diagonal configuration (*C2_V60_R075_D_NoAir*) but despite the airbag, still ten fractures would remain. Also in this case, the airbag provided a reduction of 9 mm thorax deflection was obtained, but according to Compression Criterion, the 94 mm deflection measured would still derive in a AIS 4 injury severity. Less rib fractures are obtained in horizontal configuration (*C2_V60_R075_H_Air*) where the use of the airbag would reduce to eight the number of fractured ribs. However, the airbag would be also unable to decrease the injury severity reporting a critical severity (AIS 5) in this scenario.

An airbag protector would have a similar performance in an impact at 50 km/h showing a limited influence on the protection. Although the airbag is able to absorb some of the impact energy during approximately 9 ms, it is not enough to reduce the injury severity compared to the non protected scenario. In horizontal configuration, although the airbag is able to reduce quantitative the thorax deflection measured, it would not mean a qualitative reduction of the injury severity reporting AIS 5 for both object radius (0.05 m and 0.100 m). The same trend is observed in diagonal configuration where in *C2_V50_R100_D_Air* a critical severity would be expected too. Less severity (AIS 4) was obtained compared with the other scenarios at the same impact velocity for the case of an obstacle with a radius of 0.05 m in diagonal configuration *C2_V50_R050_D_Air*, though qualitatively it would not imply a reduction of the severity compared to the situation without airbag. Comparing the four airbag scenarios at 50 km/h impact, the maximum of rib fractures occurred in *C2_V50_R100_D_Air* counting a total of 14 fractures. However, not less than 8 fracture would be obtained in any other case.

It was difficult to analyse globally an impact at 70 km/h because, as it was explained before for the vertical configuration, most of the diagonal configuration simulations were interrupted without the calculation of the whole impact phase. However, the results obtained in horizontal configuration suggest that, due to the increase of the impact speed, the performance of the airbag at those impact conditions would get even worse than in the previous cases. In the simulation *C2_V70_R050_H_Air* a total of 14 rib fractures were counted and a chest deflection of 127 mm were measured reporting an AIS 5 injury severity. Same severity would be obtained for the case of a radius of 0.100 m with a deflection of 109 mm despite the airbag protector. The partial results obtained from the simulations in diagonal configuration indicate a similar trend about the effectiveness of the airbag on such impact scenarios. Eleven and twelve rib fractures would be expected for the simulations *C2_V70_R050_D_Air* and *C2_V70_R050_D_Air* respectively, showing this last example already a deflection of 104 mm which would derive in a critical injury (AIS 5) according to the Compression Criterion.

4.3.3 Cluster 3

In Cluster 3, the possible protection effect of an airbag device is studied in an impact scenario against a large object (see Figure 4.23). As it was explained in section 4.2.2, due to the large dimension of the object, only the horizontal configuration was considered in the analysis of the impact scenarios enclosed in cluster 3. Following the same structure as for the previous clusters' result exposition, a detailed exposition of the results obtained from the simulation corresponding with the mean impact conditions of the cluster is firstly presented. Then, in section 4.3.3.2, a summary of the main results obtained from every simulations of the cluster is exposed. In total, ten simulations were conducted to analyse the whole cluster.

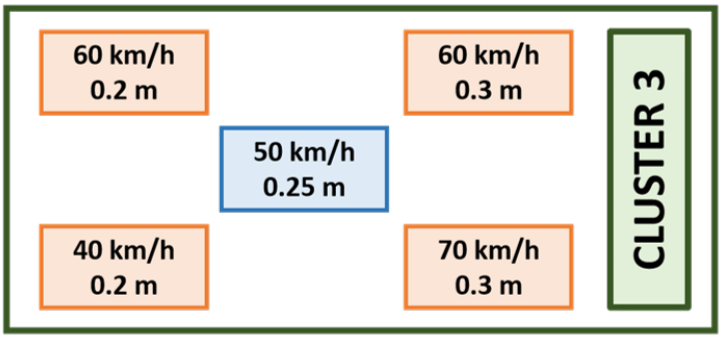

Figure 4.23: Cluster 3 impact conditions

4.3.3.1 Horizontal impact configuration at 50 km/h

The simulation of an impact at a velocity of 50 km/h against an obstacle with a 0.25 radius (*C3_V50_R250_H_NoAir*) was interrupted because of a numerical error due to some nodes having out-of-range forces. Therefore, the impact phase could not be totally assessed. At the last state calculated,it was already possible to observed on both sides the double point fracture of the 3rd rib as well as the single fracture of the 2nd, 4th and 5th ribs. The energy absorption provided by the airbag during 9 ms made possible to calculate almost the whole impact phase in *C3_V50_R250_H_Air* avoiding the quick compression of the thorax soft tissues. However, the absorption given was not significantly reflected in the number of rib fractures prevented. Attending to the strain values obtained, a single fracture of the 2nd, 3rd, 4th and 5th ribs would be still fractured and only the double point fracture of both 3rd ribs named before would be prevented. Figure 4.24 shows contour plots for both situations.

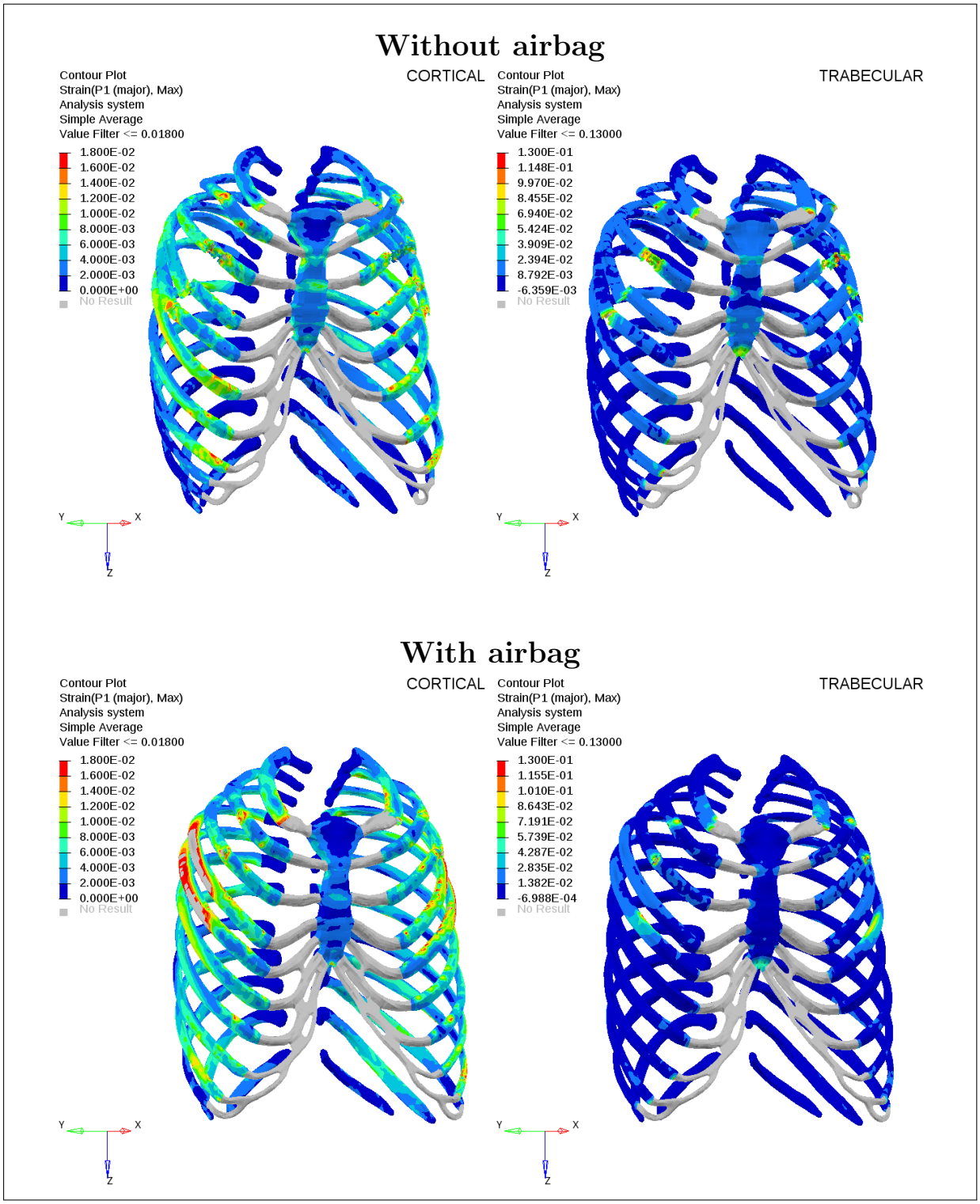

Figure 4.24: Rib principal strain at cortical and trabecular bone for an impact at 50 km/h in horizontal configuration

The thorax deflection measured at the simulations of the impacts without and with airbag were 86 mm and 100 mm respectively. Considering the 100 mm obtained for impacting with airbag and also considering that the simulation of the impact without airbag was interrupted before the calculation of the impact phase was completed, the 86 mm for the first one should not be considered as a definitive value and a higher deflection would be expected in case of the calculation of the whole impact. According to the Compression Criterion, an injury severity of AIS 4 would be reported for the case of a crash with airbag at these impact conditions. Figure 4.25 shows thorax deformation for both cases.

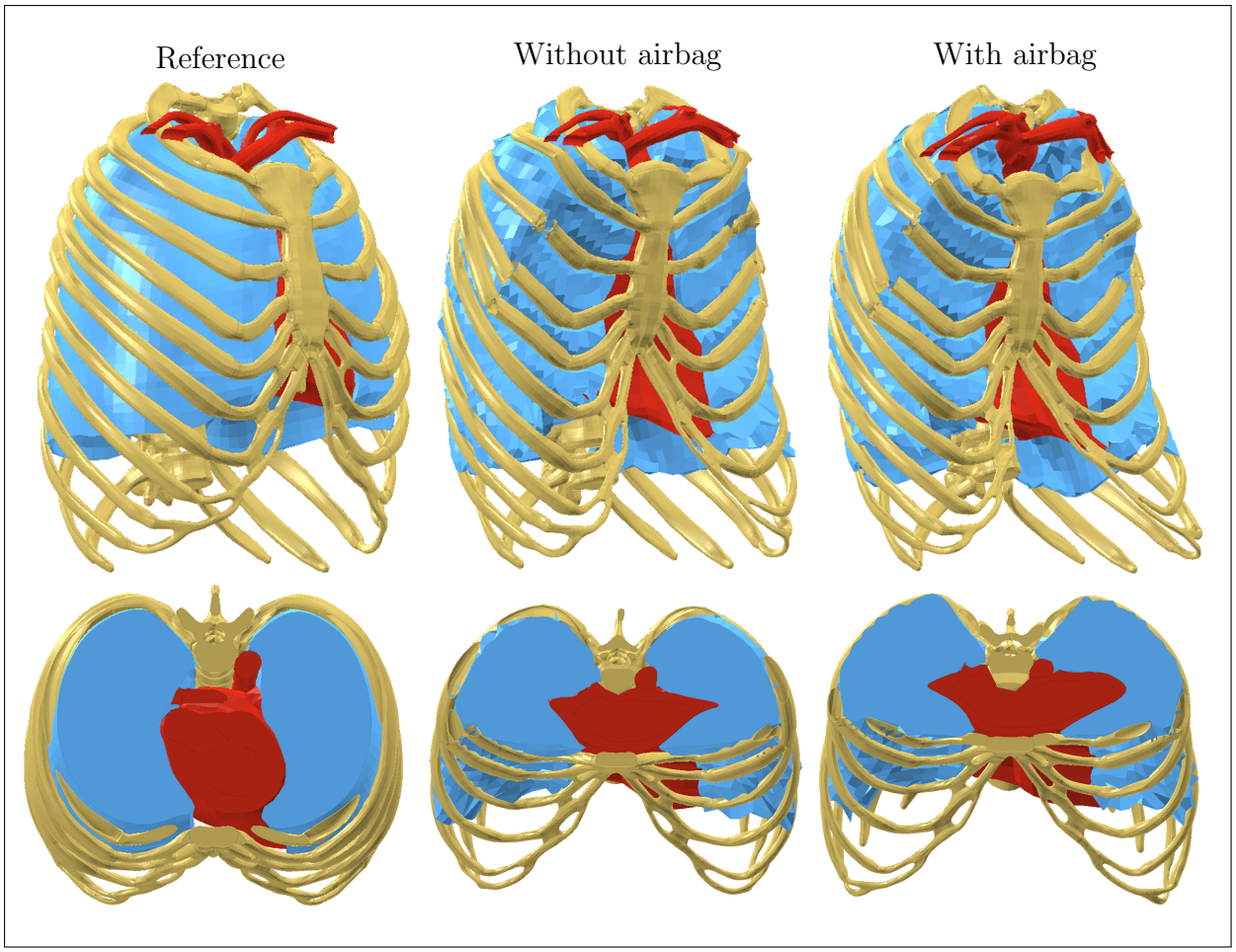

Figure 4.25: Thorax deformation by an impact of 50 km/h in horizontal configuration

4.3.3.2 Results synthesis: Cluster 3

In this section, the main results obtained from the simulation of all impact scenarios contemplated in Cluster 3 are presented. These results are summarized in table 4.4 where the number of rib fractures observed and deflection values measured are exposed for each

simulation. In the previous section 4.3.3.1, it was explained how a frontal airbag protector was not able to reduce significantly the number of rib fractures in case of impacting a large object at a velocity of 50 km/h where still a total of eight single fractures would be counted. The injury severity derived of this impact scenario according to the Compression Criterion it would be also rated as critical (AIS 4) despite of the absorption effect provided by the airbag.

Simulation	Rib fractures		Deflection (mm)	Compression Criterion	Time (ms)
	Left side	Right side			
C3_V40_R200_H_NoAir	2^{nd} 3^{rd} 4^{th} 5^{th}	2^{nd} 3^{rd} 4^{th} 5^{th}	100	AIS 4	17
C3_V40_R200_H_Air	2^{nd} 3^{rd} 4^{th} 5^{th}	2^{nd} 3^{rd} 4^{th} 5^{th}	90	AIS 3	44
C3_V40_R300_H_NoAir	2^{nd} 3^{rd} 4^{th} 5^{th}	2^{nd} 3^{rd} 4^{th} 5^{th}	97	AIS 4	13
C3_V40_R300_H_Air*	2^{nd} 3^{rd} 4^{th} 5^{th}	2^{nd} 3^{rd} 4^{th} 5^{th}	81	AIS 3	36
C3_V50_R250_H_NoAir*	2^{nd} 3^{rd} flail 4^{th} 5^{th}	2^{nd} 3^{rd} flail 4^{th} 5^{th}	85	AIS 3	11,5
C3_V50_R250_H_Air	2^{nd} 3^{rd} 4^{th} 5^{th}	2^{nd} 3^{rd} 4^{th} 5^{th}	100	AIS 4	35,4
C3_V60_R200_H_NoAir*	2^{nd} 3^{rd} 4^{th} 5^{th}	2^{nd} 3^{rd} 4^{th} 5^{th}	86,2	AIS 3	6,5
C3_V60_R200_H_Air	2^{nd} 3^{rd} 4^{th} 5^{th}	2^{nd} 3^{rd} 4^{th} 5^{th}	100	AIS 4	28,5
C3_V60_R300_H_NoAir*	2^{nd} 3^{rd} 4^{th} 5^{th} 6^{th}	2^{nd} 3^{rd} 4^{th} 5^{th}	84	AIS 3	12,4
C3_V60_R300_H_Air	2^{nd} 3^{rd} 4^{th} 5^{th} 6^{th}	2^{nd} 3^{rd} 4^{th} 5^{th}	103,5	AIS 5	29

*Results for the last state calculated.

Table 4.4: Cluster 3 - Simulation Results

Slightly more effective would be the airbag protector in an impact at 40 km/h. For an obstacle's radius of 0.2 m as well as for one with a radius of 0.3 m, the airbag would be able to reduce the thorax compression (from 100 to 90 mm in *C3_V40_R200_H_Air* and from 97 to 89 mm *C3_V40_R300_H_Air*) which would imply a mitigation of the injury severity from severe (AIS 4) to serious (AIS 3) in both cases. However, this positive contribution of the protector would not be observed in the strain-based analyses of the rib cage. In both situations the airbag would not reduce the number of rib fractures and the fracture of the 2nd, 3rd, 4th and 5th rib on both sides would be expected despite the airbag. No significant influence of the object radius was observed.

Simulation *C3_V60_R200_H_NoAir* and simulation *C3_V40_R300_H_NoAir* were both interrupted because of numerical error due nodes having out-of-range forces and was not possible to simulate the whole impact phase. Therefore, the results shown in table 4.4 for both no airbag situation correspond to the last state calculated and they should not be considered as definitive values. Especially for the chest deflection noted, a higher final compression of the thorax would be expected. An impact against an 0.2 m radius obstacle at 60 km/h (*C3_V60_R200_H_Air*) with a thorax frontal airbag would emerged in a AIS 4 injury severity level (100 mm deflection) according to the Compression Criterion. Same

impact velocity but with a larger obstacle radius (0.3 m) would derived in a critical injury level (AIS 5) because of the 103.5 mm chest deflection. Despite the airbag, at least the fracture of eight ribs would be expected in both situations.

4.3.4 Cluster 4

The effect of a frontal airbag protector in an impact against a flat surface at a velocity of 17 km/h is studied in the last cluster (see figure 4.26). As it was explained in section 4.2.1, these impact conditions could be representative of those happening when the rider falls from his own motorcycle, impacting the ground frontally with the thorax. Additionally they are also similar to those contemplated in the standard EN1621-4 for motorcyclists' airbag protectors. A total of two simulations were conducted to complete the analysis of this Cluster 4.

Figure 4.26: Cluster 3 impact conditions

4.3.4.1 Frontal impact against a flat surface

The main results of the simulation of Cluster 4 impact conditions are summarized in table 4.5. From the strain-based analysis of the rib cage it was concluded that, for the case of impacting without airbag (*C4_V17_R∞_NoAir*), no rib fracture would occurred. Same result was obtained for the simulation with airbag where also no rib fracture would be expected and the airbag contributed in a reduction of the strain values obtained at the rib cortical bone (see figure 4.27).

Simulation	Rib fractures		Deflection (mm)	Compression Criterion	Time (ms)
	Left side	Right side			
C4_V17_R∞_NoAir	None	None	53	AIS 0	50
C4_V17_R∞_Air	None	None	51	AIS 0	60

Table 4.5: Cluster 4 - Simulation Results

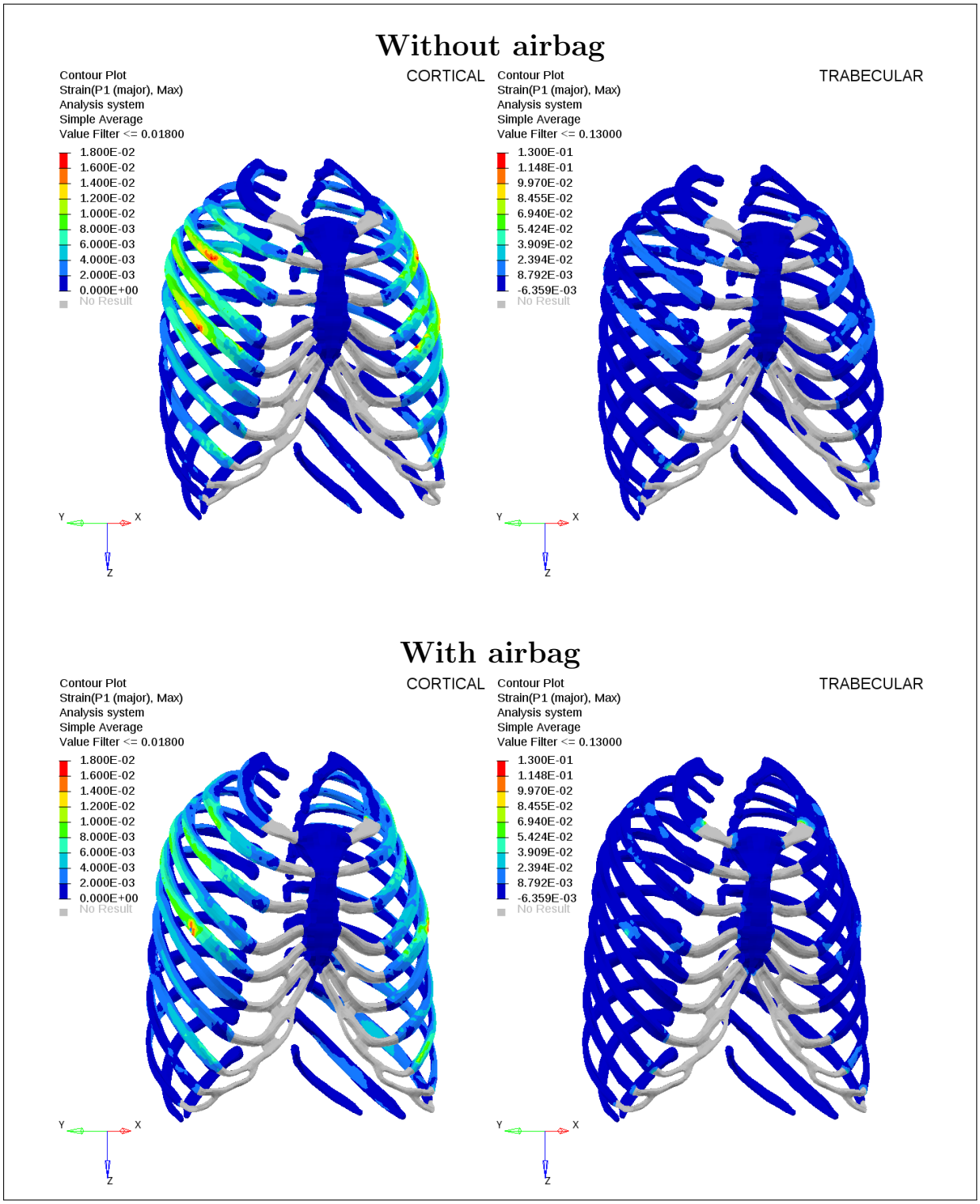

Figure 4.27: Rib principal strain at cortical and trabecular bone for an impact at 17 km/h against a flat object

The chest deflection values measured were 53 mm and 51 mm for the simulation without and with airbag respectively. Both cases would be classified as AIS 0 injury severity according to the Compression Criterion. Similar thorax deformation for both impacts is shown in figure 4.28.

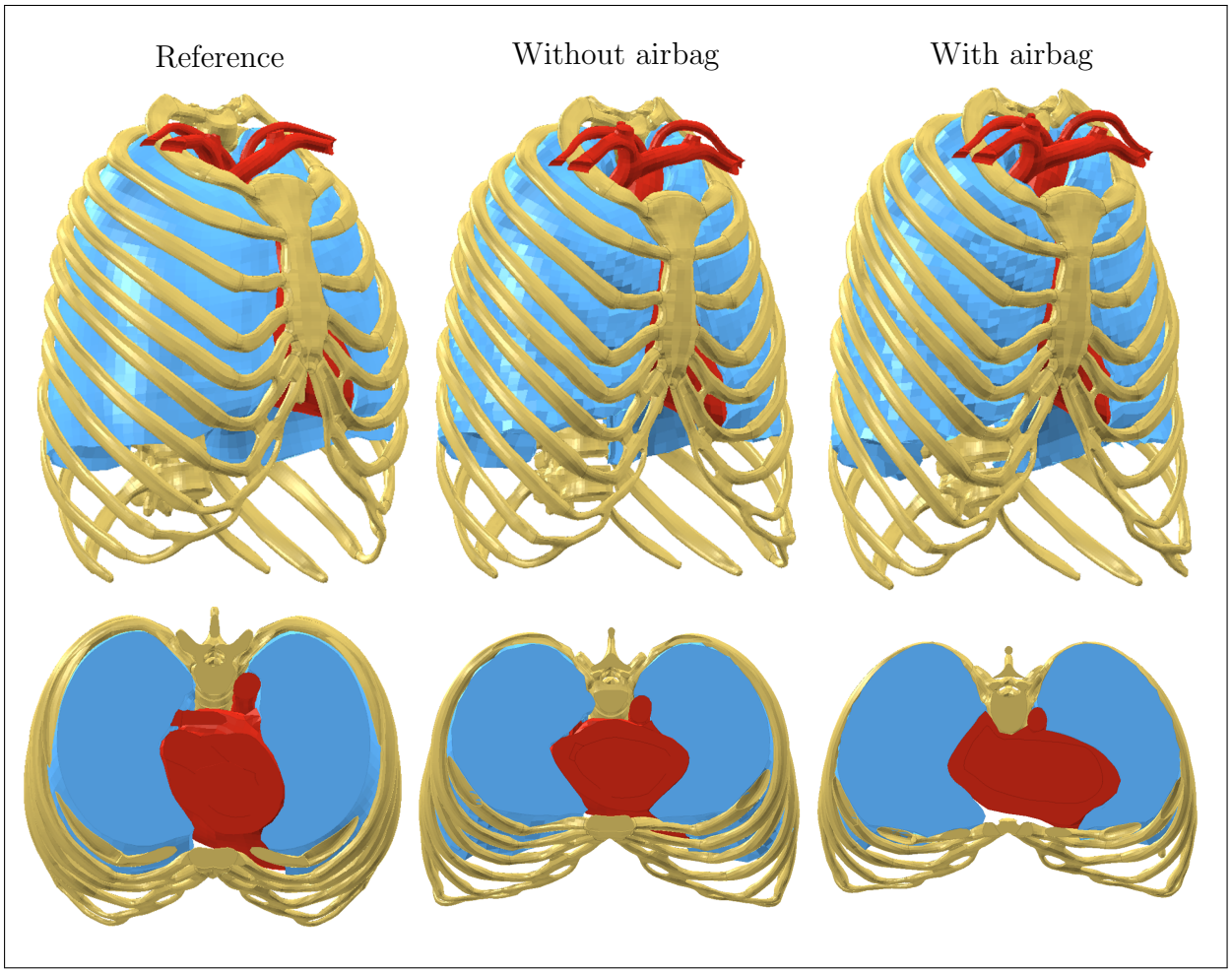

Figure 4.28: Thorax deformation by an impact at 17km/h to a flat surface.

4.3.5 Analogy between vehicle's roof edge and idealized object - Results

In this section a comparision between a frontal impact against an idealized obstacle in horizontal configuration with a radius of 0.075m and an impact against a vehicle's roof edge is presented. Both cases were simulated without airbag protector and for an impact velocity of 30 km/h. Rib strain values obtained from both situations are plotted in the next figure 4.29.

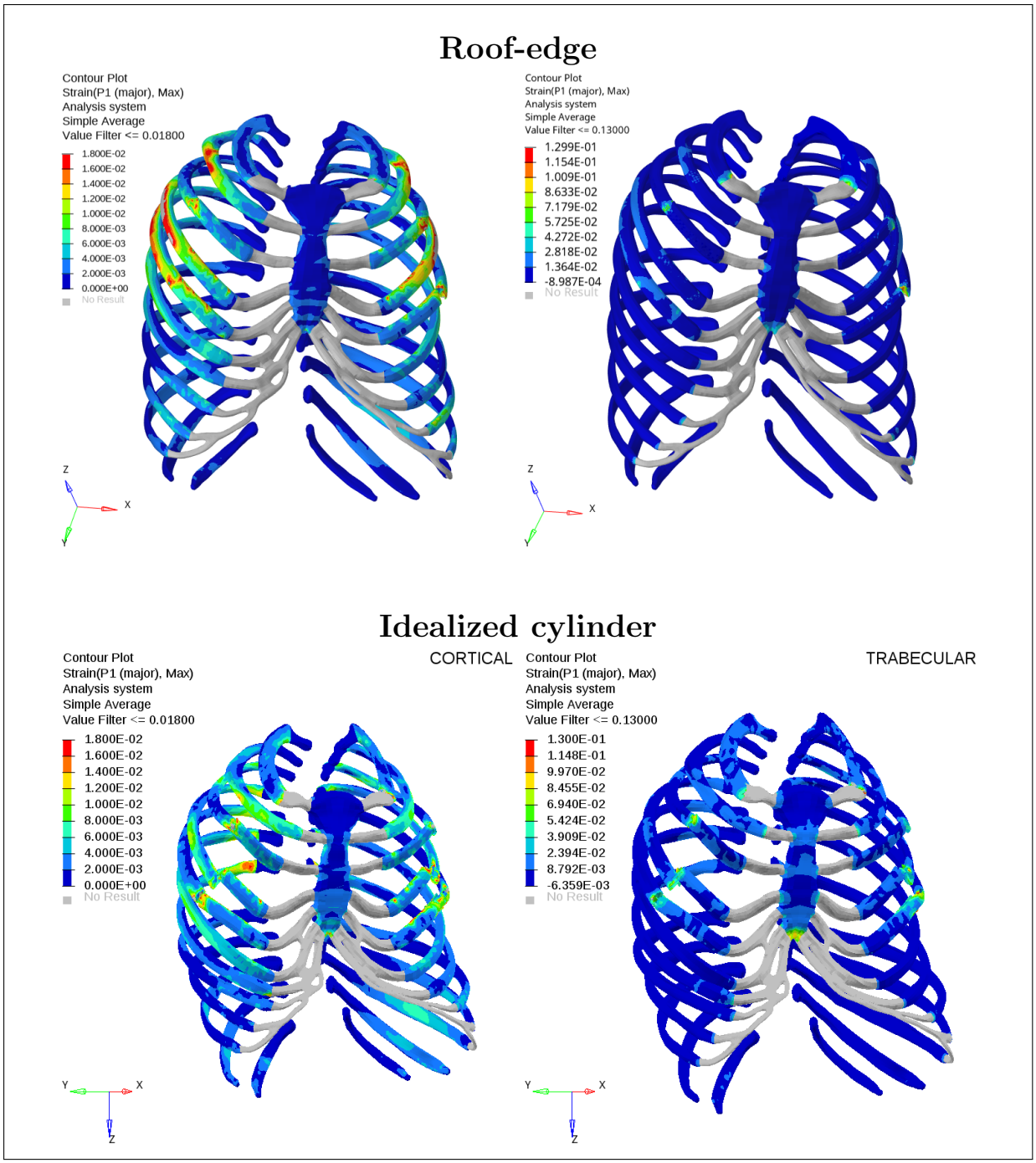

Figure 4.29: Rib principal strain at cortical and trabecular bone for an impact against a vehicle's roof edge and a cylinder with a radius of 0.075 m.

The analysis of the cortical strain values indicated that for both cases the same rib fractures would be expected: 3rd, 4th and 5th ribs of both sites. Regarding the chest deflection similar results were obtained: 94,4 mm were measured for the case of the impact against the roof-edge and 97,2 mm for the impact with the simplified impactor. According to the Compression Criterion an injury severity of AIS 4 would be reported for both situations.

4.4 Discussion

The objective of this chapter was to analyse the potential of injury mitigation of a representative current frontal thorax airbag under realistic impact conditions. Based on the interval areas or clusters identified in the accident analysis carried out by Andreas Thalhammer in his PhD Thesis [92] as those areas with a higher concentration of accidents with thorax injuries, a matrix of simulations was defined in order to study the airbag effectiveness. Every accident scenario identified in each cluster was simulated using the FE human body model GHBMC pedestrian and the frontal thorax airbag protector explained in chapter 3 and then it was compared with the simulation of the same impact situation without protector. In total, 72 simulations were performed considering the boundary conditions of each scenario in terms of velocity, object radius and obstacle orientation. The evaluation of the representative frontal thorax airbag was conducted by the analysis of its influence in the injury mitigation attending to two indicators: the reduction of the number of possible rib fractures based on a maximal principal strain analysis of the rib cage and the reduction of the thorax deflection.

It was found that the effectiveness of the airbag in the reduction of the injury severity varies depending on the cluster analysed. At a lower impact speed, like the 17 km/h of Cluster 4, the airbag was able to reduce the thorax deflection and avoid rib fractures. Also a positive effect was observed for some of the impact scenarios contemplated in Cluster 1 (see Table 4.2). At 20 km/h, the airbag would reduce considerably the injury severity in terms of thorax deflection and in number of rib fractures expected. The airbag would also globally present a significant influence in an impact at 30 km/h but at this impact speed, showing more variation on the protection effectiveness depending on the impact configuration. A total of six rib fractures could be avoided for the cases of horizontal and diagonal object configuration (from six fractures to zero and from ten to four rib fractures, respectively) but only one fracture would be avoided in case of the vertical configuration. According to the Compression Criterion, a reduction of two levels of injury severity (from AIS 4 to AIS 2) would be expected in horizontal configuration but only one (from AIS 3 to AIS 2) and none would be expected for the diagonal and vertical configuration respectively. The importance of the protective effect of the airbag was only remarkable at the horizontal configuration of the object for an impact at 40 km/h. For both object radius, the thorax deflection values measured pointed out that with the airbag the level of injury severity would be reduced from critical (AIS 5) to serious (AIS 3). However this positive result would not imply a significant reduction of the number of rib fractures obtained in the strain-based analysis,

where at least seven fractures could be predicted. Looking at Cluster 3 (Table 4.4), the same situation could be observed for the impact scenarios at 40 km/h. The airbag could provide a mitigation of the injury severity (from AIS 4 to AIS 3) according to the thorax deflection measured and the Compression Criterion but not in terms of ribs fractured where eight fractures would be expected. No significance effect of the airbag was observed in the impact situations at 50 km/h and 60 km/h of this Cluster. In those scenarios, several rib fractures could be predicted (eight or more) reporting also at least an injury severity of AIS 4 according to the measured values of thorax deflection. Similar results were obtained for the situations in Cluster 2 where impacts from 50 to 70 km/h were considered. Despite the fact that in quantitative terms the airbag could slightly reduce the thorax deflection or the number of rib fractures, this performance would not have a qualitative effect on the injury mitigation predicting in all cases a minimum level of severe injury (AIS 4) and ten or more rib fractures.

The findings presented in this chapter should be contemplated carefully because some limitations and some observed discrepancies need to be considered. Firstly, it should be mentioned that the load cases analysed in this study are more severe than those reported by other authors [14] because they are extracted from the Institute of Legal Medicine - LMU accident data which is constituted only by fatal cases. In addition, the selected impact scenarios were simplified by the representation of the obstacles with idealized rigid objects in order to minimize results scatter and reduce the computational time. To show an adequate correspondence between the idealized impact situation and an impact against the roof-edge of a vehicle, a single impact at 30 km/h was simulated and compared. However, it could be interesting to conduct in the future a sensitivity analysis to demonstrate this correpondence for other impact velocities or to identify a possible influence of the relative stiffness between the human body and the obstacle. Regarding the boundary conditions for the simulation extracted from the accident analysis it should also be mentioned that, in comparison with other publications where the effectiveness of a frontal thorax airbag is analysed by the numerical simulation of a moving object impacting a fixed human body model [25, 93], in this study the airbag performance was analysed through the simulation of the accident scenario of a moving body impacting a fixed obstacle. As it was proved for the case of the head [45], it could be supposed that the global kinematics and the inertia of the motorcyclists may also affect the thorax risk injuries. Despite the mass of a 50th percentile male thorax is considered to be around 23.4 kg [99], this value could not correspond with the equivalent mass involved in a real accident. This possibility was contemplated in this thesis and therefore, the impact configuration used should be considered to be more realistic than the one used in previous studies, implying also an analysis of the airbag performance closer to the reality.

Another limitation of the work presented in this thesis is that for the analysis of the effectiveness of a frontal thorax, a conceptual finite element model representative of a real frontal thorax airbag was used in this work and not a fully validated model reproducing exactly a product available in the market. The FE airbag was modelled with a simple shape and only the main operating characteristics of a real product regarding impact

absorption like the pressure, thickness and volume were considered for the modelling. These parameters were obtained experimentally as it was exposed in chapter 3. However, other factors that may affect the performance of the airbag like the real bag shape or the possible effect of ergonomics in the airbag coupling with the human body were not contemplated in the modelling. In addition, the analysis of the correct accident detection and airbag activation was not contemplated is this work and the airbag was modelled with a constant pressure value. Therefore, the impact situation was always calculated when the airbag was fully inflated at the prescribed value not considering possible variations during the inflation process [25]. Nevertheless, taking into account these limitations on the airbag modelling, an extensive analysis of the protection effectiveness of a frontal thorax airbag, which could be representative of some real products, was conducted. From this assessment it was found that the protection provided by an airbag in a frontal thorax impact would be strongly influenced by the impact speed. At those impact situations analyed for an impact speed below 30 km/h, the airbag was able to provide an effective protection. In alignment with the findings exposed by Serre *et al.* (2019) [84], at those accident simulations with an impact velocity from 30 to 40 km/h, the airbag could only provide a limited protection and the airbag performance would be also influenced by others factors like the impact configuration highlighting the object positioned in horizontal as the impact configuration whereby the airbag would supply more effectiveness. At higher impact speeds than 40 km/h no significant effect of the airbag in the injury mitigation was obtained.

In the understanding and examination of the results arisen in this work, some limitations of the human body model GHBMC should also be considered. Mainly, those related with the modelling of the rib cage and the costal cartilage. The costal cartilage plays a crucial role in the structural stiffness and elasticity of the thorax proportioning a flexible joint between the anterior ends of the ribs and the sternum [48]. However, the process of calcification or ossification of the hyaline cartilage mid-substance of the costal cartilage inherent with age produces inhomogeneities of the costal cartilage which vary the local material properties [41, 53]. Those inhomogeneities produced by calcification of the costal cartilage can significantly affect the mechanical response of this human structure [68, 9]. Despite some authors try to solve this issue by appliying individually-meshed cartilage segments [41, 40] or by applying an indexing system [48], the modelling of the human body model GHBMC, like at other commercial FE human body models, is a simple representation with homogeneus material properties [19, 79, 44]. This homogeneity of the material properties generates artificial limits between the cartilage part and the bone components which are modelled with other material properties. This discontinuity, which does not exist in the reality where the junction between the ribs end and the cartilage is constituted by a tissue transition region, could affect also the structural behaviour of the HBM rib cage. It was observed during the analysis of the deformations of the ribcage that these artificial limits between the anterior rib ends and the costal cartilage could be acting as stress concentrations and could lead to a false interpretation of the strain values obtained in a strain-based analysis of possible rib fractures. This effect was observed in all impact configurations but it was extremely remarkable for impacts against a vertical object where the object were

aligned with the sagittal plane and the load was very concentrated in the sternum. At the other configurations, the stress concentration was more evident at the first rib of both sides, which is the reason why the fracture of those two ribs were not considered in the analysis of any of the simulations conducted. The incorporation of calcificated areas in the modelling of the costal cartilage as well as the modelling of a more continuous transition in terms of material properties between the anterior rib ends and the costal cartilage arise as two issues to be improved in order to obtain human body models with a more biofidel thorax response to external loading. It should be also considered that global force-deflection response of the thorax of the GHBMC Pedestrian is not specifically validated against frontal impacts. The pedestrian version of the model is implemented with the same material properties as a validated model, the occupant version, but both thoraces are slightly differently positioned and this point may affect the force-deflection response at this kind of loading.

The assessment of the protective effect provided by the frontal airbag was based on two procedures implemented for the estimation of skeletal injuries. Therefore, an evaluation of the possible soft tissue injuries, for example by calculating the Viscous response like other authors [25], was not included in this study and it could be implemented in a future work to complement the results here obtained. The possible injuries derived from the impact situation were evaluated attending to two different methods or criteria. Firstly, a deterministic method based on the analysis of the maximal principal strain at the cortical bone of the ribs was used to predict the possible number of rib fractures occurring after the impact. In addition, the injury severity was estimated by the measurement of the thorax deflection and the posterior the application of the Compression Criterion. This criterion, developed by Kroell *et al.* [52], correlates the thorax compression with the AIS injury severity based on the thorax deflection measurements obtained from the author in a set of blunt thoracic impacts. However, a mismatching between both methods was noticed. For some of the impact situations, the thoracic skeletal AIS values in terms of rib fractures predicted with the Compresion Criterion differed from the number of rib fractures obtained with the estimation of those fractures following the strain-based analysis. The origin of this discrepancy in the results could be the method used for the measurement of the thorax deflection. As it was explained in the section 4.2.2, the thorax deflection was defined as the distance between the midpoint of two nodes taken on the pectoral muscles and a node taken on the skin at the level of the center of the 8th thoracic vertebra (T8) and it was calculated following the method proposed by Poulard *et al.* [73] transferred to the pedestrian version of the GHBMC. This method was proposed in the framework of the validation of the GHBMC thorax and reported as the closest to the original definition given by Kroell *et al.* [52] in their experiments. However, those experimental load cases consisted on symmetrical impact loading of the thorax and therefore the method chosen may not be the most adequate for some of the impact situations here analysed. As the midpoint between both pectoral muscles is a virtual point not physically associated with a node of the model, its position during the impact simulation was calculated in this work by the interpolation of two nodes symmetrically positioned at the pectoral muscles. This method could lead to the underestimation of the deflection value measured not only in

asymmetric load cases like the diagonal configuration of the object but also in the vertical configuration where the loading is applied symmetrically but the two points selected for the calculation of the position of the anterior midpoint were not directly hit during the impact. This underestimation was not observed at the horizontal configuration were the loading was also applied symmetrically. A possible solution for this issue could be to chose more interpolation points for the calculation of the position of the anterior midpoint in order to record more accurately the possible compression of the thorax under not symmetric loading. Another possible solution would be to conduct more experiments were the loading would not be apply symmetrically in order to evaluate the global response of the thorax against these loadings and to implement its corresponding injury risk criteria, thus extending the Compression Criterion to non symmetrical loads.

Despite all the limitations explained, in this chapter a global evaluation of the possible protection effectiveness of a representative frontal airbag protector was presented through the simulation in a finite element environment of different realistic impact situations obtained from the accident analysis. The results here presented showed that an airbag could provide a limited protection establishing a velocity of 30 km/h as the border impact velocity where an airbag could provide a significant injury mitigation. In further steps, the efficiency of such a device should be also evaluated in an experimental procedure which, in comparison with the current test standard EN1621-4 for thorax airbags, should be based on biomechanical criteria.

Chapter 5

Analysis of a potential test procedure for frontal thorax airbags

5.1 Introduction

The conjunction of a group of factors like their limited structural protection, an inherent instability, their higher power-to-weight ratios, their poor visibility because of their size and shape in comparison with other motorised vehicles, make the Powered Two-Wheelers one of the most dangerous modes of road transportation. In Europe, the risk of death for motorcyclists is 20 times higher that for car occupants [37]. Notwithstanding the high risk of suffering an accident by riding a motorcycle, the use of personal protective equipment among Powered Two-Wheelers users is significantly low [94], specially in some European countries [8]. The unique exception is the helmet which is extensively used in Europe probably because its wearing is mandatory.

The personal protective equipment available on the market in Europe is certified by different standards developed by the European Committee for Standardization (CEN), like for example the EN13594 [29] for the standardisation of gloves, the EN13634 [30] for shoes or the EN1621 [31] for impact protectors. Different available standards, like the Snell M2010 [87] or the DOT FMVSS 218 [34] from USA or the AS/NZS 1698/2006 [13] from Australia and New Zealand, regulate the standardisation of the helmets depending on the world but the European standard ECE 22.05 [76] is the most extended [75]. However, several authors like Newman (2005) [67] or Pratellesi *et al.* (2011) [75], questioned the suitability of this standard due to the low biofidelity, the impact conditions not derived from accident data and specially the obsolete pass-fail criteria. The ECE 22.05 considers only the linear acceleration for the certification of motorcyclist helmets establishing a limit of 275 g and a value of 2400 for HIC but does not considered the deceleration forces caused by the rotational kinematics of the head which are marked as the main origin of brain injuries [77]. For that reason, several studies were conducted to create FE head models where the complexity of head and brain dynamics were considered and a tissue level injury criterion

could be introduced [20, 102, 91, 81] leading to the proposal of coupled experimental-numerical test methods for the evaluation of motorcyclists helmets [21]. Inspired by the effort in the improvement of the helmet standards and facing the various airbag jackets today available on the market, some doubts about the suitability of the standard EN1621-4 for the evaluation of those devices in terms of protection have emerged. In a recent study by Aranda *et al.* [11] some of the limitations of the current standard test procedure indicating the lack of enough sensitivity of the impact test method to distinguish the optimal inflated thickness/pressure combination were described and the necessity of introduce biomechanical parameters for the protection assessment instead of the only measurement of the transmitted force suggested.

The apparently low biofidelity of the current standard for frontal airbag protectors together with the necessity of a new test procedure, which should reproduce more realistic accident impact conditions or at least closer to a real accident, motivate the research into a new assessment method of the frontal thorax airbag protection. As part of its activities, the PIONEERS project (Protective Innovations Of New Equipment for Enhanced Rider Safety) addresses this topic in order to develop a more reliable test method. For that purpose, based on the identified most common accident situations, a new test set-up [70] was developed considering biomechanical parameters as the main indicators for the evaluation of frontal thorax airbag. In the future, the procedure and test machine introduced by PIONEERS could replace the current standard test method for frontal thorax airbags or be implemented as a supplement for the airbag certification.

In this chapter, the new test procedure introduced by PIONEERS [71] is analysed in a virtual environment in order to identify its possible limitations and to explore, following the path of helmets testing, the feasibility of using this new test procedure for the development of an numerical-experimental test method for the evaluation of motorcyclists thorax airbags. The analysis presented in this work was divided into two steps. Firstly, the translation of the impact conditions identified in a real accident situation into appropiate and representative test environment impact conditions was investigated based on the thorax response and then, the difficulties entailed in this process were analysed. For that purpose, a sensitivity study evaluating the effect of the impact speed and mass was conducted calculating several numerical situations of the investigated impact configurations. A possible influence of an airbag protector was also evaluated with the simulations of those impact situations using two different airbag FE models. Then, the possible relationships between the experimental findings and the results obtained from the simulations of the rider-to-object configuration under the same boundary conditions and using the human body model GHBMC were investigated. Both processes were based on the thorax response determined by two biomechanical criteria: thorax deflection and the Viscous response [97].

5.2 Methodology

5.2.1 Bridging the gap between the accident scenario and the test impact conditions

In a motorcycle accident the rider usually impacts another object causing the loading of the thorax. In terms of boundary conditions, it means that a moving mass (the body of the rider) of approximately 75 kg (if the rider corresponds with the 50th percentile male) would impact a fixed rigid object (rider-to-object configuration). As it was shown on the previous chapter 4, this could be represented by the simulation of the impact against an obstacle using a HBM as representative of the rider's body, obtaining some information about the possible injuries like rib fractures or some indicators like the thorax deflection. However, the translation of these impact conditions into a repeatable, simple, cheap and more biofidelic and realistic test is still a challenge. Trying to fulfil these requirements, the PIONEERS project proposed a test with an inverse configuration (object-to-rider configuration) where a moving object would impact a fixed thorax [71]. An object-to-rider configuration would allow to increase the reproducibility and also would reduce the technical complexity. In addition, the use of a Hybrid III dummy thorax was proposed as a surrogate of the rider to achieve more biofidelity in comparison with the current standard test procedure. These test conditions are assumed in this work as the basis for a feasible and more realistic test for the evaluation of the protection provided by frontal thorax airbags in case of a motorcycle accident. The remaining open question is if an equivalence between both situations could be found (see Figure 5.1).

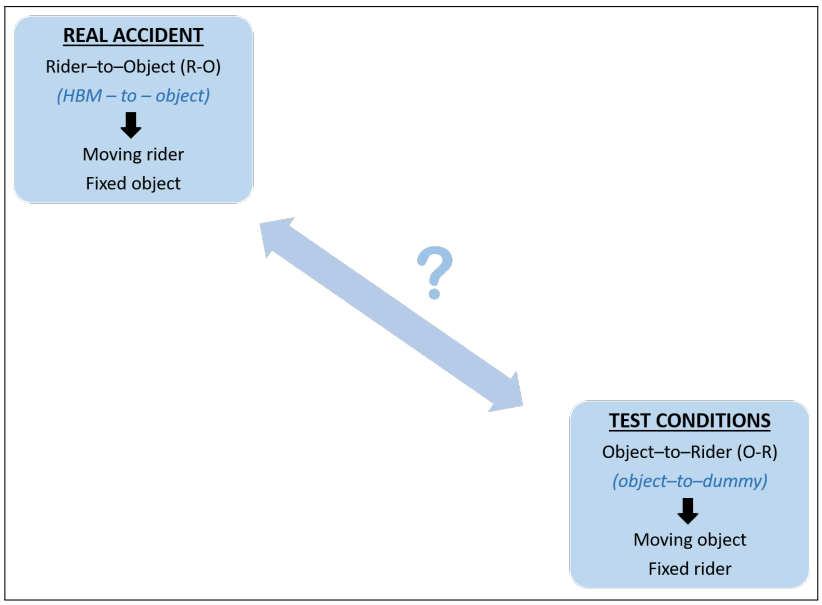

Figure 5.1: Summary of initial procedure states: accident and test impact conditions.

Starting from the requirement that the new test procedure should be as close as possible to the reality, the first step in the search of this equivalence should be the translation of the rider-to-object impact configuration into a object-to-rider configuration. This translation implies the calculation of the mass of the striker (impacting object), which should be equivalent to that portion of the mass of the rider involved in the impact situation in order to obtain the same thorax response. However, different thorax behaviours could be expected between the dummy and the HBM because of their different rigidities and therefore a direct comparison between the initial situations should not be conducted. For that reason, the representation of a real accident using a dummy in a rider-to-object configuration is needed (see Figure 5.2). The objective of this intermediate step is to determine the behaviour of the thorax of the dummy in a frontal thorax impact and compare it to the response of the dummy thorax at the inverse configuration. A sensitivity analysis to determine the mass which provides an equivalent thorax response would be needed at this point.

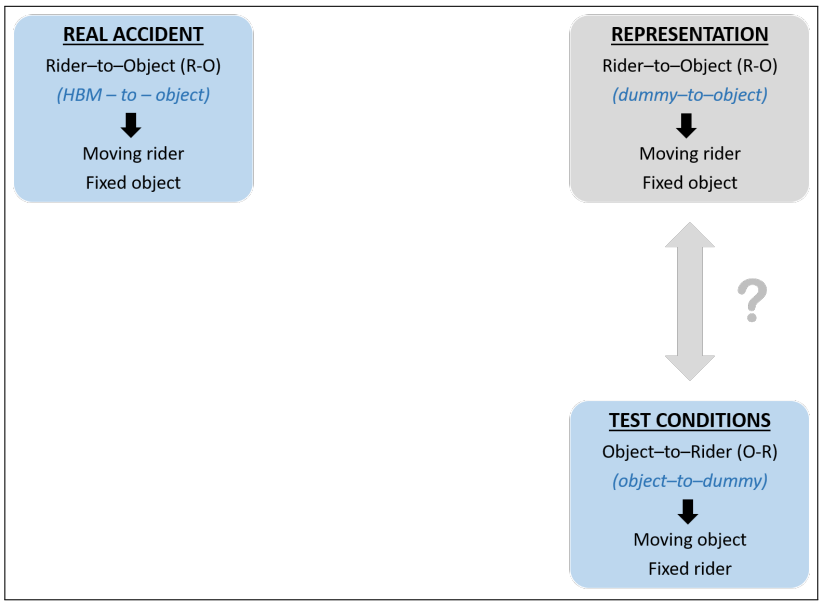

Figure 5.2: Intermediate step: Determination of the equivalent mass.

Once the equivalent mass would be obtained, the next step should be to investigate the possible relationships between the HBM and the dummy in the rider-to-object configuration. When both relationships are established, it could be possible to define an equivalence system between some of the test results and those expected in a real accident scenario (see Figure 5.3).

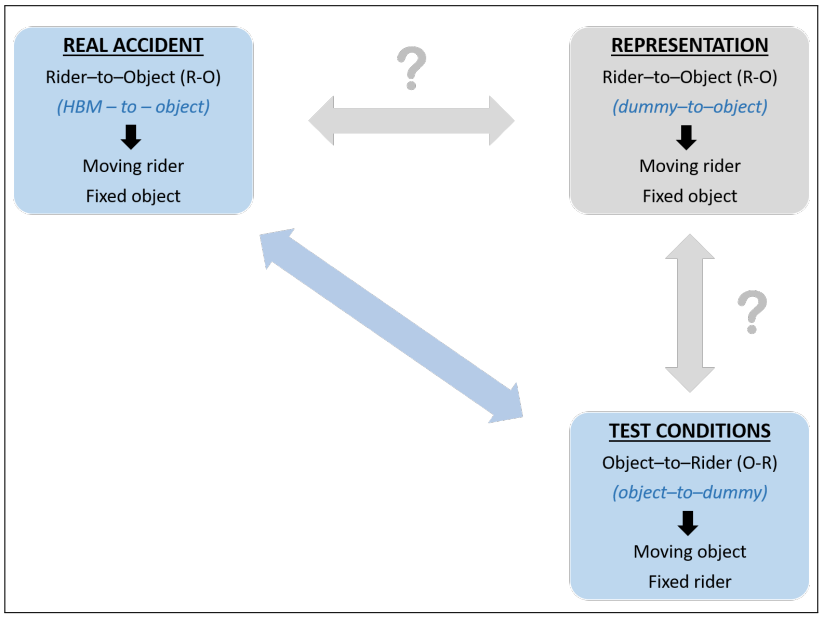

Figure 5.3: Possible equivalence between the real accident scenario and the new test procedure.

In this work, an analysis using numerical simulations was conducted, in order to find the equivalences explained before and to evaluate the feasibility of this new test procedure.

5.2.2 Feasibility of the new test procedure

The analysis of the feasibility and possible limitations of the test procedure exposed in the previous section 5.2.1 was conducted in a numerical environment and it was divided in two parts. Firstly, a sensitivity analysis was performed to determine the equivalent mass of the rider's surrogate (a Hybrid III dummy) necessary to translate the impact conditions of a rider-to-object into a object-to-rider configuration. In the second part, the response of the two rider-to-object impact situations contemplated in the procedure (HBM and Hybrid III dummy impacting a fixed obstacle) were compared in order to investigate possible similarities.

Equivalent mass: sensitivity analysis

An adequate translation of the rider-to-object configuration into an object-to-rider configuration, and therefore a reproduction of the reality by the test procedure as closely as possible, is conditioned by the determination of the mass of the impact object. This mass value should be equivalent to that portion of the mass of the rider involved in the accident and, after an impact against the fixed Hybrid III, should proportionate the same thorax response as those expected in a rider-to-object impact configuration for the same boun-

dary conditions. For that reason, a sensitivity study based on numerical simulations was conducted to estimate this mass value. In the study, a FE model of the Hybrid III dummy and a rigid cylinder with a radius of 100 cm were used for representing the rider and the impact object respectively (see Figure 5.4).

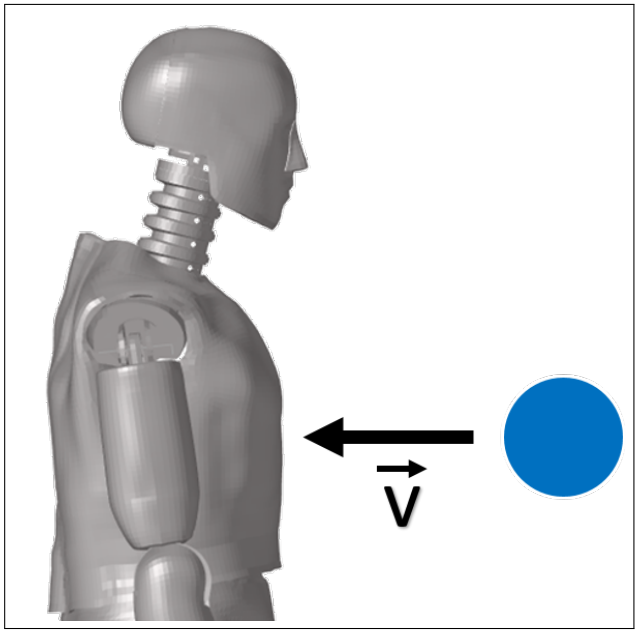

Figure 5.4: Simulation of the object-to-rider impact configuration with the Hybrid III dummy model.

To perform this sensitivity study, a table of simulations was defined. Firstly, the rider-to-object configuration was simulated at four different impact speeds. The first velocity selected was an impact at 30 km/h, which it was found in the previous chapter as the limit velocity for a remarkable protection performance of a frontal thorax airbag. The second impact speed selected was the same as the velocity used in the test procedure of the EN 1621-4 [33], 16 km/h (4.4 m/s). The third was 25 km/h, velocity chosen in PIONEERS D3.2 for the evaluation of thorax airbag devices. The last velocity selected was 20 km/h, a value between the two previous ones explained. The simulation at different impact velocities was motivated by the premise of a possible influence of the impact velocity in the value of equivalent mass. On a second step, the object-to-rider configuration was simulated for the same impact velocities with four different values of mass assigned to the impact object. The mass values considered for the study were: 23.4 kg (reported by some authors as the mass of a human thorax [101]), 37.5 kg (the half of the total mass of a 50th percentile man) and two values in between, 30 kg and 33.75 kg. Figure 5.5 summarizes both configurations. To determine the equivalent mass, both configurations were compared based on the Hybrid III thorax response attending specially two biomechamical parameters: thorax deflection

and the maximal Viscous response according to the Viscous Criterion [97].

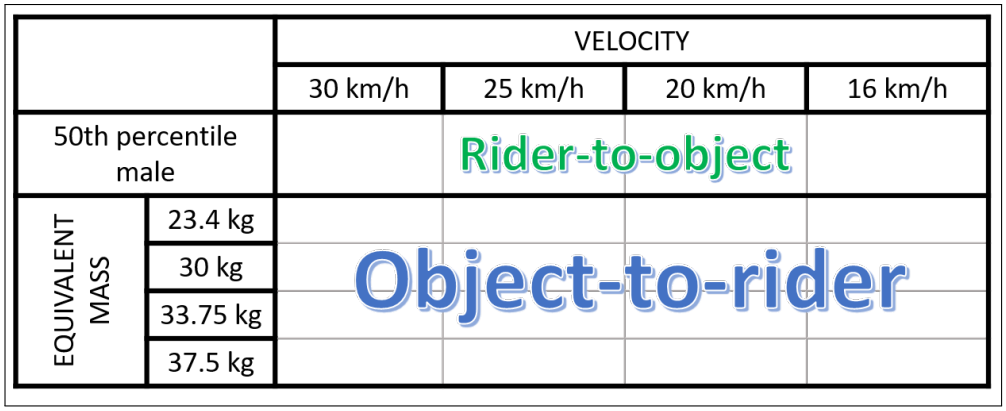

Figure 5.5: Impact conditions of the sensitivity study.

The simulations previously described were calculated not only for the case of no airbag protection, but also for the case of two different FE models of a frontal thorax airbag. The first airbag (Airbag A) integrated in the study was the one previously used in the chapter 4 and whose modelling process was explained in the chapter 3. The second airbag (Airbag B) was a variation of the previous one, modelled with a lower thickness (3.5 cm) and inflated with a higher pressure (3 bar). Both of them would be certified according to the standard EN 1621-4 impact attenuation requirements and their main characteristics are shown in table 5.1. The aim of simulating both configurations also using two different airbags is to preliminarily investigate a possible influence of the airbag in the calculation of the equivalent mass. In total 60 simulations were calculated in this sensitivity study: 12 simulations corresponding to the rider-to-object configuration and 48 to the object-to-rider.

	Thickness (cm)	Pressure (bar)	Transmitted Force (kN)	EN1621-4 Level of protection
Airbag A	8.5	0.65	0.8	2
Airbag B	3.5	3	3.2	1

Table 5.1: Main characteristics of the airbag models used in the sensitivity study.

Response comparison between HBM and the surrogate Hybrid III dummy

In this second part of the feasibility analysis of the new test procedure exposed in the previous section, the response of the Hybrid III thorax was compared with the response of the thorax of the HBM in the rider-to-object impact configuration in order to explore possible correlations. For that purpose, the impact of the GHMBC pedestrian model against a fixed object (see Figure 5.6)was simulated reproducing the same boundary conditions

described in previous section for the impact of the Hybrid III in the rider-to-object configuration. Both thorax responses were compared in terms of thorax deflection and Viscous response. Considering the four impact velocities and the three different levels of protection contemplated in the sensitivity analysis, a total of 12 simulations were conducted in this section using the human body model GHBMC pedestrian.

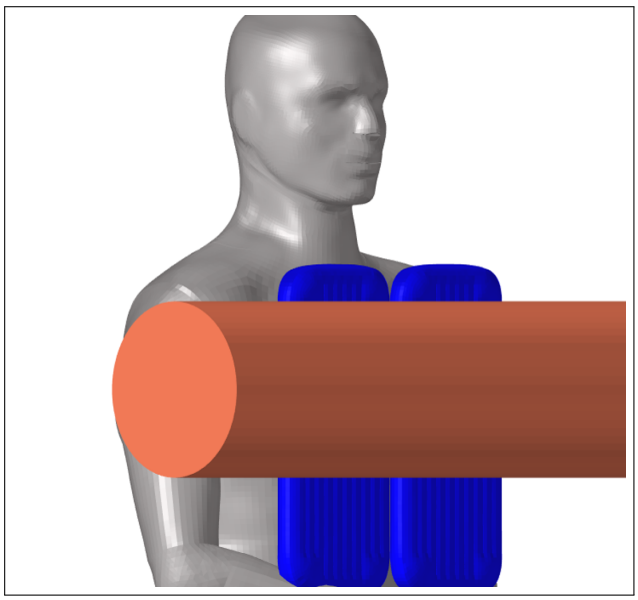

Figure 5.6: Simulation of the object-to-rider impact configuration with the Hybrid III dummy model.

5.3 Results

In this part of the study, the results obtained from the numerical simulations are presented. Considering the two steps proposed in the previous section 5.2.2 to analyse the feasibility of the new test procedure, a total of 72 simulations were calculated: 60 using a FE model of the Hybrid III dummy and 12 using the GHBMC pedestrian model.

5.3.1 Sensitivity analysis

The values of thorax deflection and Viscous response were used in this section to determine the possible equivalent mass for the translation of the rider-to-object impact configuration into a object-to-rider one and to explore the possible influence of a protective frontal thorax airbag in the calculation of this value. Considering the three different protection conditions evaluated (no airbag, airbag A and airbag B), a total of 60 simulations were conducted in

this analysis using the FE model of a 50th percentile Hybrid III dummy: 12 simulations corresponding to the rider-to-object configuration and 48 simulations corresponding to the inverse one. For all cases, the dimensions of the object were the same with a radius of 100 cm. All results obtained from the simulation of both impact configurations in terms of thorax deflection and Viscous response are presented in the tables 5.2 and 5.3 respectively.

Thorax deflection (mm)				
	NO AIRBAG			
	8.3 m/s	7 m/s	5.7 m/s	4.4 m/s
Rider-to-object	108	101.8	88.3	70.5
23.4 kg	99.4	86.5	71.9	56.5
30 kg	108	96.8	81.3	64.1
33.75 kg	110.3	101.8	86.5	68.3
37.5 kg	111.4	105.8	91.1	72.4
	AIRBAG A			
	8.3 m/s	7 m/s	5.7 m/s	4.4 m/s
Rider-to-object	97	82.8	65.2	50.3
23.4 kg	78	63	49.8	38.4
30 kg	87.2	73.7	58.3	44.4
33.75 kg	93	78.9	63.2	47.6
37.5 kg	98.6	82.9	68	50.8
	AIRBAG B			
	8.3 m/s	7 m/s	5.7 m/s	4.4 m/s
Rider-to-object	100	91.8	74.8	59.2
23.4 kg	88.4	76.2	62.2	48.3
30 kg	96.5	85.5	71	54.9
33.75 kg	100.4	89.9	75.5	58.8
37.5 kg	104	94	80	62.7

Table 5.2: Thorax deflection values obtained from the rider-to-object configuration and possible equivalent masses in object-to-rider configuration.

Attending to the thorax response observed from the simulation of both configurations without an airbag, no definitive value of equivalent mass could be determined. For an impact at 8.3 m/s, an equivalent mass of 30 kg would match the same thorax deflection value (108 mm) in an object-to-rider configuration. However, at 7 m/s, it would be necessary to increment the equivalent mass up to 33.75 kg to obtain the same deflection response (101.8 mm). In addition, an object with a mass between 33.75 kg and 37.5 kg would fit a similar deflection for an impact at 5.7 m/s km/h and 4.4 m/s respectively. Looking at the Viscous response, a mass close to 30 kg would provide similar thorax responses for an impact at 7, 5.7 and 4.4 m/s respectively. Nevertheless, the Viscous response obtained at

30 km/h with an impactor of 30 kg would be slightly higher (2.64 m/s) than the response obtained in a rider-to-object impact configuration (2.52 m/s).

Viscous Criterion response (m/s)				
	NO AIRBAG			
	8.3 m/s	7 m/s	5.7 m/s	4.4 m/s
Rider-to-object	2.52	1.84	1.21	0.72
23.4 kg	2.28	1.66	1.08	0.57
30 kg	2.64	1.88	1.22	0.7
33.75 kg	2.82	2.02	1.3	0.74
37.5 kg	2.96	2.17	1.39	0.78
	AIRBAG A			
	8.3 m/s	7 m/s	5.7 m/s	4.4 m/s
Rider-to-object	1.83	1.19	0.52	0.27
23.4 kg	1.04	0.58	0.32	0.19
30 kg	1.68	0.78	0.43	0.23
33.75 kg	1.88	0.91	0.49	0.26
37.5 kg	2.05	1.13	0.54	0.27
	AIRBAG B			
	8.3 m/s	7 m/s	5.7 m/s	4.4 m/s
Rider-to-object	2.22	1.51	0.96	0.58
23.4 kg	1.7	1.13	0.69	0.39
30 kg	1.83	1.34	0.88	0.49
33.75 kg	1.91	1.53	1	0.57
37.5 kg	2.04	1.69	1.1	0.61

Table 5.3: Maximal Viscous Criterion response values obtained from the rider-to-object configuration and possible equivalent masses in object-to-rider configuration.

The thorax response in terms of thorax deflection and Viscous Criterion obtained from the simulations with airbag A and B show variation in the equivalent mass required for translation of the rider-to-object into a object-to-rider configuration and also differ with the no airbag condition. Figure 5.7 summarize the thorax responses showed by the three protective conditions varying the velocity for prescribed equivalent masses in comparison with the thorax response obtained in the rider-to-object configuration.

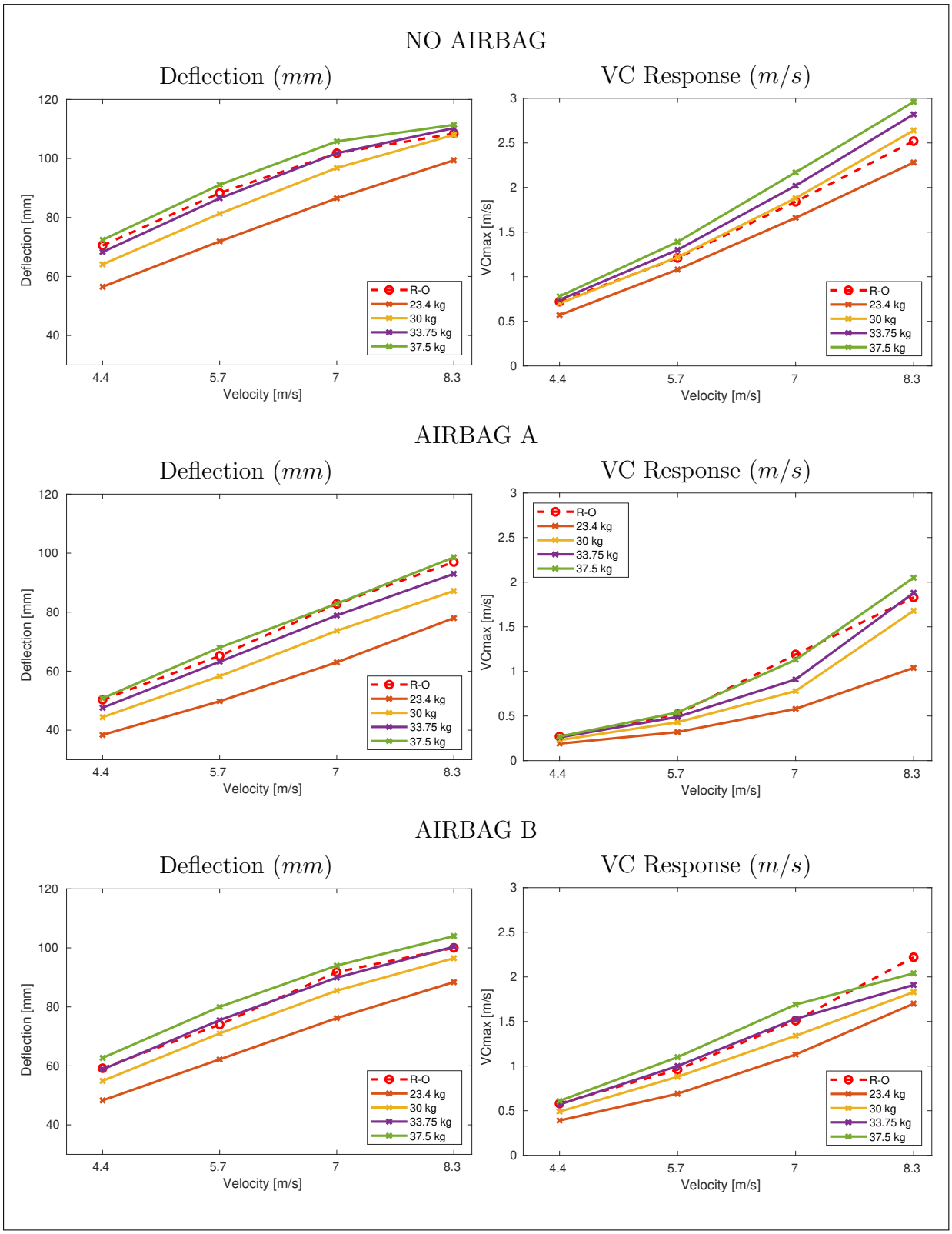

Figure 5.7: Comparison of thorax deflection and maximal Viscous Criterion response of both impact configurations under three different protective conditions for a variable equivalent mass and the applied velocities.

For the case of airbag A, the thorax deflection values measured indicates a correspondence with an impact using a mass of 37.5 kg at 7 m/s and 4.4 m/s. At 8.3 m/s and 5.7 m/s the thorax deflection would match with an equivalence mass lighter than 37.5 kg but heavier than 33.75 kg. A higher variety of the possible equivalent mass has been observed considering the the Viscous Criterion response. For each different impact velocity, a different value of the necessary equivalent mass is found in order to generate the same Viscous response in the object-to-rider configuration compared with the one obtained in the rider-to-object configuration. Less variation can be observed with airbag B, where a mass of 33.75 kg for the impact object would generate similar thorax responses obtained in rider-to-object configuration for the most of the velocities contemplated in the sensitivity analysis. Only a significant discrepancy would appeared in the Viscous response at 30 km/h where a mass higher than 37.5 kg would be required to provide the 2.22 m/s maximal Viscous response expected in the rider-to-object configuration. Figure 5.8 summarizes all the deflection and Viscous Criterion response value for all mass-velocity combinations simulated and for the three protection levels evaluated (no airbag, airbag A and airbag B).

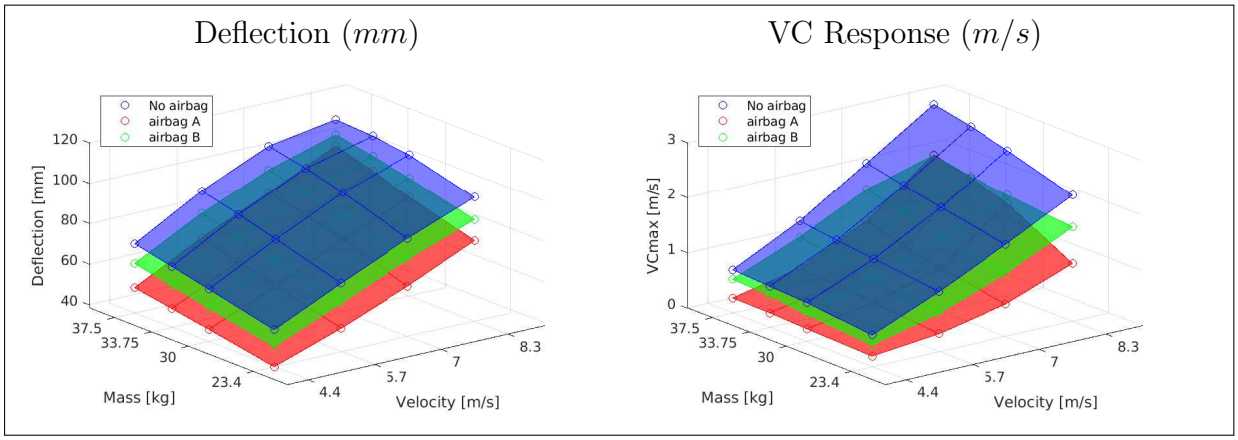

Figure 5.8: Thorax deflection and Viscous Criterion response as a function of the combination of equivalent-mass velocity for three different protection levels.

5.3.2 HBM vs Dummy thorax response: Results

In this section, the thorax responses of the Hybrid III dummy an the GHBMC were compared in order to find a possible correlation. For that purpose, in addition to the rider-to-object simulations calculated in the previous section 5.3.1 with the Hybrid III dummy, 12 new simulations using GHBMC pedestrian were conducted also in the rider-to-object configuration following the same boundary conditions: four different impact velocities (8.3 m/s, 7 m/s, 5.7 m/s and 4.4 m/s), an impact object with a radius of 100 cm and three different protection levels (no airbag, airbag A and airbag B). Table 5.4 collects the thorax deflection and Viscous response values obtained from the GHBMC simulations.

Thorax deflection (mm)				
	8.3 m/s	7 m/s	5.7 m/s	4.4 m/s
No airbag	88.5	83	77	72
Airbag A	74.6	67.8	60.8	53.5
Airbag B	80	74.3	68	58.8
Viscous Criterion response (m/s)				
	8.3 m/s	7 m/s	5.7 m/s	4.4 m/s
No airbag	2.73	2.13	1.55	1
Airbag A	0.77	0.64	0.43	0.4
Airbag B	1.92	1.45	1.1	0.81

Table 5.4: Thorax response in terms of thorax deflection and Viscous Criterion response obtained from the simulation of the rider-to-object configuration with GHBMC pedestrian.

Attending to the results obtained, the change of the response of the GHBMC and Hybrid III dummy are mostly different. Only for the no airbag situation a nearly linear estimation could be defined between the Viscous response of GHBMC and Hybrid III dummy (see figure 5.9). Some further observations can be summarised. Firstly, looking at the thorax deflection, a virtually linear behaviour with respect to the velocity of the GHBMC thorax response was observed, in contrast to the dummy response. Despite similar values of deflection were reported at 4.4 m/s for all protection levels, the deflection increment observed between 4.4 m/s and 8.3 m/s was between two and four times larger for the dummy than for the HBM: 38 mm versus 13 mm for no airbag, 47 mm versus 11 mm for airbag A and 41 mm versus 22 mm. In addition, a saturation behaviour of the dummy thorax is perceptible as of 90 mm deflection. Secondly, the positive effect of the airbag protectors with respect to the no airbag situation was more evident in the HBM simulations, especially for the Viscous Criterion response.

The thorax deflection reduction provided by the two airbags used was similar for the case of HBM as well as the dummy. For example, for airbag A, at 4.4 m/s impact speed a reduction of 20 mm was measured with the HBM against the 19 mm measured with the dummy. Or at 8.3 m/s, -11 mm would be reported with the dummy versus -14 mm with the HBM. At the same mentioned impact speeds, the airbag B would reduce the thorax deflection by 11 mm versus a reduction of 14 mm measured with the HBM and -8 mm for the dummy against the -14 mm measured with the HBM would be reported at 8.3 m/s. However, larger differences were observed attending to the Viscous response values. At high impact speed (8.3 m/s) this divergence would be remarkable obtaining with the Hybrid III dummy a reduction of the maximal Viscous response of 0.7 m/s and 0.4 m/s for airbags A and B respectively against a reduction of 2 m/s and 0.8 m/s at the simulation of the same impact scenario with the GHBMC.

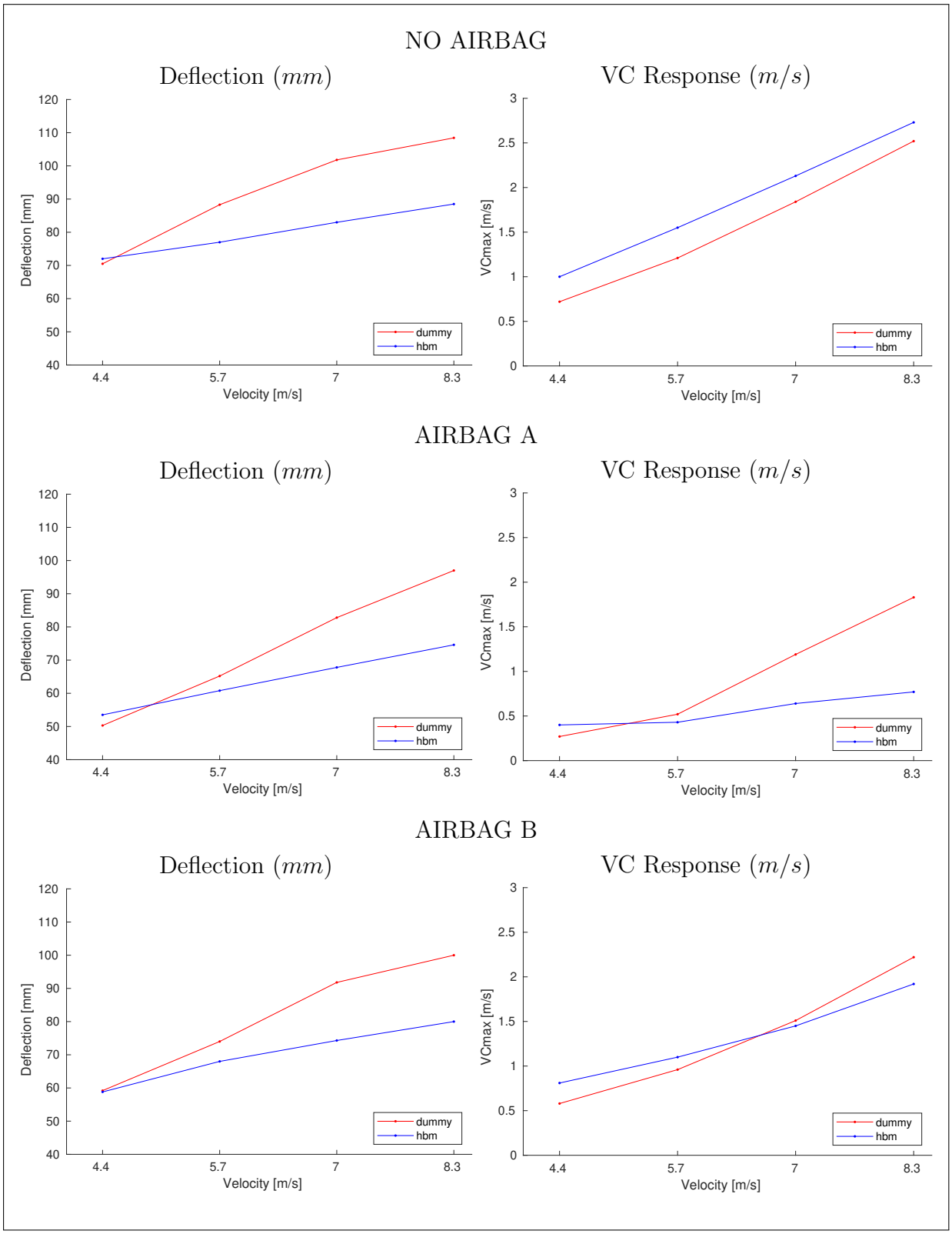

Figure 5.9: Comparison of thorax deflection and maximal Viscous Criterion response in rider-to-object configuration between the GHBMC and the Hybrid III dummy FE model.

5.4 Discussion

The objective of this chapter was to analyse a potential test procedure for frontal thorax airbags for motorcyclists and to explore the feasibility of using this procedure for the development of a future numerical-experimental test method. This analysis was divided in two parts and conducted in a Finite Element environment with a total of 72 simulations. Firstly, a sensitivity analysis was conducted to determine the equivalent mass of the Hybrid III dummy (used as a surrogate of the motorcyclist) necessary to translate the impact conditions of a rider-to-object impact configuration into an object-to-rider configuration. In a second step, the behaviour of the Hybrid III dummy and the human body model GHBMC were compared in a rider-to-object impact configuration. In both parts, the possible influence of an airbag protector was also investigated. All analyses were conducted based on the thorax response obtained in terms of thorax deflection and Viscous Criterion maximal response.

The results obtained from the sensitivity analysis suggest that the possible equivalent mass, which would provide a similar thorax response in the object-to-rider configuration as in the inverse one, would depend on the impact velocity and on the airbag protector. Attending to the values of thorax deflection and Viscous Criterion response provided by the simulation of the no-airbag condition, it was not possible to determine an unique value of equivalent mass which would replicate the same thorax response as the expected one in the rider-to-object configuration for all impact conditions considered in this study. In addition, the results indicate that the introduction of different airbag protective systems (airbag A and B) would also vary the value of equivalent mass at an specific impact velocity in comparison with the no airbag condition. Therefore, the expected thorax response in the object-to-rider configuration in terms of thorax deflection and Viscous Criterion response respectively, should be defined as a different combination of mass-velocity for each protecting condition and could be correspondingly represented as surface (see figure 5.8).

The comparison between the behaviour of the GHBMC and Hybrid III in a rider-to-object impact configuration showed that the thoracic responses are mostly different. Assuming the behaviour of the GHBMC as the closer to the reality, the differences between both responses were expected because of the construction of the Hybrid III dummy and the higher sensitivity of the HBM. The Hybrid III dummy is a test instrument which provides measurements at specific locations and is constructed with durability and repeatability requirements, while a FE Human Body Model is implemented with a more detailed anatomy, able to provide a wider range of data measurement and further reproduce the behaviour and internal interactions of the different human body structures. The higher stiffness of the Hybrid III dummy in comparison with the human body would also explain the differences obtained in the thoracic responses. In a direct comparison with data obtained from PMHS tests, several studies reported the higher stiffness of the Hybrid III dummy as the main cause of the kinematic differences presented by the dummy in frontal [18],

rear [100] and roll-over crash experiments [103] as well as it was presented as a factor which might also affect the thorax response [86]. Despite the different thoracic responses obtained, some similarities between the GHBMC and Hybrid III dummy where observed at the measurement of the protective effect provided by both considered airbag protectors in terms of thorax deflection. The reduction of the deflection values given by the airbag A and the airbag B measured with the Hybrid III dummy were proportionally similar to those obtained for both airbags at the GHBMC for the lower impact speed (4.4 m/s) as well as for a higher impact speed (8.3 m/s). However, for the case of the Viscous Criterion response, the protective effect provided by the airbags was only comparable at the lower impact speed. At an impact speed of 8.3 m/s, the reduction of the Viscous response provided by both airbags measured with the Hybrid III was around 2.5 times lower than those ones calculated with the GHBMC. Those results could be caused by the primitive stage of the soft tissues implemented at the Hybrid III dummy and could be as well considered another indicator of the high stiffness of the overall structure.

The analysis conducted in this chapter showed that the described test procedure was able to distinguish two different concepts of airbag protector based on the evaluation of their protective effect through biomechanical indicators like the thorax deflection and Viscous Criterion response. This ability is more evident if the airbag performances are expressed in terms of injury risk. Based on the existing injury risk curves for the Hybrid III dummy (see figure 2.10 for sternal compression and 2.11 for Viscous Criterion response), the values of thorax deflection and Viscous Criterion response can be translated into an injury risk probability. For example, translating the values of thorax deflection obtained from the test configuration into the risk of suffering an AIS$\geq$3 skeletal injury, the airbag A would report an injury risk between 72% and 13% depending on the impact mass and impact velocity. In comparison, the airbag B provided worse performance reporting a risk of an AIS$\geq$3 injury that would vary from 77% to 19% depending on the impact mass and velocity. The translation of the Viscous Criterion response in terms of injury risks indicates the same tendency; the risk of suffering AIS$\geq$4 soft tissue injury would be lower by wearing airbag A than airbag B. Comparing with the no-airbag impact situation, both airbags performed well at low impact speeds but airbag A could provide more significant injury risk reduction at an 30 km/h impact.

The current standard test for frontal thorax airbags assigned three levels of protection (fail, level 1 and level 2) depending of the transmitted force values measured during the testing. However, the origin and background of those force transmitted thresholds are unknown. The presented test method could be used to develop a new standard test procedure which could classify the protection effect of an airbag in terms of injury risk. After the translation of the values of thorax deflection and Viscous Criterion response into injury risk probability, the airbags could be classified into three levels of protection following the initial statement considered by the EN1621. A possible classification proposal for the new test procedure for an impact velocity of 8.3 m/s (30 km/h) could be: to qualify an airbag as "fail" if the thorax deflection obtained during the test implies a risk of an AIS$\geq$3 bone

injury higher than 67% and the Viscous Criterion response correspond to a risk of suffering an AIS≥4 soft tissue injury higher than 86%. These injury risks values correspond to the performance of airbag A at 30 km/h. A level 1 of protection would be assigned to those airbags reporting a 67% or lower risk of AIS≥3 for the thorax compression and a 86% risk or lower of an AIS≥4 or according to the Viscous Criterion. Those airbags able to provide a maximal risk of AIS≥3 skeletal injury of 50% for thorax compression and a maximal of 21% risk of AIS≥4 soft tissue injury for the Viscous Criterion would be labelled with the level 2 of protection. The injury risk probabilities of the level 2 correspond to the protection provided by airbag A at an impact velocity of 25 km/h.

Together with the findings exposed before, some other limitations should be mentioned. Firstly, the new test procedure was only analysed for one impact object symmetric configuration (horizontal), shape (cylinder) and dimension (a radius of 0.1 m). Further studies should evaluate the feasibility of the test method with other type of impact objects like a flat impactor and also analyse the procedure considering an asymmetric loading configuration, especially in a diagonal impact configuration which, as it was shown in the previous chapter 4, was revealed as a demanding loadcase for a frontal airbag protector. In addition, no eccentric impact with respect to middle-sternum was considered in this work. However, this impact configuration would be difficult at this test set-up. A low number of test and impact conditions (combinations of mass and velocity) have been conducted with this test set-up [72] and still potential reproducibility and repeatability problems could appear. Before the implementation of eccentric impacts could be addressed, a trustworthy operation of the test set-up should be developed. In addition, the development of another surrogate would be needed because the Hybrid III dummy is only equipped with a deflection measuring device at the centre of the thorax. Secondly, during the logic contemplated for the transformation of a real world accident into a laboratory test procedure, it was assumed that the performance of a Human Body Model would loyally reproduce the real behaviour of the human body in a frontal thorax impact. This statement should be carefully considered because even if the biofidelity of the HBMs (in this case the GHBMC) has been reported as promising [12, 90, 82], there are still some open issues to be improved like the possible effects of soft tissue mechanical properties in the model kinematic response [46] or the implementation of models with different weighs, statures and shapes to represent a more diverse population [49, 50].

Despite all the limitations explained, this chapter exposed the proposal of a potential test procedure for motorcyclist frontal airbags. Starting from the requirement that the test procedure should be as close as possible to the reality, a logic to translate the complex impact conditions of a frontal thorax impact situation into a potential simple and realistic laboratory test was presented. The different steps of that logic were analysed in order to identify the possible difficulties and explore its limitations. The results obtained in this chapter presented a test procedure able to distinguish different airbag protectors and classify them in different protection levels based on biomechanical parameters supporting the discussion about the necessity of a new standard for motorcyclists airbags.

Chapter 6

Conclusions and Outlook

Powered-Two-Wheeler users are considered vulnerable road users and present a higher risk of being involved in a fatal accident than car occupants. In the European Union, traffic accidents involving motorcycle and moped users account the 17% of the traffic fatalities. Despite the thorax is not the most frequent body region injured in a motorcycle accident, it was pointed out as the region with the highest rate of severe injuries. The solution of a wearable airbag was proposed to mitigate and prevent thoracic injuries in case of accident. Several airbag protective systems are available in the market with the certification of the European Standard EN1621. However, due to its low biofidelity, the suitability of the current standard EN1621 for the evaluation of those devices has been revealed as a questionable procedure and the effectiveness of a frontal thorax airbag in a real accident remains still unknown. Based on biomechanical criteria and the use of finite element human body models, this thesis investigates both open questions and contributes to the further development of motorcyclists airbags by firstly, assessing the protection efficiency and performance limitations of a representative current airbag device in more realistic impact scenarios and secondly, analysing a potential test procedure for the evaluation of frontal thorax airbags under impact conditions closer to a real accident.

This thesis begins with a review of the state of the art in chapter 2. In chapter 3, a finite element frontal thorax airbag model representative of a real airbag was modelled and characterized on basis of the parameters and performance of a real standard airbag available on the market. This model was used in the next chapter 4 to analyse the ability of injury mitigation of a representative current standard frontal thorax airbag under realistic accident impact conditions using numerical situations.

According to previous accident statistical studies, three interval areas or clusters were identified as those with a higher concentration of severe accidents with thorax injuries. The impact velocities and impact object radius of those identified clusters were used in chapter 4 to define the impact conditions of the numerical study. Using the FE human body model

GHBMC 50th percentile male pedestrian, every impact situation was simulated with and without an airbag protector to assess the current protection potential and limits of a representative frontal thorax airbag. Considering the different impact speeds, impact object radius, object configuration and the protective condition, a total of 72 simulations were conducted and analysed in this chapter. The number of rib fractures obtained on the basis of an ultimate strain analysis from the rib cage together with the measurement of the thorax deflection and the application of the Compression Criterion were used to determine the possible benefit in terms of injury mitigation of wearing an airbag protector. The results obtained from the simulation of all contemplated impact situations showed that the effectiveness of a frontal thorax airbag in the reduction of the injury severity is highly conditioned by the impact velocity and, to a lesser degree, by the object configuration. According to the results, an airbag could provide a limited protection up to 30 km/h of impact velocity. At a lower impact velocity, like the 17 km/h of Cluster 4 or the 20 km/h of Cluster 1, the airbag was able to provide a protective effect, reducing considerably the number of rib fractures and thorax deflection. In addition, at 30 km/h impact velocity, the airbag would also globally present a significant influence on the injury mitigation, showing specially a positive benefit for the cases of horizontal and diagonal impact configuration. However, over an impact speed of 30 km/h, the airbag was not able to provide a significant reduction of the injury severity obtaining a high number of rib fractures and high values of thorax compression at the most impact situations simulated. Only for the case of an impact at 40 km/h against a horizontal object, a partial benefit was observed being the airbag able to reduce the thorax compression but without a significant reduction of the number of rib fractures predicted. Looking at potential solutions to increment the potential frontal airbag protection from the airbag technology perspective, an airbag with a higher volume could improve the injury mitigation and may also increase slightly the impact velocity limit of 30 km/h for a significant protection performance. However, to achieve a real effective protection at higher impact speeds would entail some challenges for the development of technical solutions. Preliminary calculations showed that to avoid all rib fractures at an impact velocity of 60 km/h against an horizontal object, an airbag with a volume higher than 100 litres and a pressure over 1 bar would be needed. In addition, a higher volume and pressure might not be enough and this possible high volume airbag should be also equipped with a system of valves which would regulate the energy absorption.

Another measure to increment the airbag protection effectiveness could be to develop new test methods based on biomechanical criteria for the evaluation and certification of frontal airbags. A potential test procedure proposes to reproduce the impact conditions observed on a real motorcycle accident in a laboratory environment using a surrogate, the measurement of the thorax response through two biomechanical parameters (thorax deflection and Viscous Criterion response) for the evaluation of airbag protection performance. Chapter 5 presented and analysed the logic the potential test procedure is based on, in order to find its possible limitations and to explore the feasibility of using this procedure for the development of a numerical-experimental test method. This analysis was divided in two parts

and a total of 72 simulations were conducted. Firstly, a sensitivity study was conducted to determine the equivalent mass of the Hybrid III dummy (used as a surrogate of the motorcyclist during the test procedure) necessary to translate the impact conditions of a ride-to-object configuration into an object-to-rider configuration. Secondly, the behaviour of the Hybrid III dummy and the human body model GHBMC were compared in a rider-to-object impact configuration. In addition, during both parts of the analysis, the possible influence of an airbag protector was investigated. The sensitivity analysis showed that there is no unique value of equivalent mass which would replicate the expected response from the rider-to-object configuration in the object-to-rider one. In addition, it was found that the possible equivalent mass, which would reproduce a similar thorax response, would depend on the impact velocity and on the airbag protector. Those results suggest that the thorax response in the object-to-rider impact configuration should be defined as a different mass-velocity combination for each protector. The different behaviour showed by the Hybrid III dummy in comparison with the GHBMC was expected because of their different structure and purpose. Despite those differences, a proportional response between them was found when the performance of the airbags in terms of thorax deflection was evaluated. The test procedure presented in this thesis stays at a preliminary stage and only few experimental information is available [72]. Apart from more necessary experiments to improve this procedure, it may also be necessary to develop an specific surrogate for this application due to the implicit limitations of the Hybrid III dummy. However, facing the low biofidelity of the EN1621-4 and the unknown origin of the transmitted-force thresholds established to classify the performance of the protectors, the analysis conducted in this thesis showed the potential of the new test method as a possible substitute of the standard procedure not only evaluating its larger correspondence with a real accident impact conditions, but also proposing an evaluation of the airbag protective effect in terms of the injury risks derived from the measurement of biomechanical parameters.

In conclusion, this thesis contributes to the improvement of motorcyclists safety, specially in the protection of frontal thorax with airbag protectors. Based on numerical simulations and biomechanical criteria, this thesis exposes which are the protection limits of a representative current standard frontal airbag under realistic impact conditions and also contributes to the discussion about the necessity of a more realistic and biomechanically based standard procedure for the evaluation and certification of future thorax airbags. In addition, this thesis presents the possible benefit and potential of the use of the virtual assessment and human body models, not only for the evaluation of impact situations and injury assessment, but also for developing more effective new airbag devices.

Bibliography

[1] [Online]. Available: https://www.jsol-cae.com/

[2] [Online]. Available: https://www.helite.de/

[3] [Online]. Available: https://www.motoairbag.com/

[4] "EU Horizon 2020 PIONEERS - Protective Innovations of New Equipment for Enhanced Rider Safety." [Online]. Available: http://pioneers-project.eu/

[5] "EU Marie Curie Action FP7 Project MOTORIST - MOTOrcycle Rider Integrated SafeTy." [Online]. Available: https://cordis.europa.eu/project/id/608092

[6] "Unfallforschung kompakt Nr. 91 - Optimierte Schutzkleidung für Motorradfahrer," Unfallforschung der Versicherer (UDV), Tech. Rep., Aug. 2019.

[7] B. Albanese, T. Gibson, T. Whyte, L. Meredith, G. Savino, L. de Rome, M. Baldock, M. Fitzharris, and J. Brown, "Energy attenuation performance of impact protection worn by motorcyclists in real-world crashes," *Traffic injury prevention*, vol. 18, no. sup1, pp. S116–S121, 2017.

[8] Alexandri, V. et al., "The use of motorcycle in greece: Protective equipment, injuries and physiotherapy." *Ephitorese Klinikes Farmakologias kai Farmakokinetikes*, vol. 31, no. 3, pp. 243–248, 2013.

[9] J. Antona-Makoshi, Y. Yamamoto, R. Kato, F. Sato, S. Ejima, Y. Dokko, and T. Yasuki, "Age-dependent factors affecting thoracic response: a finite element study focused on japanese elderly occupants," *Traffic injury prevention*, vol. 16, no. sup1, pp. S66–S74, 2015.

[10] R. Aranda and S. Peldschus, "Feasibility of analysing the effects of personal protective equipment using virtual human body models," in *ifz Forschungsheft Nr. 17, Tagungsband der 11. Internationalen Motorradkonferenz*, Collogne, Germany, 2016.

[11] R. Aranda, W. Wei, T. Serre, P. Sanchez, and E. Gonzalez, "Limitations of the Standard Test Procedure for Assessing the Protection of Motorcyclist Airbag Jackets in a Realistic Impact Scenario," in *IRCOBI Conference Proceedings*, 2020.

[12] M. W. Arun, S. Umale, J. R. Humm, N. Yoganandan, P. Hadagali, and F. A. Pintar, "Evaluation of kinematics and injuries to restrained occupants in far-side crashes using full-scale vehicle and human body models," *Traffic injury prevention*, vol. 17, no. sup1, pp. 116–123, 2016.

[13] AS/NZS 1698: 2006, "Protective helmets for vehicle users," 2006.

[14] O. C. Ballester, M. Llari, S. Afquir, J.-L. Martin, N. Bourdet, V. Honoré, C. Masson, and P.-J. Arnoux, "Analysis of trunk impact conditions in motorcycle road accidents based on epidemiological, accidentological data and multibody simulations," *Accident Analysis & Prevention*, vol. 127, pp. 223–230, 2019.

[15] M. R. Bambach and R. Mitchell, "The rising burden of serious thoracic trauma sustained by motorcyclists in road traffic crashes," *Accident Analysis & Prevention*, vol. 62, pp. 248–258, 2014.

[16] K. Bauer, S. Peldschus, and S. Schick, "Retrospektive Analyse tödlicher Motorradunfälle und Ableitung von Schutzmaßnahmen bei komplexen Bremsmanövern," in *ifz Forschungsheft Nr. 16, Tagungsband der 10. Internationalen Motorradkonferenz*, Collogne, Germany, 2014.

[17] K. Bauer, S. Schick, R. Aranda, A. Thalhammer, S. Peldschus, M. Kühn, and A. Lang, "Optimierte Schutzkleidung für Motorradfahrer - Forschungsbericht 68," Unfallforschung der Versicherer (UDV), Berlin, Tech. Rep., 2020. [Online]. Available: https://udv.de/de/publikationen/forschungsberichte/optimierte-schutzkleidung-fuer-motorradfahrer

[18] S. M. Beeman, A. R. Kemper, M. L. Madigan, C. T. Franck, and S. C. Loftus, "Occupant kinematics in low-speed frontal sled tests: Human volunteers, hybrid iii atd, and pmhs," *Accident Analysis & Prevention*, vol. 47, pp. 128–139, 2012.

[19] M. Behr, P.-J. Arnoux, T. Serre, S. Bidal, H. Kang, L. Thollon, C. Cavallero, K. Kayvantash, and C. Brunet, "A human model for road safety: from geometrical acquisition to model validation with radioss," *Computer Methods in Biomechanics & Biomedical Engineering*, vol. 6, no. 4, pp. 263–273, 2003.

[20] N. Bourdet, C. Deck, V. Tinard, and R. Willinger, "Behaviour of helmets during head impact in real accident cases of motorcyclists," *International journal of crashworthiness*, vol. 17, no. 1, pp. 51–61, 2012.

[21] N. Bourdet, S. Mojumder, S. Piantini, C. Deck, M. Pierini, and R. Willinger, "Proposal of a new motorcycle helmet test method for tangential impact," in *Proc. of the International IRCOBI Conference on the Biomechanics of Impacts*, 2016, pp. 503–504.

[22] D. A. Bruneau and D. S. Cronin, "Head and neck response of an active human body model and finite element anthropometric test device during a linear impactor helmet test," *Journal of Biomechanical Engineering*, vol. 142, no. 2, 2020.

[23] R. Capitani, S. Pellari, and R. Lavezzi, "Design and numerical evaluation on an airbag-jacket for motorcyclists," Hannover, Germany, 2010.

[24] D. Caroline and W. Rémy, "Head injury prediction tool for protective systems optimisation," in *7th European LS-DYNA Conference*, 2009.

[25] O. Cherta Ballester, M. Llari, V. Honoré, C. Masson, and P.-J. Arnoux, "An evaluation methodology for motorcyclists' wearable airbag protectors based on finite element simulations," *International Journal of Crashworthiness*, pp. 1–10, 2019.

[26] COST, "Motorcycle Safety Helmets Final report," European Commission, Tech. Rep., 2001. [Online]. Available: https://ec.europa.eu/transport/road_safety/sites/roadsafety/files/pdf/projects/cost_327.pdf

[27] L. de Rome, R. Ivers, M. Fitzharris, W. Du, N. Haworth, S. Heritier, and D. Richardson, "Motorcycle protective clothing: protection from injury or just the weather?" *Accident Analysis & Prevention*, vol. 43, no. 6, pp. 1893–1900, 2011.

[28] DESTATIS, "Verkehrsunfälle zeitreihen 2018," Statistisches Bundesamt, Wiesbaden, Tech. Rep., 2019.

[29] DIN EN 13594, "Protective gloves for motorcycle riders - requirements and test methods," 2015.

[30] DIN EN 13634, "Protective footwear for motorcycle riders - requirements and test methods," 2017.

[31] DIN EN 1621-1:2013-03, "Motorcyclists' protective clothing against mechanical impact - part 1: Motorcyclists' limb joint impact protectors - requirements and test methods." 2013.

[32] DIN EN 1621-3:2019-03, "Motorcyclists' protective clothing against mechanical impact - part 3: Motorcyclists' chest protectors - requirements and test methods." 2013.

[33] DIN EN 1621-4:2013-03, "Motorcyclists' protective clothing against mechanical impact - part 4: Motorcyclists' inflatable protectors - requirements and test methods." 2013.

[34] DOT FMVSS-218, "Federal motor vehicle safety standard no. 218 - motorcycle helmets," 2013.

[35] Editoriale Domus, "Dueruote - Arbag per motociclisti," Sep. 2019.

[36] ERSO, "Annual accident report 2018," European Road Safety Observatory, Tech. Rep., 2018. [Online]. Available: https://ec.europa.eu/transport/road_safety/sites/roadsafety/files/pdf/statistics/dacota/asr2018.pdf

[37] European Commission - SafetyNet, (Accessed: October 2020). [Online]. Available: http://ec.europa.eu/transport/road_safety/specialist/knowledge/vehicle/safety_design_needs/motorcycles_en

[38] F. A. Fernandes, R. J. Alves de Sousa, R. Willinger, and C. Deck, "Finite element analysis of helmeted impacts and head injury evaluation with a commercial road helmet," in *IRCOBI Conference*, 2013, pp. 431–442.

[39] J. Forman, H. Lin, B. Gepner, T. Wu *et al.*, "Occupant safety in automated vehicles," *International journal of automotive engineering*, vol. 10, no. 2, pp. 139–143, 2019.

[40] J. L. Forman and R. W. Kent, "Modeling costal cartilage using local material properties with consideration for gross heterogeneities," *Journal of biomechanics*, vol. 44, no. 5, pp. 910–916, 2011.

[41] ——, "The effect of calcification on the structural mechanics of the costal cartilage," *Computer methods in biomechanics and biomedical engineering*, vol. 17, no. 2, pp. 94–107, 2014.

[42] R. Fredriksson and B. Sui, "Fatal Powered Two-Wheeler (PTW) crashes in Germany–an in-depth study of the events, injuries and injury sources," in *Proceedings of Conference IRCOBI*, 2015.

[43] ——, "Powered two-wheeler accidents in Germany with severe injury outcome—accident scenarios, injury sources and potential countermeasures," in *IRCOBI Conference Proceedings*, 2016.

[44] K. Furusu, I. Watanabe, C. Kato, K. Miki, and J. Hasegawa, "Fundamental study of side impact analysis using the finite element model of the human thorax," *JSAE review*, vol. 22, no. 2, pp. 195–199, 2001.

[45] M. Ghajari, U. Galvanetto, L. Iannucci, and R. Willinger, "Influence of the body on the response of the helmeted head during impact," *International journal of crashworthiness*, vol. 16, no. 3, pp. 285–295, 2011.

[46] D. Gierczycka, A. Rycman, and D. Cronin, "Importance of passive muscle, skin, and adipose tissue mechanical properties on head and neck response in rear impacts assessed with a finite element model," *Traffic injury prevention*, pp. 1–6, 2021.

[47] C. C. Gordon, T. Churchill, C. E. Clauser, B. Bradtmiller, and J. T. McConville, "Anthropometric survey of us army personnel: methods and summary statistics 1988," Anthropology Research Project Inc Yellow Springs OH, Tech. Rep., 1989.

[48] Y. Huang, Q. Zhou, S. Wang, B. Nie, and S. Holcombe, "An anatomic indexing system for costal cartilage and its application in calcification representation in finite-element human body models," in *Proceedings of IRCOBI Conference*, 2019.

[49] E. Hwang, J. Hu, C. Chen, K. F. Klein, C. S. Miller, M. P. Reed, J. D. Rupp, and J. J. Hallman, "Development, evaluation, and sensitivity analysis of parametric finite element whole-body human models in side impacts," SAE Technical Paper, Tech. Rep., 2016.

[50] E. Hwang, J. Hu, and M. P. Reed, "Validating diverse human body models against side impact tests with post-mortem human subjects," *Journal of biomechanics*, vol. 98, p. 109444, 2020.

[51] K. Kayvantash, S. Bidal, and F. Delcroix, "HUMOS - An FE Model for Advanced Safety and Comfort Assessments," in *6th Altair CAE Technology Conference*, 2009.

[52] C. K. Kroell, D. C. Schneider, and A. M. Nahum, "Impact tolerance and response of the human thorax ii," *SAE Transactions*, pp. 3724–3762, 1974.

[53] A. G. Lau, M. W. Kindig, R. S. Salzar, and R. W. Kent, "Micromechanical modeling of calcifying human costal cartilage using the generalized method of cells," *Acta biomaterialia*, vol. 18, pp. 226–235, 2015.

[54] I. V. Lau and D. C. Viano, "The viscous criterion—bases and applications of an injury severity index for soft tissues," *SAE transactions*, pp. 672–691, 1986.

[55] H. Liers, L. Hannawald, and M. Prohn, "Analysis of the accident scenario of powered two-wheelers on the basis of real accidents," *Forschungshefte Zweiradsicherheit*, no. 16, 2014.

[56] M.-R. Lin and J. F. Kraus, "A review of risk factors and patterns of motorcycle injuries," *Accident Analysis & Prevention*, vol. 41, no. 4, pp. 710–722, 2009.

[57] T. Lobdell, C. Kroell, D. Schneider, W. Hering, and A. Nahum, "Impact response of the human thorax," in *Human impact response*. Springer, 1973, pp. 201–245.

[58] MAIDS, "In-depth investigations of accidents involving powered two wheelers," ACEM, European Commission, Tech. Rep., 2009.

[59] E. Marconi, F. Gatto, and M. Massaro, "Numerical and experimental assessment of the performance of wearable airbags for motorcycle riders," in *Proceedings of the World Congress on Engineering*, vol. 2, 2018.

[60] H. J. Mertz, P. Prasad, and A. L. Irwin, "Injury risk curves for children and adults in frontal and rear collisions," *SAE transactions*, pp. 3563–3580, 1997.

[61] F. Meyer, C. Deck, and R. Willinger, "Protection from motorcycle neck–braces using fe modelling," *Sports Engineering*, vol. 21, no. 4, pp. 267–276, 2018.

[62] G. Milne, C. Deck, N. Bourdet, R. Carreira, Q. Allinne, A. Gallego, and R. Willinger, "Bicycle helmet modelling and validation under linear and tangential impacts," *International journal of crashworthiness*, vol. 19, no. 4, pp. 323–333, 2014.

[63] MOSAFIM, "MOtorcyclists road SAFety IMprovement through better behaviour of the quipment and first aid devices." European Commission, Tech. Rep., 2013.

[64] A. Moskal, J.-L. Martin, E. Lenguerrand, and B. Laumon, "Injuries among motorised two-wheelers in relation to vehicle and crash characteristics in rhone, france," in *Enhanced Safety Vehicle Conference, Lyon*, 2007.

[65] A. M. Nahum and J. W. Melvin, *Accidental injury: biomechanics and prevention*. Springer Science & Business Media, 2012.

[66] National Highway Traffic Safety Administration (NHTSA), (Accessed: April 2019). [Online]. Available: https://www.nhtsa.gov/crash-simulation-vehicle-models

[67] J. Newman, "The biomechanics of head trauma and the development of the modern helmet. how far have we really come," in *Proceedings of the IRCOBI Conference*, 2005, p. 10.

[68] M. Oyen, D. Murakami, and R. Kent, "Mechanical characterization of costal cartilage," in *33rd Proceedings, International Workshop on Human Subjects for Biomechanical Research*, 2005.

[69] S. Piantini, M. Pierini, M. Delogu, N. Baldanzini, A. Franci, M. Mangini, and A. Peris, "Injury analysis of powered two-wheeler versus other-vehicle urban accidents," in *Proceedings of IRCOBI Conference*, 2016.

[70] PIONEERS - Protective Innovations of New Equipment for Enhanced Rider Safety, "D3.1 - Test procedures for PPE, helmet and full vehicle," European Commission, Grant Agreement No. 769054, Horizon 2020, Tech. Rep., 2020.

[71] ——, "D3.2 - Associated Assessment Method," European Commission, Grant Agreement No. 769054, Horizon 2020, Tech. Rep., 2020.

[72] ——, "D3.3 - Test Results," European Commission, Grant Agreement No. 769054, Horizon 2020, Tech. Rep., 2020.

[73] D. Poulard, R. W. Kent, M. Kindig, Z. Li, and D. Subit, "Thoracic response targets for a computational model: a hierarchical approach to assess the biofidelity of a 50th-percentile occupant male finite element model," *Journal of the mechanical behavior of biomedical materials*, vol. 45, pp. 45–64, 2015.

[74] P. Prasad, H. J. Mertz, D. J. Dalmotas, J. S. Augenstein, and K. Digges, "Evaluation of the field relevance of several injury risk functions," SAE Technical Paper, Tech. Rep., 2010.

[75] A. Pratellesi, S. Turrin, T. Haag, A. Scippa, and N. Baldanzini, "On the effect of testing uncertainties in the homologation tests of motorcycle helmets according to ece 22.05," *International journal of crashworthiness*, vol. 16, no. 5, pp. 523–536, 2011.

[76] E. Regulation, "22.05 (2002)," *Uniform provision concerning the approval of protective helmets and their visors for driver and passengers of motor cycles and mopeds*.

[77] M. Richter, D. Otte, U. Lehmann, B. Chinn, E. Schuller, D. Doyle, K. Sturrock, and C. Krettek, "Head injury mechanisms in helmet-protected motorcyclists: prospective multicenter study," *Journal of Trauma and Acute Care Surgery*, vol. 51, no. 5, pp. 949–958, 2001.

[78] S. Robin, "Humos: Human model for safety˜ a joint effort towards the development of refined human-like car occupant models," SAE Technical Paper, Tech. Rep., 2001.

[79] J. S. Ruan, R. El-Jawahri, S. Barbat, and P. Prasad, "Biomechanical analysis of human abdominal impact responses and injuries through finite element simulations of a full human body model," SAE Technical Paper, Tech. Rep., 2005.

[80] D. Sahoo, C. Deck, and R. Willinger, "Axonal strain as brain injury predictor based on real-world head trauma simulations," in *Proceedings of the IRCOBI Conference, Lyon, France IRC-15-30*, 2015.

[81] ——, "Brain injury tolerance limit based on computation of axonal strain," *Accident Analysis & Prevention*, vol. 92, pp. 53–70, 2016.

[82] J. M. Schap, B. Koya, and F. S. Gayzik, "Objective evaluation of whole body kinematics in a simulated, restrained frontal impact," *Annals of biomedical engineering*, vol. 47, no. 2, pp. 512–523, 2019.

[83] K.-U. Schmitt, P. Niederer, M. Muser, and F. Walz, *Trauma biomechanics*. Springer, 2010.

[84] T. Serre, C. Llari, M. Masson, B. Canu, M. Py, and C. Perrin, "Airbag Jacket for Motorcyclists: Evaluation of Real Effectiveness," in *IRCOBI Conference Proceedings*, 2019.

[85] T. Serre, C. Masson, C. Perrin, J.-L. Martin, A. Moskal, and M. Llari, "The motorcyclist impact against a light vehicle: epidemiological, accidentological and biomechanic analysis," *Accident Analysis & Prevention*, vol. 49, pp. 223–228, 2012.

[86] G. Shaw, D. Lessley, J. Ash, J. Crandall, and D. Parent, "Response comparison for the hybrid iii, thor mod kit with sd-3 shoulder, and pmhs in a simulated frontal crash," in *23rd ESV Conference, Paper*, no. 13-0130, 2013.

[87] Snell Memorial Foundation, Inc. North Highlands, CA, USA, "Snell M2010 Standard for Motorcycling Helmet," 2010.

[88] K. Somasundaram, L. Zhang, D. Sherman, P. Begeman, D. Lyu, and J. Cavanaugh, "Evaluating thoracolumbar spine response during simulated underbody blast impact using a total human body finite element model," *Journal of the mechanical behavior of biomedical materials*, vol. 100, p. 103398, 2019.

[89] J. T. Somers, N. J. Newby, C. Lawrence, R. L. DeWeese, D. Moorcroft, and S. E. Phelps, "Investigation of the thor anthropomorphic test device for predicting occupant injuries during spacecraft launch aborts and landing," *Frontiers in bioengineering and biotechnology*, vol. 2, p. 4, 2014.

[90] E. Song, P. Petit, and J. Uriot, "Modelling of an adjustable generic simplified vehicle for pedestrian impact and simulations of corresponding reference pmhs tests using the ghbmc 50 th percentile male pedestrian simplified model," SAE Technical Paper, Tech. Rep., 2018.

[91] E. G. Takhounts, S. A. Ridella, V. Hasija, R. E. Tannous, J. Q. Campbell, D. Malone, K. Danelson, J. Stitzel, S. Rowson, and S. Duma, "Investigation of traumatic brain injuries using the next generation of simulated injury monitor (simon) finite element head model," SAE Technical Paper, Tech. Rep., 2008.

[92] A. Thalhammer, "Entwicklung einer funktionalen Methodik zur Eingrenzung kinematischer Anprallparameter verunfallter Motorradfahrer auf Basis von Realunfalldaten und Ableitung von Anforderungen an innovative Schutzkleidung," Ph.D. dissertation, Ludwig-Maximilians-Universität München , 2022.

[93] L. Thollon, Y. Godio, S. Bidal, and C. Brunet, "Evaluation of a new security system to reduce thoracic injuries in case of motorcycle accidents," *International journal of crashworthiness*, vol. 15, no. 2, pp. 191–199, 2010.

[94] Transport for London, "Motorcycle safety action point. working together, towards roads free from death and serious accidents." Tech. Rep., 2014. [Online]. Available: http://content.tfl.gov.uk/motorcycle-safety-action-plan.pdf

[95] C. D. Untaroiu, J. B. Putnam, J. Schap, M. L. Davis, and F. S. Gayzik, "Development and preliminary validation of a 50th percentile pedestrian finite element model," ser. International Design Engineering Technical Conferences and Computers and Information in Engineering Conference, vol. Volume 3: 17th International Conference on Advanced Vehicle Technologies; 12th International Conference on Design Education; 8th Frontiers in Biomedical Devices, 08 2015.

[96] N. A. Vavalle, M. L. Davis, J. D. Stitzel, and F. S. Gayzik, "Quantitative validation of a human body finite element model using rigid body impacts," *Annals of biomedical engineering*, vol. 43, no. 9, pp. 2163–2174, 2015.

[97] D. C. Viano and I. V. Lau, "A viscous tolerance criterion for soft tissue injury assessment," *Journal of Biomechanics*, vol. 21, no. 5, pp. 387–399, 1988.

[98] WHO, "Global status report on road safety 2018," World Health Organization, Geneva, Switzerland, Tech. Rep., 2018.

[99] T. Wu, T. Kim, V. Bollapragada, D. Poulard, H. Chen, M. B. Panzer, J. L. Forman, J. R. Crandall, and B. Pipkorn, "Evaluation of biofidelity of thums pedestrian model under a whole-body impact conditions with a generic sedan buck," *Traffic injury prevention*, vol. 18, no. sup1, pp. S148–S154, 2017.

[100] M. Yaguchi, K. Ono, M. Kubota, and F. Matsuoka, "Comparison of biofidelic responses to rear impact of the head/neck/torso among human volunteers, pmhs, and dummies," in *Proc 2006 Int'l IRCOBI Conf on the Biomechanics of Impacts*, 2006, pp. 20–22.

[101] J. Yang, P. Lövsund, C. Cavallero, and J. Bonnoit, "A human-body 3d mathematical model for simulation of car-pedestrian impacts," *Traffic Injury Prevention*, vol. 2, no. 2, pp. 131–149, 2000.

[102] L. Zhang, K. H. Yang, R. Dwarampudi, K. Omori, T. Li, K. Chang, W. N. Hardy, T. B. Khalil, and A. I. King, "Recent advances in brain injury research: a new human head model development and validation," SAE Technical Paper, Tech. Rep., 2001.

[103] Q. Zhang, D. J. Lessley, P. Riley, J. Toczyski, J. Lockerby, P. Foltz, B. Overby, J. Seppi, J. R. Crandall, and J. R. Kerrigan, "Occupant kinematics in laboratory rollover tests: Atd response and biofidelity," SAE Technical Paper, Tech. Rep., 2014.

[104] J. Z. Zhao, M. Katagiri, W. Decker, S. Lee, and F. Gayzik, "A human body model study on restraints for side-facing occupants in frontal crashes of an automated vehicle," SAE Technical Paper, Tech. Rep., 2020.

LMU LUDWIG-MAXIMILIANS-UNIVERSITÄT MÜNCHEN

Promotionsbüro
Medizinische Fakultät

MMRS MUNICH MEDICAL RESEARCH SCHOOL

Eidesstattliche Versicherung

Aranda Marco, Raúl

Name, Vorname

Ich erkläre hiermit an Eides statt,

dass ich die vorliegende Dissertation mit dem Titel

Biomechanical effectiveness assessment of motorcyclist airbags in realistic impact scenarios using human body models

selbständig verfasst, mich außer der angegebenen keiner weiteren Hilfsmittel bedient und alle Erkenntnisse, die aus dem Schrifttum ganz oder annähernd übernommen sind, als solche kenntlich gemacht und nach ihrer Herkunft unter Bezeichnung der Fundstelle einzeln nachgewiesen habe.

Ich erkläre des Weiteren, dass die hier vorgelegte Dissertation nicht in gleicher oder in ähnlicher Form bei einer anderen Stelle zur Erlangung eines akademischen Grades eingereicht wurde.

30.11.2022, München

Ort, Datum

Raúl Aranda Marco

Unterschrift Doktorandin bzw. Doktorand